Supporting Information for

Alternating Copolymerization of Propylene Oxide and Cyclohexene Oxide with Tricyclic Anhydrides: Access to Partially Renewable Aliphatic Polyesters with High Glass Transition Temperatures

Maria J. Sanford,[‡] Leticia Peña Carrodeguas,[§] Nathan J. Van Zee,[‡] Arjan W. Kleij,*[,§,#] and Geoffrey W. Coates*[,‡]

[‡]*Department of Chemistry and Chemical Biology, Baker Laboratory, Cornell University, Ithaca, NY 14853-1301, USA*

[§]*Institute of Chemical Research of Catalonia (ICIQ), the Barcelona Institute of Science and Technology, Av. Països Catalans 16, 43007 Tarragona, Spain*

[#] *Catalan Institute of Research and Advanced Studies (ICREA), Pg. Lluis Companys 23, 08010, Barcelona, Spain*

1. General considerations

All manipulations of air and water sensitive compounds were carried out under nitrogen in an MBraun Labmaster glovebox or by using standard Schlenk line technique. ^{1}H NMR spectra were recorded on Varian INOVA 400 (^{1}H, 400 MHz), INOVA 500 (^{1}H, 500 MHz), or INOVA 600 (^{1}H, 600 MHz) spectrometers. Spectra were referenced to the residual chloroform (7.26 ppm) or DMSO-d_5 (2.50 ppm) signals. ^{13}C NMR spectra were recorded on a Varian INOVA 500 (^{13}C, 126 MHz) spectrometer and referenced to the residual chloroform (77.23 ppm) or DMSO-d_6 (39.50 ppm) signals. HRMS analyses were performed on a Thermo Scientific Exactive Orbitrap MS system equipped with an Ion Sense DART ion source.

Flash column chromatography was performed using silica gel (particle size 40–64 μm, 230–400 mesh). Gel permeation chromatography (GPC) analyses were carried out using an Agilent 1260 Infinity GPC System equipped with a refractive index detector as well as an Agilent 1260 Infinity autosampler. The Agilent GPC system was equipped with two Agilent PolyPore columns (5 micron, 4.6 mm ID which were eluted with THF at 30 °C at 0.3 mL/min and calibrated using monodisperse polystyrene standards.

Differential scanning calorimetry (DSC) measurements of polymer samples were performed on a Mettler-Toledo Polymer DSC instrument equipped with a chiller and an autosampler. Samples were prepared in aluminum pans. All polyesters were analyzed using the following heating program: −70 °C to 200 °C at 25 °C/min, 200 to −70 °C at 10°C/min, and then −70 °C to 200 °C at 25 °C/min. Data were processed using StarE software. All reported glass transition temperatures were observed on the second heating cycle. MALDI-TOF-MS analyses were performed on a BRUKER Autoflex system with a 20 Hz N_2 UV laser (337 nm) and based on a previously reported procedure.[1] Crude polymer samples were dissolved in THF at 1 mg·mL^{-1}. Sodium trifluoroacetate was used as the cationization agent and dissolved in THF at 5 mg·mL^{-1}. The matrix *trans*-2-[3-(4-*tert*-butylphenyl)-2-methyl-2-propenylidene]malononitrile (DCTB) was dissolved in THF at 40 mg·mL^{-1}. Solutions for analysis were prepared by mixing polymer, cationization agent, and matrix solutions in a volume ratio of 80:10:40, respectively. The sample was left to air dry after spotting on a stainless steel MALDI target plate. All spectra were recorded in linear mode and mass-locked to the residual signal of $[PPN]^+$ (538 *m*/*z*). The resulting spectra were analyzed using the Flex Analysis software package. Polymer thermal degradation experiments were performed on a Mettler Toledo Thermogravimetric Analyzer (TGA), model TGA/SDTA851. The heating program was 30 °C to 500 °C at 10 °C/min under a

nitrogen atmosphere. Data were processed using START software. Onset thermal decomposition temperatures were reported.

2. Materials

Solvents used for cyclic anhydride and ligand syntheses, including methanol (Macron), absolute ethanol (Koptec), methylene chloride (Fisher), hexanes (Macron), ethyl acetate (Fisher), chloroform (Fisher), and diethyl ether (J. T. Baker), were used as received. Toluene (Fisher) and hexane (Fisher) used in salicylaldehyde and complex syntheses were dried and degassed by passing them through two columns packed with neutral alumina and copper(II) oxide. α–Terpinene (Aldrich, ≥ 89%), α-phellandrene (Aldrich, Hallal/Kosher), 1,3-cyclohexadiene (Aldrich, 97%), citraconic anhydride (Aldrich, 98%), 2,5-dimethylfuran (Aldrich, 99%) and maleic anhydride (Aldrich, ≥ 99.0%) were used as received. Hydrogen (Airgas, 99.99%) was used as received.

Propylene oxide (PO) was purchased from Aldrich, stirred over freshly ground CaH_2 for three days, vacuum transferred to a dry Straus flask, degassed by three freeze-pump-thaw cycles and stored in a glovebox. Cyclohexene oxide (CHO) was purchased from Aldrich, stirred over freshly ground CaH_2 for one day, vacuum distilled onto a new portion of freshly ground CaH_2 in a dry roundbottom flask with Straus adapter, stirred one day and then vacuum distilled again before being degassed by three freeze-pump-thaw cycles. Palladium on activated carbon (5%, reduced, dry powder, Strem) was used as received. Bis(triphenylphosphine)iminium chloride ([PPN]Cl, 97%, Aldrich) was recrystallized by layering a saturated methylene chloride solution with diethyl ether. The resulting crystals were ground to a fine powder and then dried at 60 °C under vacuum prior to use. All other chemicals and reagents were purchased from commercial sources (Aldrich, Combi-Blocks, Strem, Acros, TCI, and Alfa Aesar) and used without further purification.

3. General Copolymerization Procedures

Copolymerization of propylene oxide with cyclic anhydrides. In a glovebox, the appropriate amount of metal complex (4.3 μmol) and [PPN]Cl (2.2 mg, 3.8 μmol) were placed in an oven-dried 4-mL vial equipped with a magnetic stir bar. The appropriate amount of cyclic anhydride (1.3 mmol) was added, followed by propylene oxide (0.45 mL, 6.4 mmol). The vial was sealed with a Teflon-lined cap, removed from the glovebox, and placed in an aluminum heating block preheated to 60 °C. After the appropriate amount of time, an aliquot was taken for ^{1}H NMR spectroscopic analysis to determine conversion of the cyclic anhydride. The reaction mixture was

then diluted with approximately 0.5 mL methylene chloride and precipitated into 10 mL of methanol with vigorous stirring, after which the methanol was decanted. Poly(PO-*alt*-**1e**) was precipitated into hexanes due to its higher solubility in methanol. Precipitation was repeated as necessary to remove excess monomer and catalyst. The polymer was dried under vacuum at 60 °C.

Copolymerization of cyclohexene oxide with cyclic anhydrides. In a glovebox, the appropriate amount of metal complex (4.3 μmol) and [PPN]Cl (2.2 mg, 3.8 μmol) were placed in an oven-dried 4-mL vial equipped with a magnetic stir bar. The appropriate amount of cyclic anhydride (1.3 mmol) was added, followed by cyclohexene oxide (0.39 mL, 3.84 mmol) and dry, degassed toluene (0.2 mL). The vial was sealed with a Teflon-lined cap, removed from the glovebox, and placed in an aluminum heating block preheated to 60 °C. After the appropriate amount of time, an aliquot was taken for ^{1}H NMR spectroscopic analysis to determine conversion of the cyclic anhydride. The reaction mixture was then diluted with approximately 0.5 mL methylene chloride and precipitated into 10 mL of methanol with vigorous stirring, after which the methanol was decanted. Poly(CHO-*alt*-**1e**) was precipitated into hexanes due to its higher solubility in methanol. Precipitation was repeated as necessary to remove excess monomer and catalyst. The polymer was dried under vacuum at 60 °C.

4. Synthesis of Complexes 2a–2c

4.1 Synthesis of 3-*tert*-butyl-5-chlorosalicylaldehyde

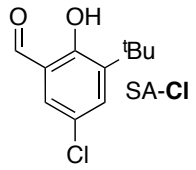

3-*tert*-butyl-5-chlorosalicylaldehyde (SA-Cl). Prepared according to the literature procedure.[2]

^{1}H NMR (400 MHz, $CDCl_3$): δ 11.72 (s, 1H), 9.82 (s, 1H), 7.46 (d, 1H), 7.38 (d, 1H), 1.41 (s, 9H).

4.2 Synthesis of (salph)H_2 Ligands

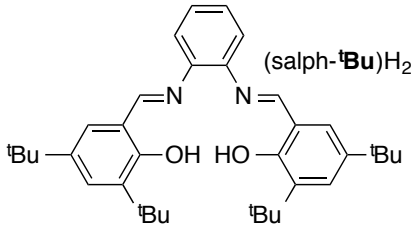

N,N'-bis(3,5-di-*tert*-butylsalicylidene)-1,2-diaminobenzene [(salph-^{t}Bu)H_2]. Prepared according to the literature procedure using 3,5-di-*tert*-butylsalicylaldehyde that was purchased from AK Scientific.[3]

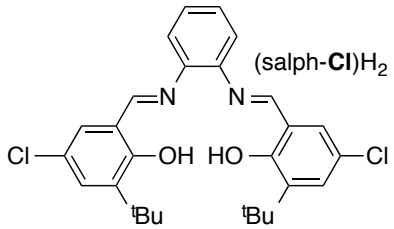

N,N'-bis(3-*tert*-butyl-5-chlorosalicylidene)-1,2-diaminobenzene [(salph-Cl)H_2].

Salicylaldehyde SA-**Cl** (0.50 g, 2.3 mmol, 2.0 equiv.) and 1,2-diaminobenzene (0.13 g, 1.2 mmol, 1.0 equiv.) were refluxed in absolute ethanol (20 mL). The reaction mixture was cooled to 22 °C, and the resulting precipitate was isolated by filtration. The solids were washed with small amounts of cold ethanol then dried under vacuum at 60 °C overnight to give **(salph-Cl)H_2** (0.32 g, 55%) as an orange solid. **^{1}H NMR** (600 MHz, $CDCl_3$): δ 13.70 (s, 2H), 8.58 (s, 2H), 7.34–7.38 (m, 2H), 7.32 (d, 2 H), 7.24–7.27 (m, 2H), 7.23 (d, 2H), 1.41 (s, 18 H). **^{13}C NMR** (125 MHz, $CDCl_3$): δ 163.38, 159.56, 142.20, 140.40, 130.91, 129.50, 128.23, 123.17, 119.89–119.95, 35.41, 29.33. **HRMS** (DART-MS): *m/z* calculated for ($M-H^+$) 497.17571 found 497.17513.

4.3 Synthesis of aluminum complexes

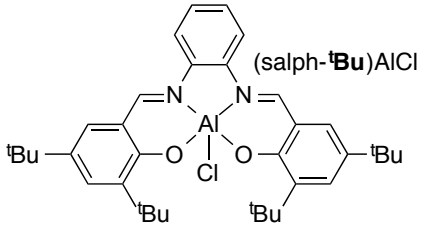

(salph-^{t}Bu)AlCl (2a). Prepared using (salph-^{t}Bu)H_2 according to the literature procedure.[4]

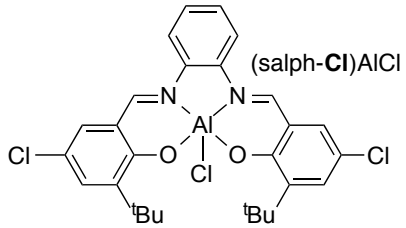

(salph-Cl)AlCl (2b). In a glovebox, (salph-**Cl**)H_2 (0.30 g, 0.60 mmol, 1.0 equiv.) was dissolved in approximately 20 mL dry, degassed toluene in a dry schlenk flask. A 1.020 M solution of Et_2AlCl (0.65 mL, 0.66 mmol, 1.1 equiv.) was added dropwise with stirring, resulting in yellow solids precipitating from the reaction mixture. After stirring at 22 °C for 5 minutes in the glovebox, the flask was sealed and removed from the glovebox. The mixture was then heated at 90 °C for 16 h. After cooling to 22 °C, the resulting solids were filtered, washed with hexanes, and dried under vacuum overnight to give (salph-**Cl**)AlCl (0.19 g, 55%) as a yellow microcrystalline solid. **^{1}H NMR** (600 MHz, DMSO-d_6): δ 9.41 (s, 2H), 8.24-8.17 (m, 2H), 7.74 (d, *J* = 2.59 Hz, 2H), 7.58-7.52 (m, 2H), 7.36 (d, *J* = 2.59 Hz, 2H), 1.52 (s, 18H). **^{13}C NMR** (125 MHz, DMSO-d_6): δ 163.40, 161.01, 142.66, 137.16, 132.80, 132.39, 129.09, 120.41, 119.13, 117.11, 35.33, 29.25 **HRMS** (DART-MS): *m/z* calculated for $C_{28}H_{30}N_2O_3AlCl_2$ ($M-Cl^-+H_2O$) 539.14434, found 539.14680.

4.4 Synthesis of iron complex

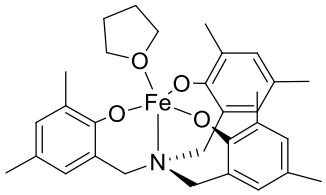

Fe (III) amino complex (2c) and the corresponding ligand were synthesized according to literature procedure.[5]

5. Synthesis of Tricylic Anhydrides

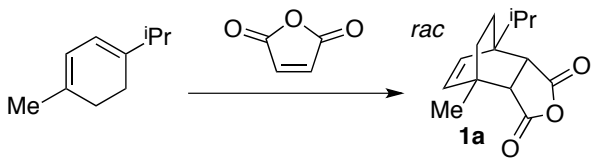

***rac-cis-endo*-1-isopropyl-4-methyl-bicyclo[2.2.2]oct-5-ene-2,3-dicarboxylic anhydride [1a]:** Synthesized according to literature procedure.[6]

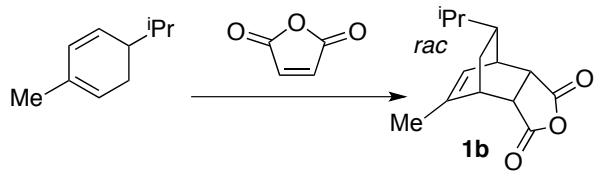

***rac-cis-endo*-7-Isopropyl-5-methyl-bicyclo[2.2.2]oct-5-ene-2,3-dicarboxylic anhydride [1b]:** Synthesized according to literature procedure.[6]

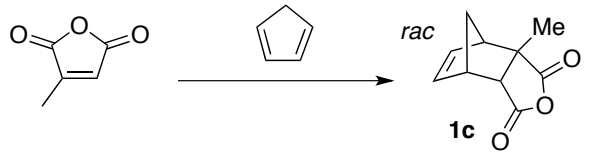

***rac-cis-endo*-2-methyl-bicyclo[2.2.1]hept-5-ene-2,3-dicarboxylic anhydride [1c]**: Synthesized according to literature procedure.[7]

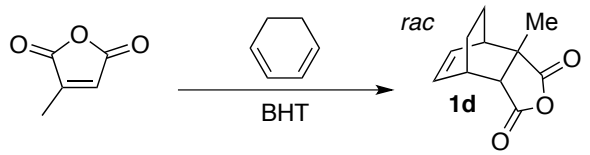

***rac-cis-endo*-2-methyl-bicyclo[2.2.2]hept-5-ene-2,3-dicarboxylic anhydride [1d]:** In a 20 mL vial equipped with a magnetic stir bar and sealed with a Teflon-lined cap, 1,3-cyclohexadiene (6.00 mL, 62.8 mmol), citraconic anhydride (6.20 mL g, 69.2 mmol) and 10 mg dibutylhydroxytoluene (BHT) were stirred at 60 °C for 48 hours. The yellow oil was purified by column chromatography with 70:30 hexanes: ethyl acetate then crystallized from 80:20 hexanes: ethyl acetate and dried under vacuum overnight to yield 4.7 g (39 %) of a white, crystalline solid**.** **^{1}H NMR** (500 MHz, $CDCl_3$): δ 6.42 (t, *J* = 7.3 Hz, 1H), 6.24 (t, *J* = 7.3 Hz, 1H), 3.16 (s,1H), 2.83 (s, 1H), 2.62 (d, *J* = 3.2 Hz, 1H), 1.84 (m, 1H), 1.55 (m, 1H), 1.45 (m, 1H), 1.26 (m, 1H) **^{13}C NMR** (125 MHz, $CDCl_3$): δ 176.76, 172.57, 135.82, 131.83, 52.29, 48.16, 36.73, 33.10, 22.70, 21.31, 19.01 **HRMS** (DART-MS): *m/z* calculated for $C_{11}H_{13}O_3$ (M+H) 193.0865, found 193.0850.

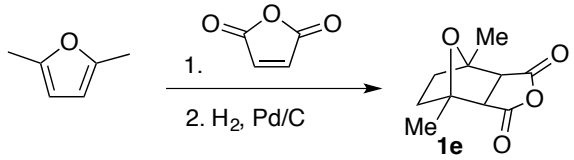

***cis-exo*-1,4-dimethyl-7-oxabicyclo[2.2.1]heptane-2,3-dicarboxylic anhydride [1e]:** Maleic anhydride (5.0 g, 51.0 mmol, 1.0 equiv.) and 2,5-dimethyl furan (8.3 mL, 76.5 mmol, 1.5 equiv.) were stirred at 22 °C for 16 h. The resulting off white solid was filtered and washed with hexanes. A portion of the crude product (4.0 g, 20.5 mmol, 1.0 equiv.) was dissolved in 20 mL THF in a Parr reactor and palladium on carbon (5%, reduced, dry powder, 2.0 g) was added. The reactor was pressurized with hydrogen gas to 600 psi and the heterogeneous mixture stirred at 22 °C for 60 h. The mixture was filtered and stripped, and the product purified by crystallization in 80:20 hexanes: ethyl acetate to yield 1.98 g (49 %) of a white crystalline solid) **^{1}H NMR** (500 MHz, $CDCl_3$): δ 3.14 (s, 2 H), 1.78 (m, 4 H), 1.63 (s, 6H) **^{13}C NMR** (125 MHz, $CDCl_3$): δ 170.13, 86.12, 54.41, 37.69, 17.96 **HRMS** (DART-MS): *m/z* calculated for $C_{10}H_{13}O_4$ (M+H) 197.0808 found 197.0808.

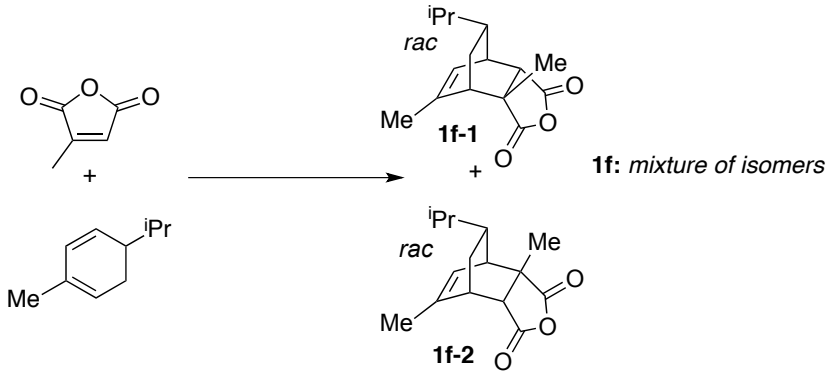

Mixture of *rac*-7-isopropyl-2,5-dimethylbicyclo[2.2.2]oct-5-ene-2,3-dicarboxylic anhydride and *rac*-8-isopropyl-2,6-dimethylbicyclo[2.2.2]oct-5-ene-2,3-dicarboxylic anhydride [1f]

Citraconic anhydride (4.13 mL, 44.6 mmol) and α-phellandrene (6.07 g, 44.6 mmol) were combined in a 20 mL vial equipped with a magnetic stir bar and sealed with a Teflon-lined cap and stirred at 60 °C for 4 days. The yellow oil was purified by column chromatography with 90:10 hexanes: ethyl acetate then dried under vacuum overnight to yield 4.6 g 40 (%) of a colorless oil which was found to be a 56:44 mixture of isomers **1f-1** and **1f-2** respectively. **^{1}H NMR** (600 MHz, $CDCl_3$): δ 5.88 (d, *J* = 6.39, 1H), 5.70 (d, *J* = 6.39 Hz, 1H), 3.13 (m, 1H), 2.90 (s, 1H), 2.81 (dd, *J* = 2.01, 6.31 Hz, 1H) 2.56 (m, 4H), 1.99 (m, 2H), 1.77 (m, 9H), 1.49 (m, 1H), 1.43 (m, 8H), 1.27 (m, 2H), 1.12 (m, 4H), 0.90 (m, 10H), 0.83 (m, 8H) **^{13}C NMR** (125 MHz,

$CDCl_3$): δ 177.05, 176.52, 172.90, 172.60, 144.94, 141.41, 125.25, 121.91, 53.76, 51.58, 49.57, 47.94, 44.30, 43.18, 40.22, 39.49, 39.29, 36.83, 33.30, 32.78, 30.00, 26.29, 21.17, 21.12, 21.10, 20.92, 20.70, 20.68, 20.57, 20.48 **HRMS** (DART-MS): *m/z* calculated for $C_{15}H_{21}O_3$ (M+H) 249.1485, found 249.1481.

6. Supplementary Polymerization Data

The initial screen with CHO used 1500 eq of CHO and no toluene, making these polymerizations analogous to those with PO (Table 1). However, we found that while reducing the amount of CHO from 1500 eq to 900 eq and replacing the volume with toluene led to slower polymerizations, we could obtain higher molecular weights and narrower $Đ$ in general. These optimized conditions are reported in Table 2. For comparison, representative polymerizations run under the initial conditions are shown in Table S1. We propose that the higher molecular weights and narrower dispersity when a smaller amount of CHO is used are due to a reduction in the number of new alcohols generated via the MPVO reaction as outlined in the manuscript.

Table S1. Copolymerization of **1a**, **1d,** and **1f** with 1500 eq cyclohexene oxide.[a]

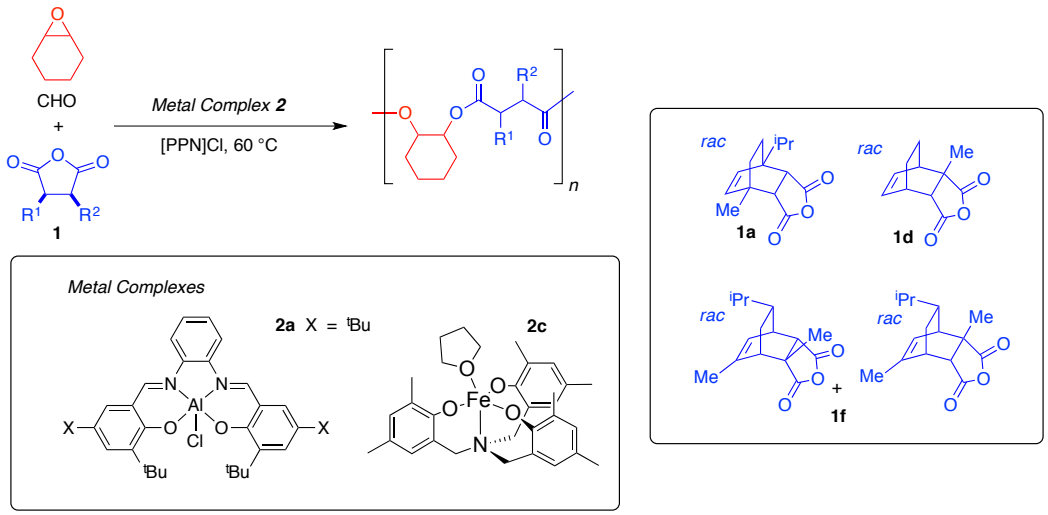

Entry	Anhyd.	Complex	t_{rxn} (h)	Conv. (%)[b]	M_n (kDa)[c]	$Đ$[c]
1	**1a**	**2a**	48	43	2.9	1.31
2	**1a**	**2c**	144	87	4.1	1.52
3	**1d**	**2a**	10	96	6.6	1.62
4	**1d**	**2c**	20	>99	7.6	1.57
5	**1f**	**2a**	10	91	6.1	1.36
6	**1f**	**2c**	15	>99	3.9	1.40

[a] [CHO]:[**1**]:[**2**]:[(PPN)Cl] = 1500:300:1:0.9 [b] Conversion of cyclic anhydride, determined by ^{1}H NMR spectroscopy. [c] Determined by GPC in THF, calibrated with polystyrene standards.

7. Stereochemistry of Polyester Diester Units

The stereochemistry of the polyester diester units was examined by degradation of the polyesters and comparison with model compounds.

7.1 Synthesis of *cis* and *trans* diol model compounds

Rac-cis-endo-1-Isopropyl-4-methyl-bicyclo[2.2.2]oct-5-ene-2,3-dicarbinol and *rac-trans*-1-Isopropyl-4-methyl-bicyclo[2.2.2]oct-5-ene-2,3-dicarbinol (mixture of diastereomers), the model compounds for **1a**, were synthesized according a literature procedure.[6] The other diols were synthesized according to the following procedures.

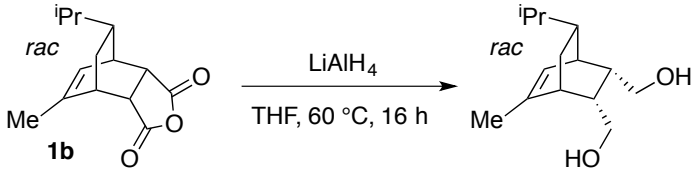

***Rac-cis-endo*-7-isopropyl-5-methylbicyclo[2.2.2]oct-5-ene-2,3-diyl)dimethanol**

Anhydride **1b** (200 mg, 0.85 mmol) and $LiAlH_4$ (324 mg, 8.54 mmol) were combined with 20 mL of dry THF in a 50-mL vial equipped with a magnetic stir bar and sealed with a Teflon-lined cap. The suspension was stirred at 60 °C for 16 h, then diluted with 20 mL of diethyl ether, cooled to 0 °C and then quenched with 0.30 mL of deionized water, 0.6 mL of 1M NaOH, and 0.6 mL of deionized water. After drying over $MgSO_4$, the mixture was filtered through a pad of Celite and the solvent was removed by rotary evaporation to yield 138 mg (72%) of a clear viscous oil. **^{1}H NMR** (400 MHz, $CDCl_3$): δ 5.59 (d, *J* = 6.67 Hz, 1H), 3.64 (m, 2H), 3.55 (m, 2H), 2.43 (m, 1H) 2.20 (m, 2H), 2.10 (m, 2H), 1.72 (m, 4H), 1.25 (m, 3H), 1.04 (m, 1H), 0.86 (m, 5 H), 0.77 (m, 3H) **^{13}C NMR** (125 MHz, $CDCl_3$): δ 141.73, 122.43, 65.54, 65.17, 46.83, 46.29, 44.69, 40.91, 37.88, 33.29, 32.67, 21.43, 21.36, 20.54 **HRMS** (DART-MS): *m/z* calculated for $C_{14}H_{25}O_2$ (M+H): 225.1855, found 225.1841.

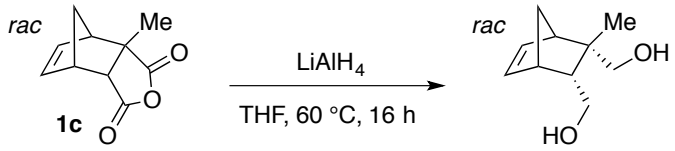

***Rac-cis-endo*-2-methylbicyclo[2.2.1]hept-5-ene-2,3-diyl)dimethanol**

Anhydride **1c** (250 mg, 1.40 mmol) and $LiAlH_4$ (531 mg, 14 mmol) were combined with 20 mL of dry THF in a 50-mL vial equipped with a magnetic stir bar and sealed with a Teflon-lined cap. The suspension was stirred at 60 °C for 16 h, then diluted with 20 mL of diethyl ether, cooled to 0 °C and then quenched with 0.30 mL of deionized water, 0.6 mL of 1M NaOH, and 0.6 mL of deionized water. After drying over $MgSO_4$, the mixture was filtered through a pad of Celite and the solvent was removed by rotary evaporation to yield 158 mg (67%) of a clear viscous oil.**^{1}H NMR** (400 MHz, $CDCl_3$): δ 6.06 (m, 1H), 5.97 (m, 1H), 4.67 (br s, 2H), 3.46 (m, 2H), 3.24 (m, 2H), 2.64 (s, 1H), 2.28 (s, 1H), 2.00 (m, 1H), 1.66 (d, J = 8.19 Hz, 1H), 1.32 (d, J = 8.19 Hz, 1H), 1.25 (s, 3H). **^{13}C NMR** (125 MHz, $CDCl_3$): δ 136.42, 133.91, 67.45, 64.33, 53.29, 52.70, 47.44,

46.78, 46.62, 29.90. **HRMS** (DART-MS): *m/z* calculated for $C_{10}H_{17}O_2$ (M+H): 169.1229, found 169.1218.

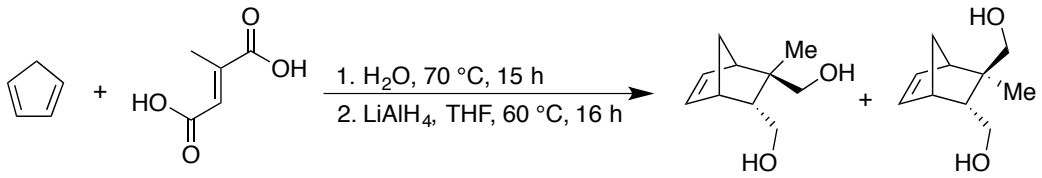

***Rac-trans* -2-methylbicyclo[2.2.1]hept-5-ene-2,3-diyl)dimethanol**

Mesaconic acid (1.00 g, 7.63 mmol) was disolved in 25 mL of water in a round bottom flask with a magnetic stir bar and a reflux condenser. Under stirring, freshly distilled cyclopentadiene (600 mg, 10.08 mmol) was added dropwise. Afterwards the mixture was refluxed at 70 °C for 15 h. The reaction mixture was extracted with ethyl acetate (3x15 mL) and the organic and aqueous layers separated. The organic layers were combined, dried over anhydrous $MgSO_4$ and the solvent was removed by rotary evaporation to yield a yellow viscous oil. A portion of the crude product (500 mg, 2.54 mmol) was dissolved in dry THF without further purification and placed in a 50 mL vial equipped with a magnetic stir bar. $LiAlH_4$ (967 mg, 25 mmol) was added and the vial was sealed with a Teflon-lined cap. The suspension was stirred at 60 °C for 16 h, then diluted with 20 mL of diethyl ether, cooled to 0 °C and then quenched with 0.30 mL of deionized water, 0.6 mL of 1M NaOH, and 0.6 mL of deionized water. After drying over $MgSO_4$, the mixture was filtered through a pad of Celite and the solvent was removed by rotary evaporation. The product was purified by column chromatography (silica gel, 60:40 hexanes:ethyl acetate) and then dried under vacuum to yield 346 mg (58%) of a clear viscous oil. **^{1}H NMR** (400 MHz, $CDCl_3$): δ 6.04 (d, 2H), 5.93 (d, 2H), 4.22 (br s, 4H), 3.45 (t, *J* = 8.74 Hz, 1H), 3.35 (m, 3H), 3.12 (m, 3H), 2.98 (d, *J* = 10.26 Hz, 1H) 2.69 (s, 1H), 2.49 (s, 1H), 2.33 (s, 1H), 2.27 (s,1H), 1.78 (s, 1H), 1.52 (d, *J* = 8.57 Hz, 1H), 1.43 (d, *J* = 8.57 Hz, 1H), 1.23 (t, *J* = 7.99 Hz, 2H), 1.06 (t, *J* = 8.20 Hz, 1H), 1.01 (s, 3H), 0.69 (s, 3H) **^{13}C NMR** (125 MHz, $CDCl_3$): δ 137.63, 137.02, 134.48, 133.88, 72.00, 71.06, 63.44, 62.75, 51.27, 49.88, 48.83, 47.38, 46.73, 45.85, 45.66, 45.21, 45.04, 44.86, 19.34, 17.00 **HRMS** (DART-MS): *m/z* calculated for $C_{10}H_{17}O_2$ (M+H): 169.1229, found 169.1218.

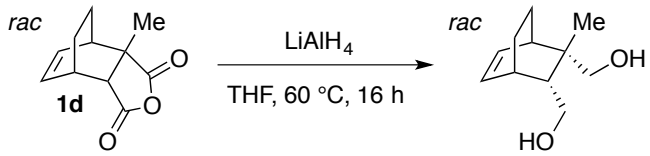

***rac*- 2-methylbicyclo[2.2.2]oct-5-ene-2,3-diyl)dimethanol:**

Anhydride **1d** (63 mg, 0.33 mmol) and $LiAlH_4$ (125 mg, 3.30 mmol) were combined with 10 mL dry THF in a 20-mL vial equipped with a magnetic stir bar and sealed with a Teflon-lined cap. The suspension was stirred at 60 °C for 16 h then diluted with 20 mL diethyl ether, cooled to 0 °C, then quenched with 0.15 mL deionized water, 0.3 mL1M NaOH, and 0.3 mL deionized water. After drying with $MgSO_4$, the mixture was filtered through a pad of Celite and the solvent removed by rotary evaporation to yield 39 mg (65%) of a clear viscous oil. **^{1}H NMR** (500 MHz, $CDCl_3$): δ 6.24 (t, *J* = 7.3 Hz, 1H), 6.08 (t, *J* = 7.3 Hz, 1H), 3.77 (d, *J* = 12.0 Hz, 1H), 3.54 (m, 2H), 3.24 (d, *J* = 12.0 Hz, 1H), 2.76 (br s, 1H), 2.38 (s, 1H), 1.91 (m,1H), 1.65 (ddd, *J* = 1.5, 4.2, 10.2 Hz, 1H), 1.54 (m, 1H), 1.25 (m, 1H), 1.21 (s, 3H), 1.04 (m,1H) **^{13}C NMR** (125 MHz, $CDCl_3$): δ 135.00, 130.87, 69.36, 66.59, 53.04, 43.96, 40.73, 35.44, 25.86, 25.28, 20.54 **HRMS** (DART-MS): *m/z* calculated for $C_{11}H_{19}O_2$ (M+H): 183.1380, found 183.1379.

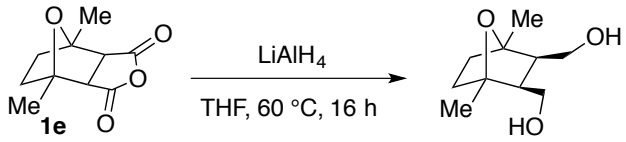

***cis-endo*-1,4-dimethyl-7-oxabicyclo[2.2.1]heptane-2,3-diyl)dimethanol**

Anhydride **1e** (196 mg, 1.00 mmol) and $LiAlH_4$ (379 mg, 10 mmol) were combined with 20 mL of dry THF in a 50-mL vial equipped with a magnetic stir bar and sealed with a Teflon-lined cap. The suspension was stirred at 60 °C for 16 h, then diluted with 20 mL of diethyl ether, cooled to 0 °C and then quenched with 0.30 mL of deionized water, 0.6 mL of 1M NaOH, and 0.6 mL of deionized water. After drying over $MgSO_4$, the mixture was filtered through a pad of Celite and the solvent was removed by rotary evaporation to yield 117 mg (63%) of a clear viscous oil. **^{1}H NMR** (400 MHz, $CDCl_3$): δ 3.82 (m, 4H), 3.39 (br s, 2H), 2.25 (m, 2H), 1.66 (m, 6H), 1.41 (s, 6H) **^{13}C NMR** (125 MHz, $CDCl_3$): δ 84.56, 60.97, 51.56, 39.85, 18.37 **HRMS** (DART-MS): *m/z* calculated for $C_{10}H_{19}O_3$ (M+H): 187.1334, found 187.1323.

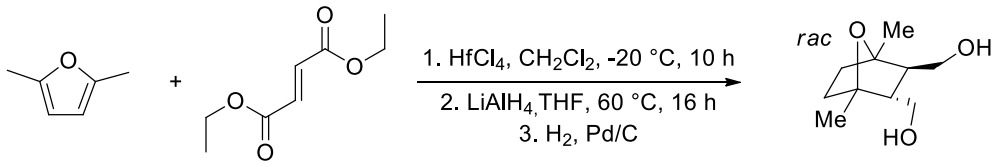

***Rac-trans*-1,4-dimethyl-7-oxabicyclo[2.2.1]heptane-2,3-diyl)dimethanol**

Diethylfumarate (220 mg, 1.28 mmol) and freshly distilled dimethylfuran (2.46 g, 25.6 mmol) were added successively at -20 °C to a suspension of $HfCl_4$ (450 mg, 1.41 mmol) in CH_2Cl_2 (1 mL) and stirred for 10 h at -20 ºC. Then, the reaction mixture was allowed to reach room temperature and aqueous $NaHCO_3$ (10 mL) was added. After filtration of the insoluble materials, the crude was extracted with $CHCl_3$ (3x15 mL) and the combined organic layers were dried over anhydrous $MgSO_4$, filtered and concentrated under high vacuum to obtain a yellow oil. A portion of the crude product (166 mg, 0.61 mmol) was dissolved in dry THF without further purification and placed in a 50 mL vial equipped with a magnetic stir bar. $LiAlH_4$ (234 mg, 6.1 mmol) was added and the vial was sealed with a Teflon-lined cap. The suspension was stirred at 60 °C for 16 h, then diluted with 20 mL of diethyl ether, cooled to 0 °C and then quenched with 0.30 mL of deionized water, 0.6 mL of 1M NaOH, and 0.6 mL of deionized water. After drying over $MgSO_4$, the mixture was filtered through a pad of Celite and the solvent was removed by rotary evaporation to obtain a yellow oil. Without further purification, a portion of this oil (75 mg , 0.40 mmol) was dissolved in 15 mL of THF in a Parr reactor and palladium on carbon (5%, reduced, dry powder, 2.0 g) was added. The reactor was pressurized with hydrogen gas to 600 psi and the heterogeneous mixture was stirred at 22 °C for 24 h. The mixture was filtered,stripped and the residue was purified by column chromatography (silica gel, 60:40 hexanes:ethyl acetate) and dried under vacuum to yield 71 mg (28%) of a clear viscous oil.**^{1}H NMR** (400 MHz, $CDCl_3$): δ 3.77 (dd, *J* = 4.60, 9.39 Hz, 1H) 3.70 (dd, *J* = 4.60, 9.39 Hz, 1H) , 3.04 (br s, 2H), 1.85 (m, 1H), 1.72 (m, 2H), 1.63 (m, 3H), 1.52 (m, 3H), 1.45 (s, 3H), 1.34 (s, 3H) **^{13}C NMR** (125 MHz, $CDCl_3$): δ 84.51, 84.36, 64.02, 63.68, 57.25, 54.88, 39.75, 32.70, 20.83, 18.11 **HRMS** (DART-MS): *m/z* calculated for $C_{10}H_{19}O_3$ (M+H): 187.1334, found 187.1324.

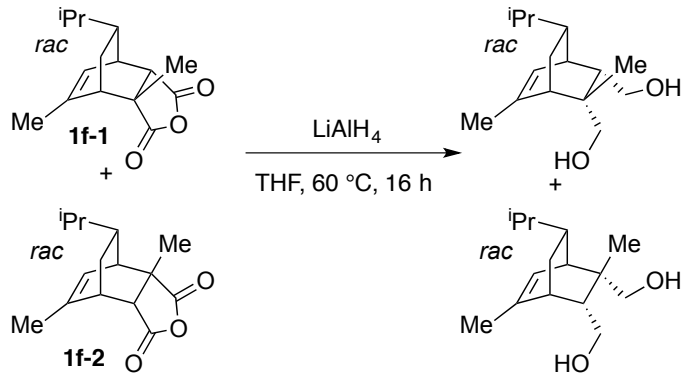

1f*: mixture of isomers*

Mixture of *rac*-7-isopropyl-2,5-dimethylbicyclo[2.2.2]oct-5-ene-2,3-diyl)dimethanol and *rac*-8-isopropyl-2,6-dimethylbicyclo[2.2.2]oct-5-ene-2,3-diyl)dimethanol:

Mixture of anhydrides **1f** (82 mg, 0.33 mmol) and $LiAlH_4$ (125 mg, 3.30 mmol) were combined with 10 mL dry THF in a 20-mL vial equipped with a magnetic stir bar and sealed with a Teflon-lined cap. The suspension was stirred at 60 °C for 16 h then diluted with 20 mL diethyl ether, cooled to 0 °C then quenched with 0.15 mL deionized water, 0.3 mL1M NaOH, and 0.3 mL deionized water. After drying with $MgSO_4$, the mixture was filtered through a pad of Celite and the solvent removed by rotary evaporation to yield 61 mg (77%) of a clear viscous oil. **^{1}H NMR** (500 MHz, $CDCl_3$): δ, 5.65 (d, *J* = 6.95 Hz, 1H), 5.49 (d, *J* = 6.95 Hz, 1H), 4.27 (br s, 4H), 3.76 (m, 1H), 3.65(m, 2H), 3.47 (m, 5H), 3.15 (dd, *J* = 4.1, 11.05 Hz, 3H), 2.30 (m, 1H), 2.07 (s, 1H), 2.01 (m, 1H), 1.71 (m, 11H), 1.58 (m, 2H), 1.51 (m, 1H), 1.24 (m, 2H), 1.15 (m, 8H), 1.00(m, 3H), 0.92–0.79 (m, 10H), 0.76 (dd, *J* = 2.84, 6.65 Hz, 8H), 0.66 (m, 1H) **^{13}C NMR** (125 MHz, $CDCl_3$): δ 143.01, 139.57, 124.23, 120.75, 69.40, 69.06, 66.63, 66.12, 53.30, 51.93, 47.23, 46.65, 44.17, 43.97, 43.11, 41.71, 40.34, 38.66, 33.47, 33.04, 32.68, 27.96, 25.64, 25.49, 21.54, 21.40, 21.30, 21.09, 20.69, 20.48 **HRMS** (DART-MS): *m/z* calculated for $C_{15}H_{27}O_2$ (M+H): 239.2006 found: 239.2005.

7.2 Degradation of polyesters

Polyesters were degraded to the corresponding diols with lithium aluminum according to a previously published procedure.[6] The degraded samples were then analyzed by ^{1}H NMR spectroscopy and the resulting spectra compared to the spectra of the appropriate *cis* and *trans* diols to determine the percent *cis* linkages in the polymer. For some of the polymers, because it was immediately apparent after degradation that there were no signals that could correspond to

the *trans* diols, and the *trans* diols were significantly harder to synthesize, the degraded polymers were compared only to the *cis* diol.

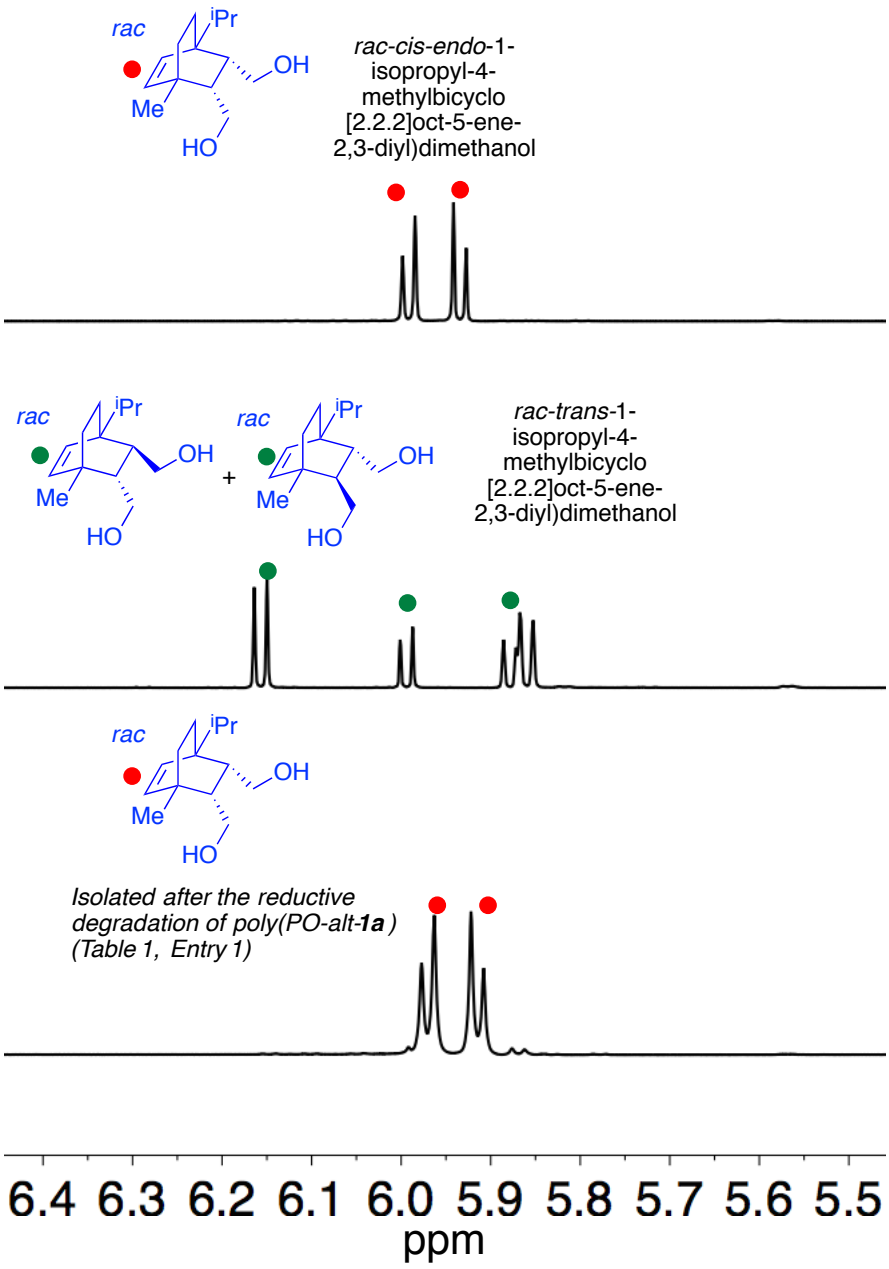

Figure S1. Comparison of vinylic region of ^{1}H NMR spectrum of degraded poly(PO-*alt*-**1a**) (Table 1, Entry 1) and corresponding *cis* and *trans* diols.

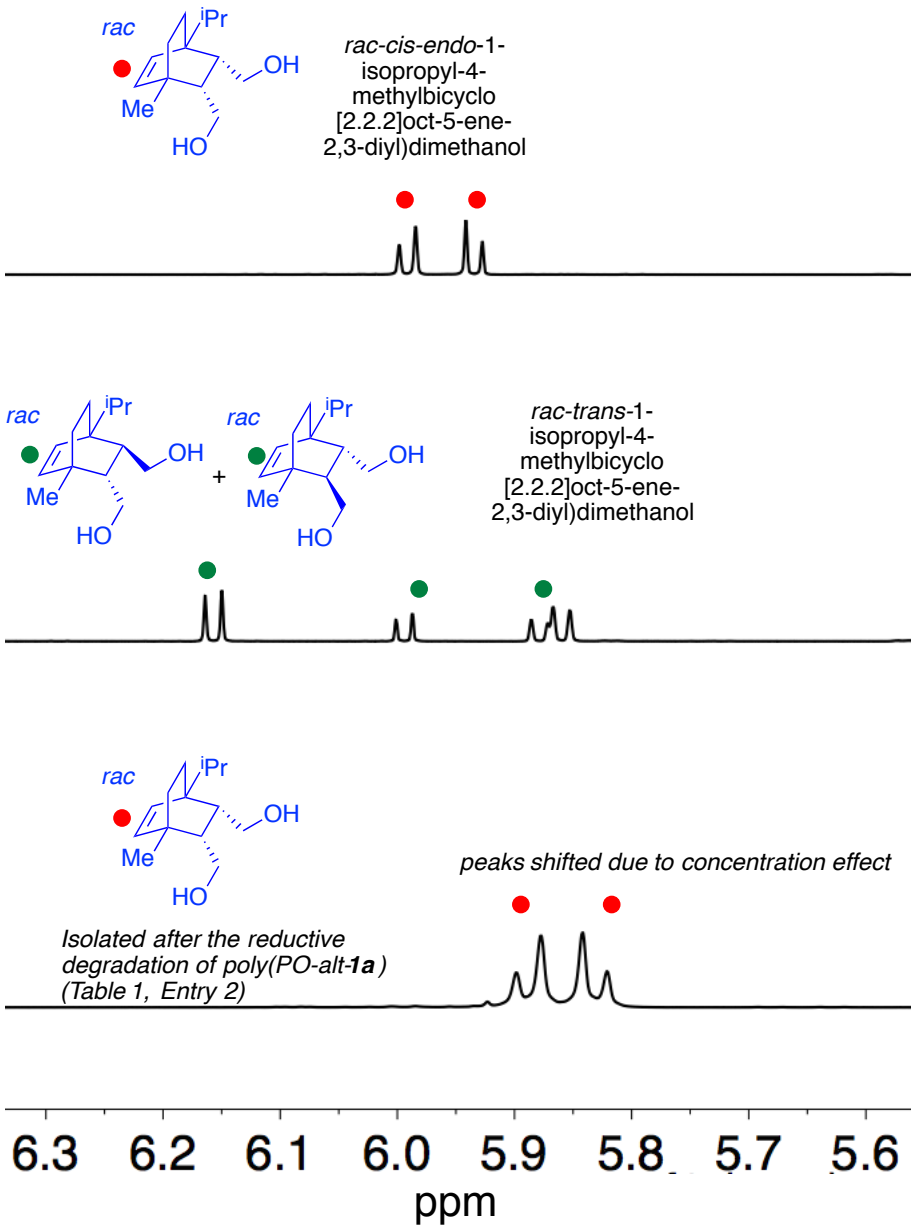

Figure S2. Comparison of vinylic region of ^{1}H NMR spectrum of degraded poly(PO-*alt*-**1a**) (Table 1, Entry 2) and corresponding *cis* and *trans* diols.

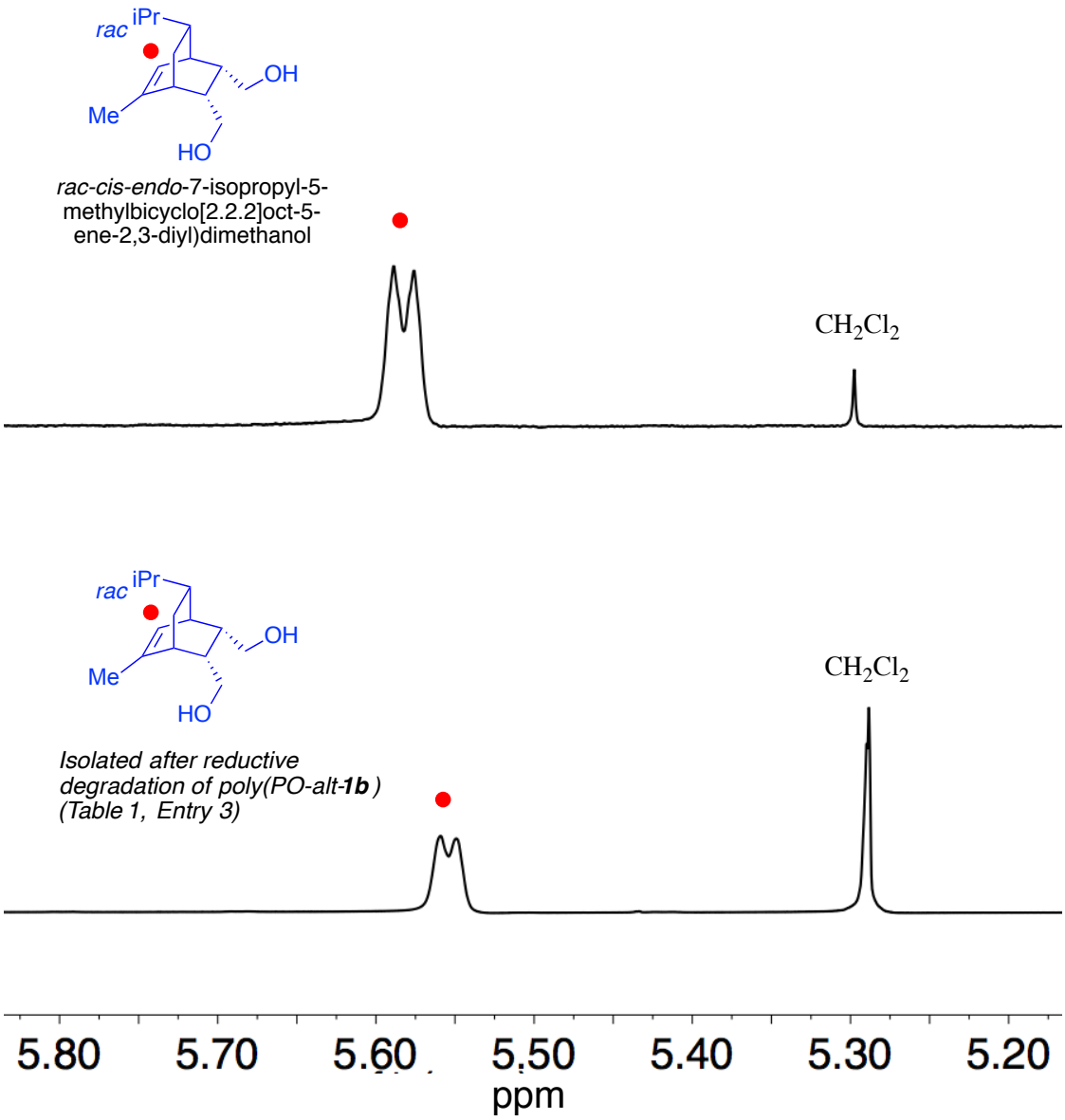

Figure S3. Comparison of vinylic region of ^{1}H NMR spectrum of degraded poly(PO-*alt*-**1b**) (Table 1, Entry 3) and corresponding *cis* diol.

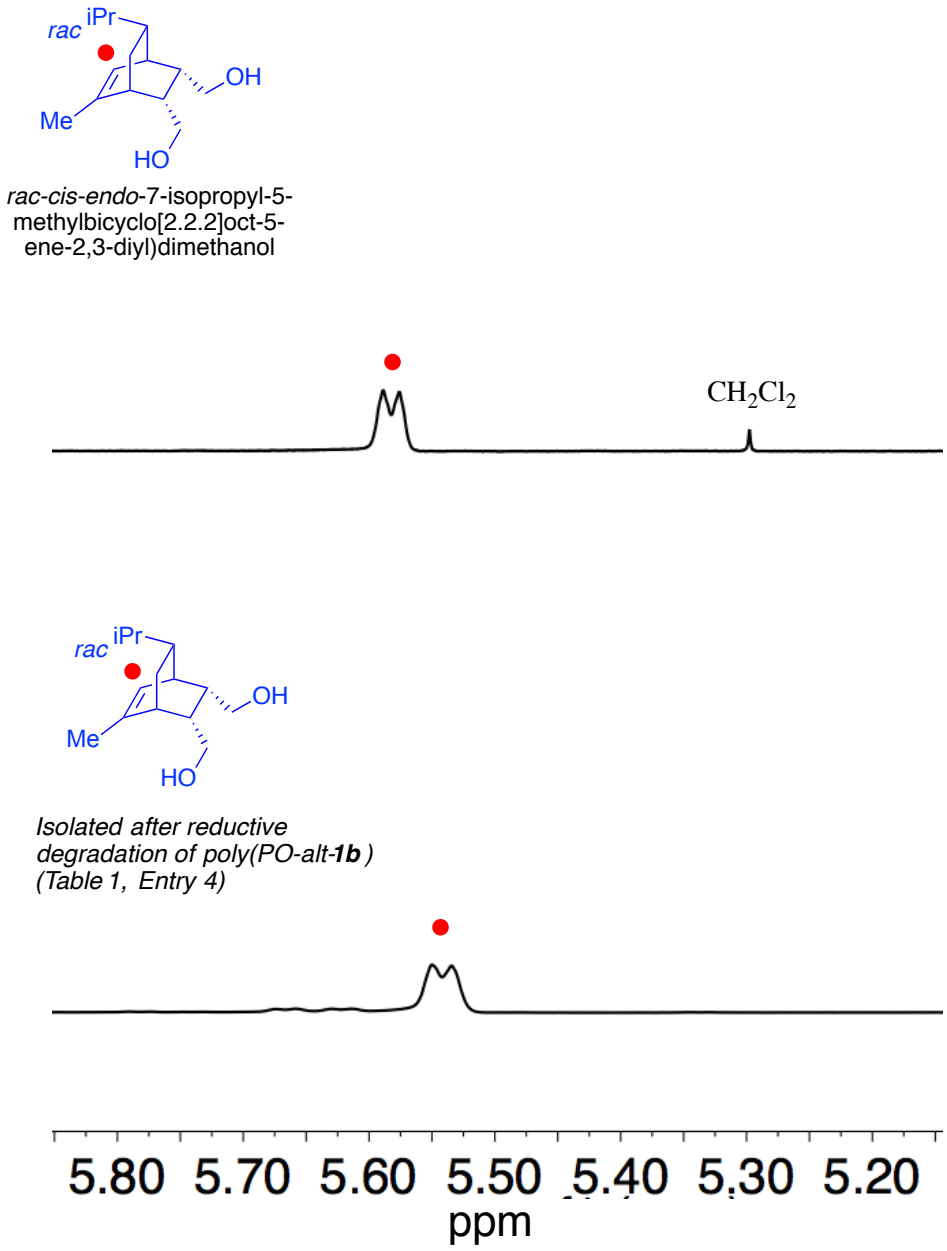

Figure S4. Comparison of vinylic region of ^{1}H NMR spectrum of degraded poly(PO-*alt*-**1b**) (Table 1, Entry 4) and corresponding *cis* diol.

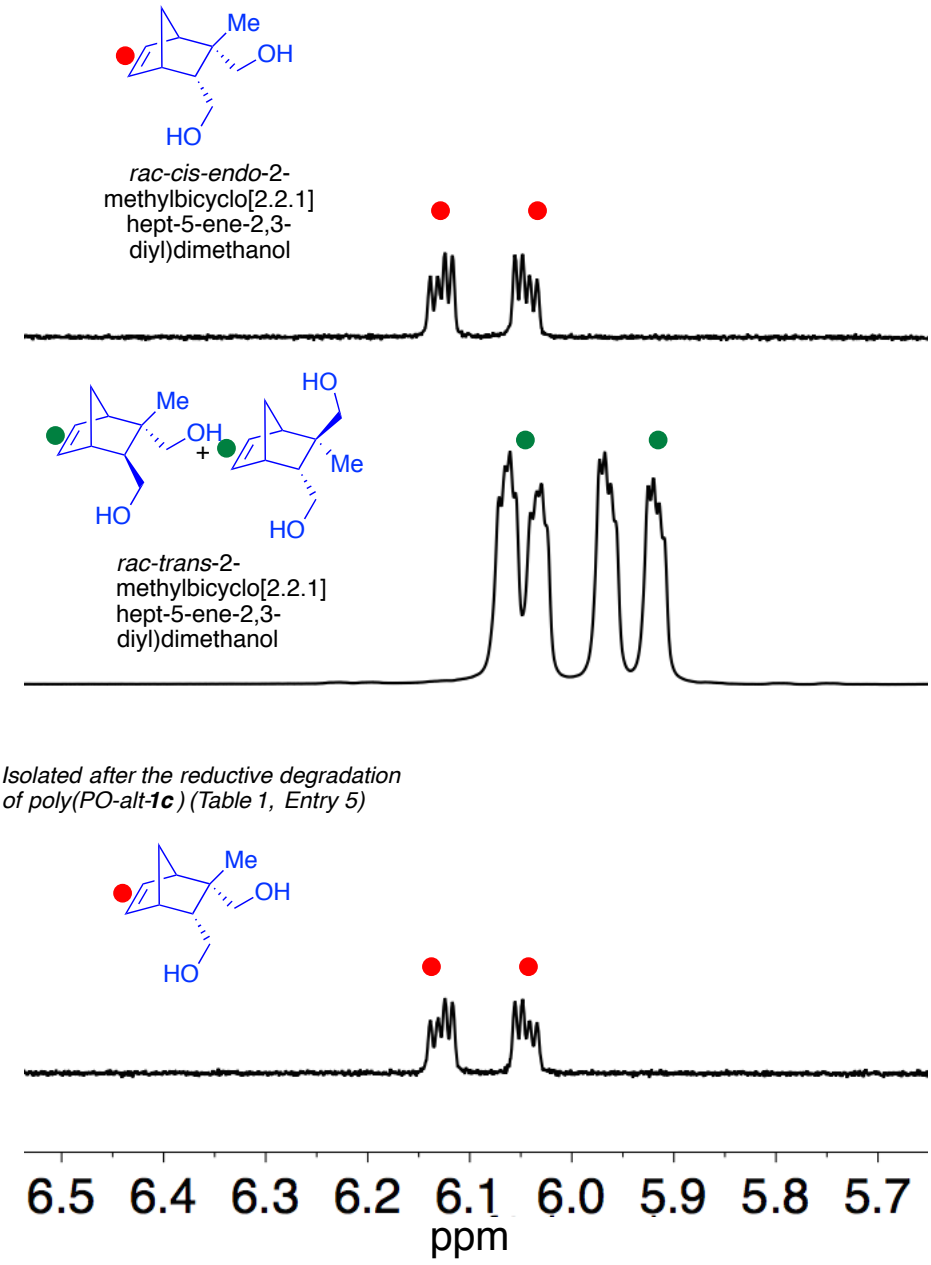

Figure S5. Comparison of vinylic region of ^{1}H NMR spectrum of degraded poly(PO-*alt*-**1c**) (Table 1, Entry 5) and corresponding *cis* and *trans* diols.

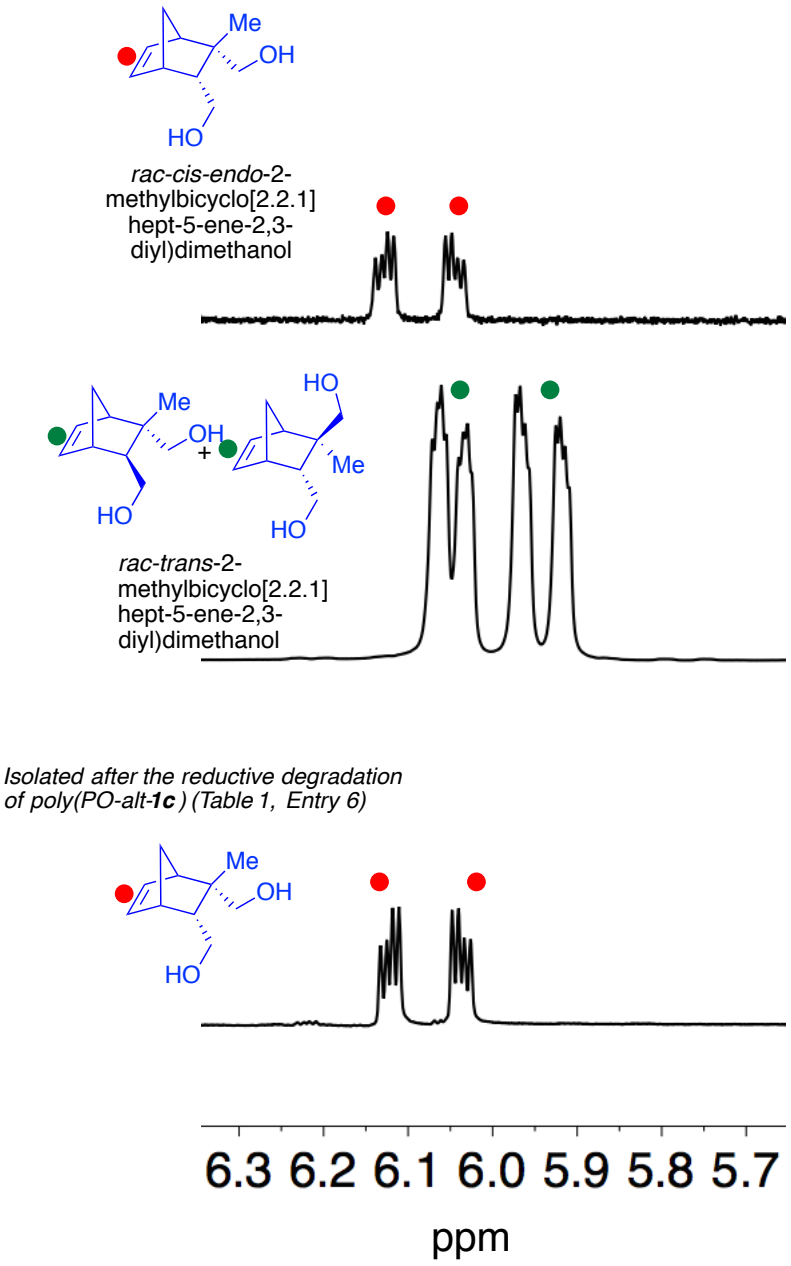

Figure S6. Comparison of vinylic region of ^{1}H NMR spectrum of degraded poly(PO-*alt*-**1c**) (Table 1, Entry 6) and corresponding *cis* and *trans* diols.

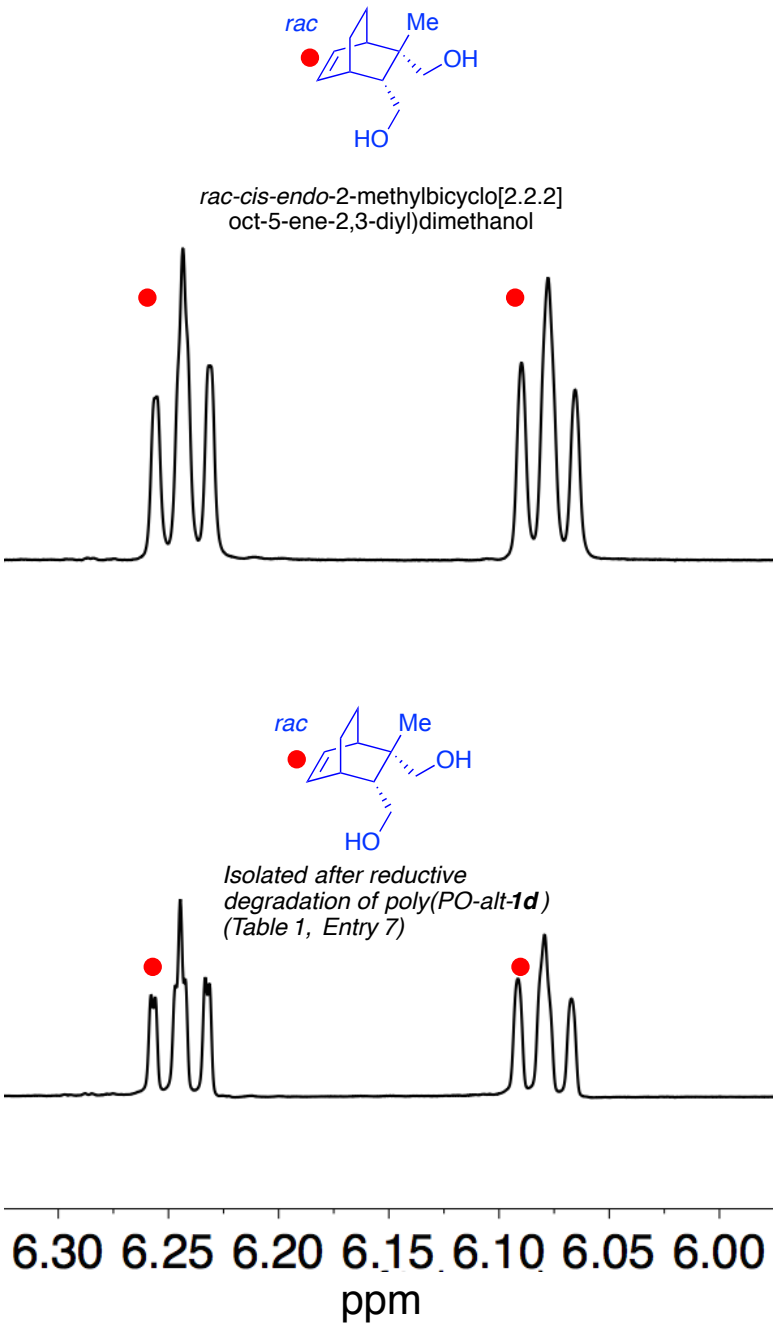

Figure S7. Comparison of vinylic region of ^{1}H NMR spectrum of degraded poly(PO-*alt*-**1d**) (Table 1, Entry 7) and corresponding *cis* diol.

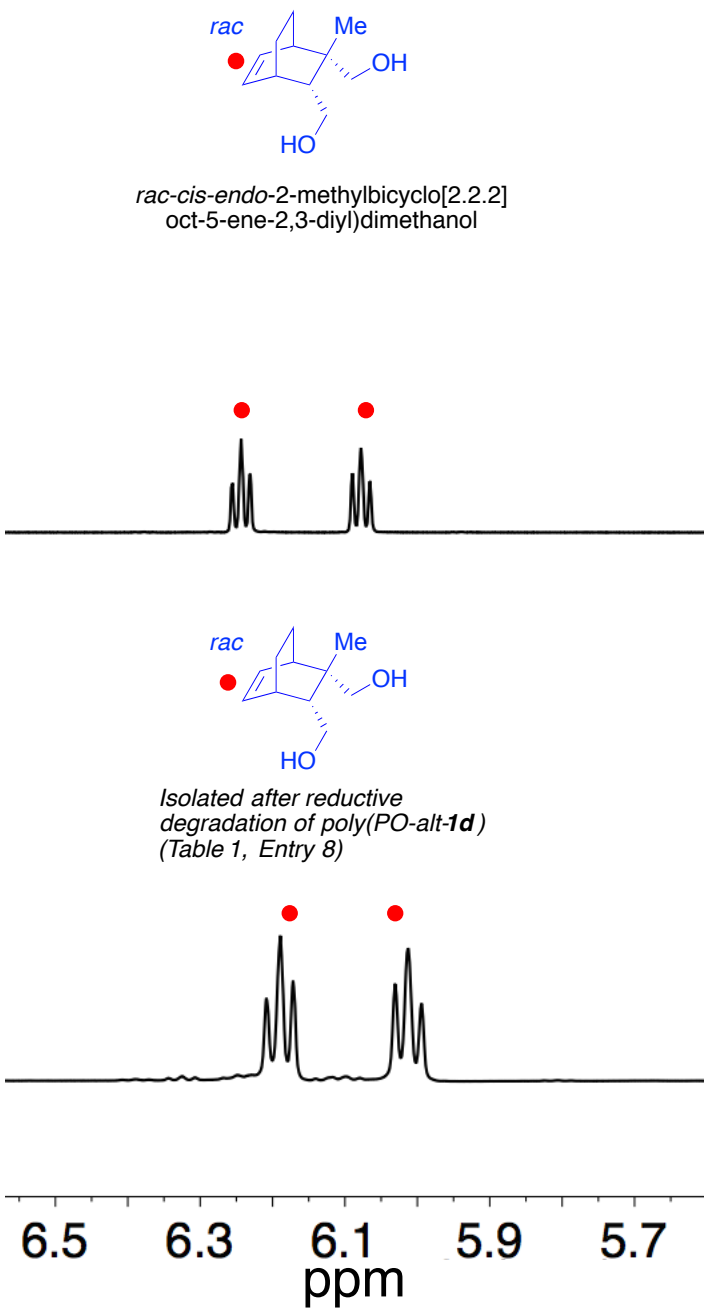

Figure S8. Comparison of vinylic region of ^{1}H NMR spectrum of degraded poly(PO-*alt*-**1d**) (Table 1, Entry 8) and corresponding *cis* diol.

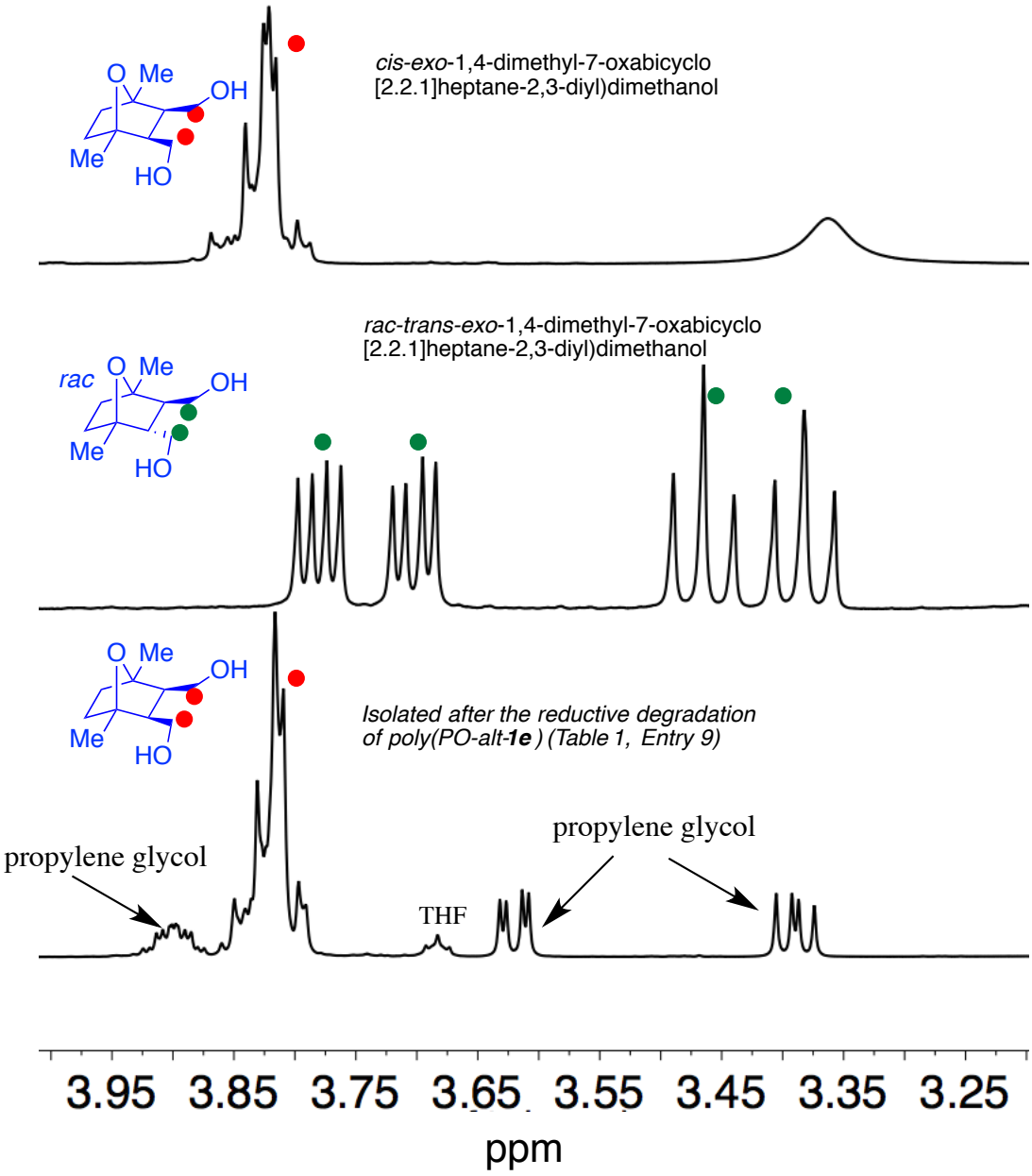

Figure S9. Comparison of diagnostic region of ^{1}H NMR spectrum of degraded poly(PO-*alt*-**1e**) (Table 1, Entry 9) and corresponding *cis* and *trans* diols.

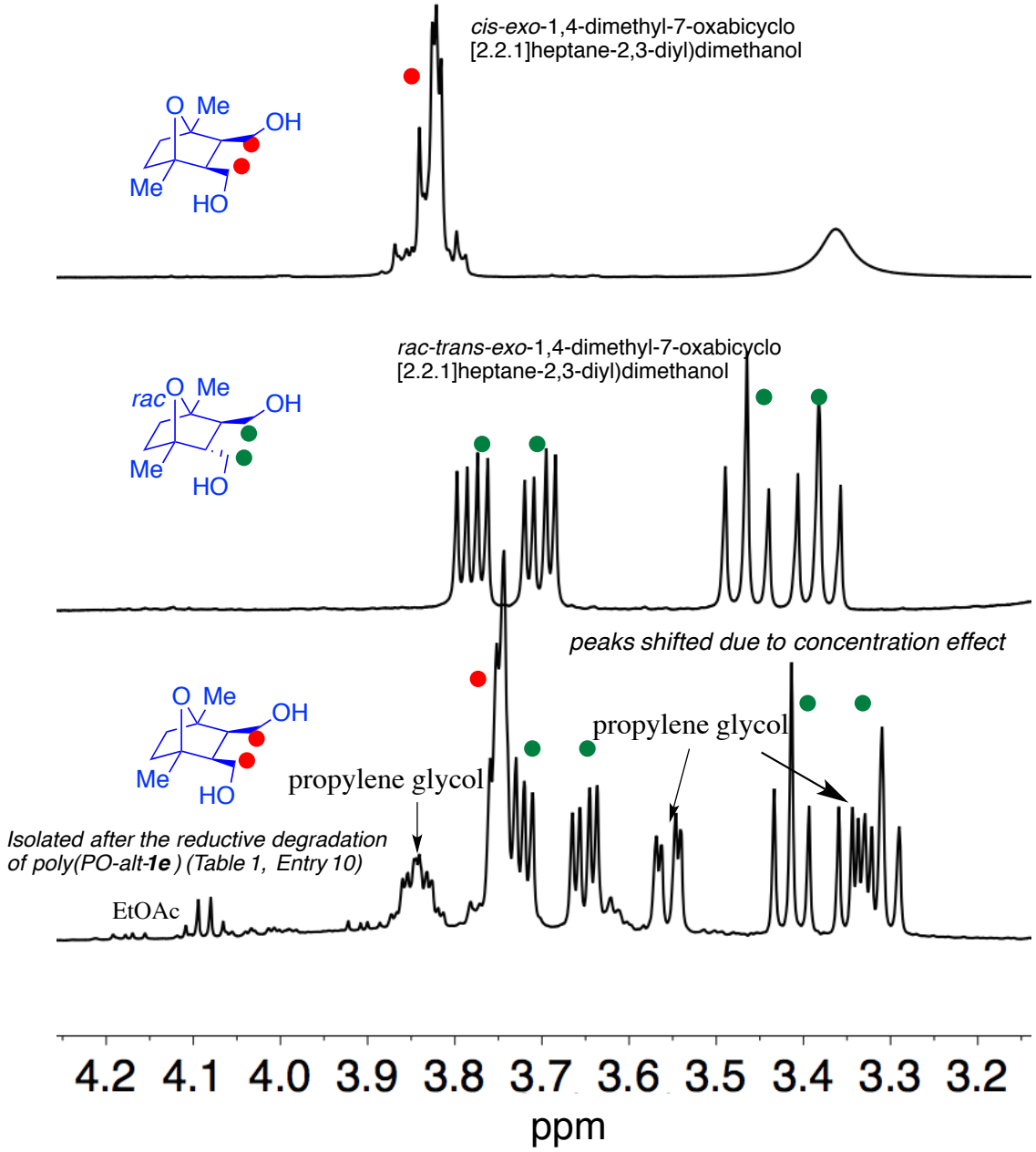

Figure S10. Comparison of diagnostic region of ^{1}H NMR spectrum of degraded poly(PO-*alt*-**1e**) (Table 1, Entry 10) and corresponding *cis* and *trans* diols.

Mixture of *rac-cis*-7-isopropyl-2,5-dimethylbicyclo[2.2.2]oct-5-ene-2,3-diyl)dimethanol and *rac-cis*-8-isopropyl-2,6-dimethylbicyclo[2.2.2]oct-5-ene-2,3-diyl)dimethanol

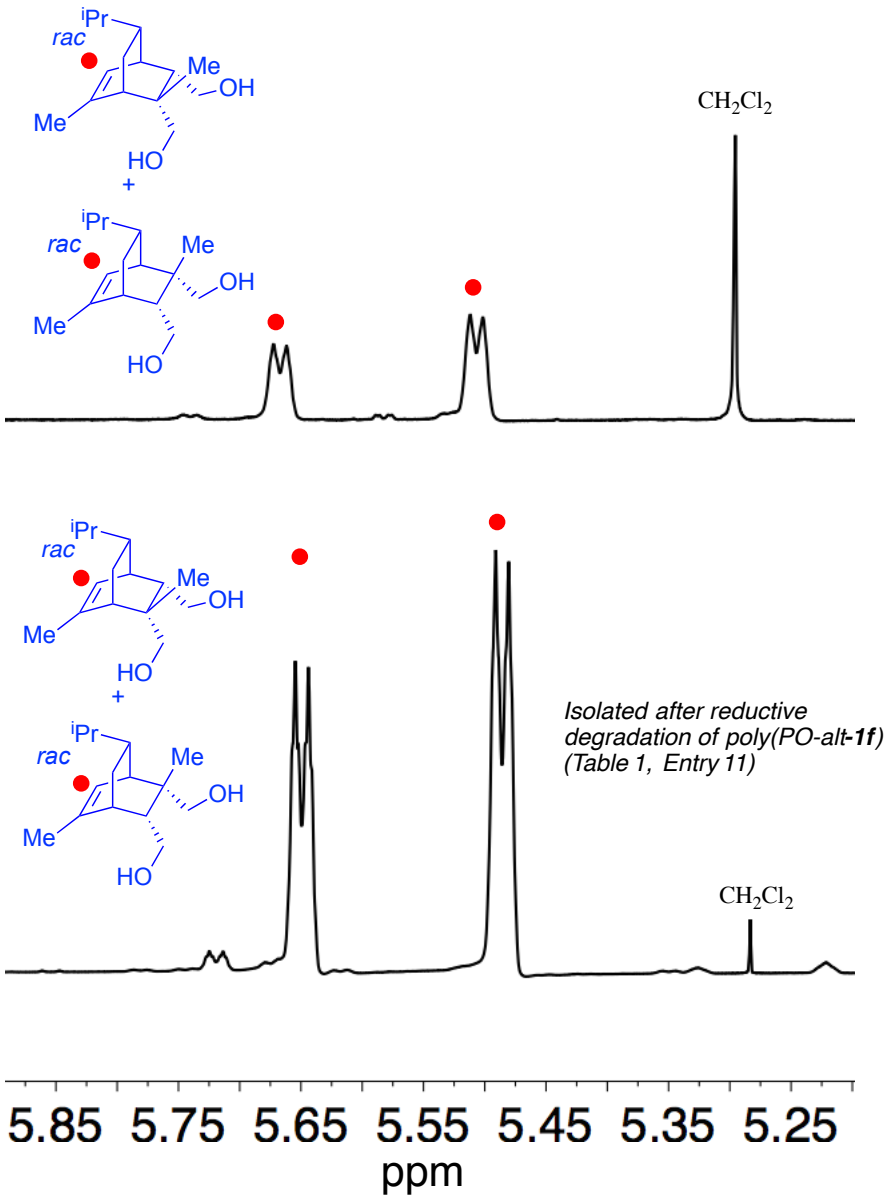

Figure S11. Comparison of vinylic region of ^{1}H NMR spectrum of degraded poly(PO-*alt*-**1f**) (Table 1, Entry 11) and corresponding *cis* diols.

Mixture of *rac-cis*-7-isopropyl-2,5-dimethylbicyclo[2.2.2]oct-5-ene-2,3-diyl)dimethanol and *rac-cis*-8-isopropyl-2,6-dimethylbicyclo[2.2.2]oct-5-ene-2,3-diyl)dimethanol

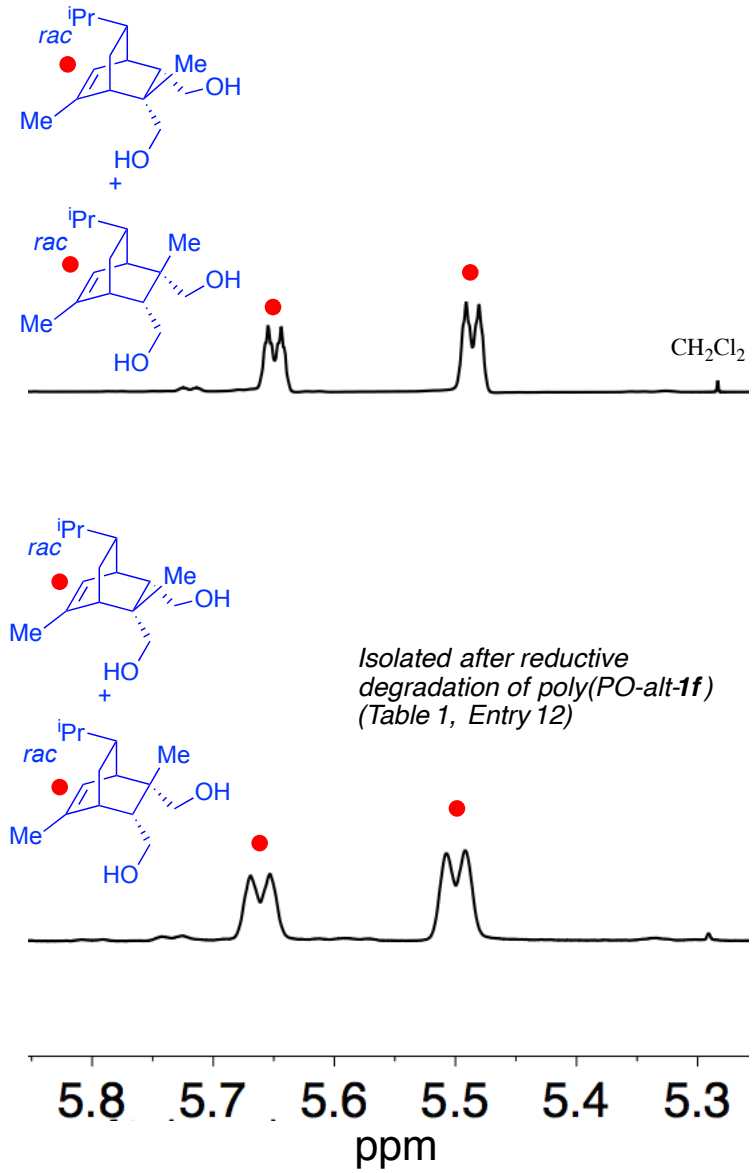

Figure S12. Comparison of vinylic region of ^{1}H NMR spectrum of degraded poly(PO-*alt*-**1f**) (Table 1, Entry 12) and corresponding *cis* diols.

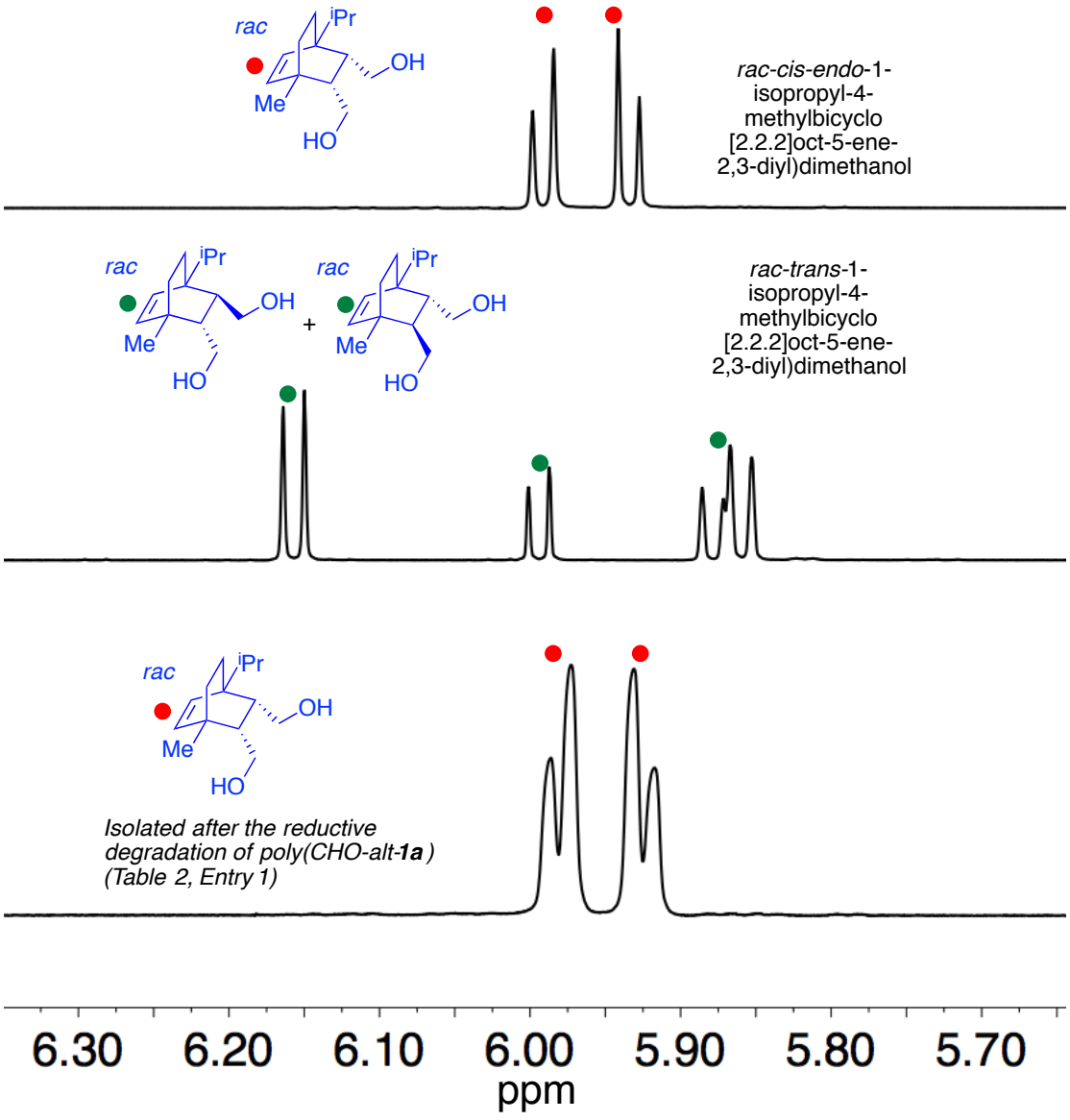

Figure S13. Comparison of vinylic region of ^{1}H NMR spectrum of degraded poly(CHO-*alt*-**1a**) (Table 2, Entry 1) and corresponding *cis* and *trans* diols.

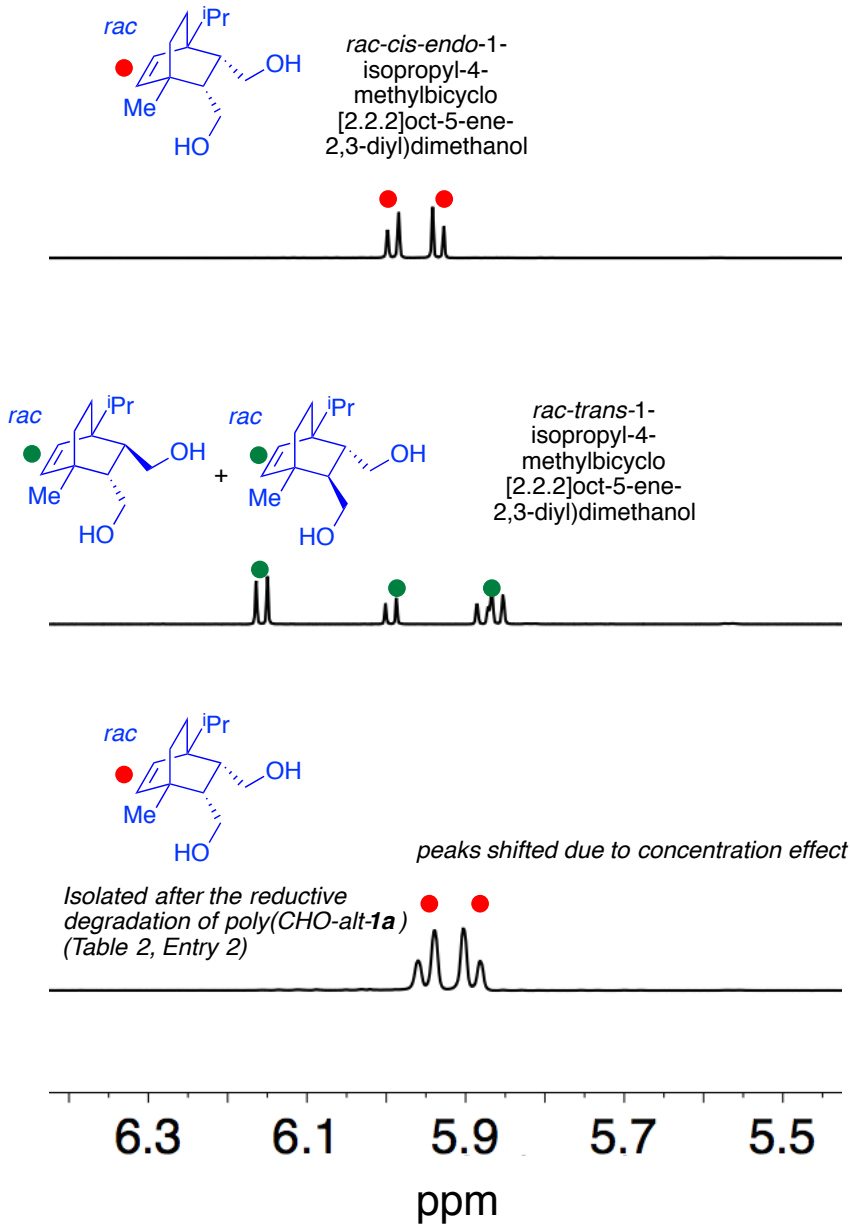

Figure S14. Comparison of vinylic region of ^{1}H NMR spectrum of degraded poly(CHO-*alt*-**1a**) (Table 2, Entry 2) and corresponding *cis* and *trans* diols.

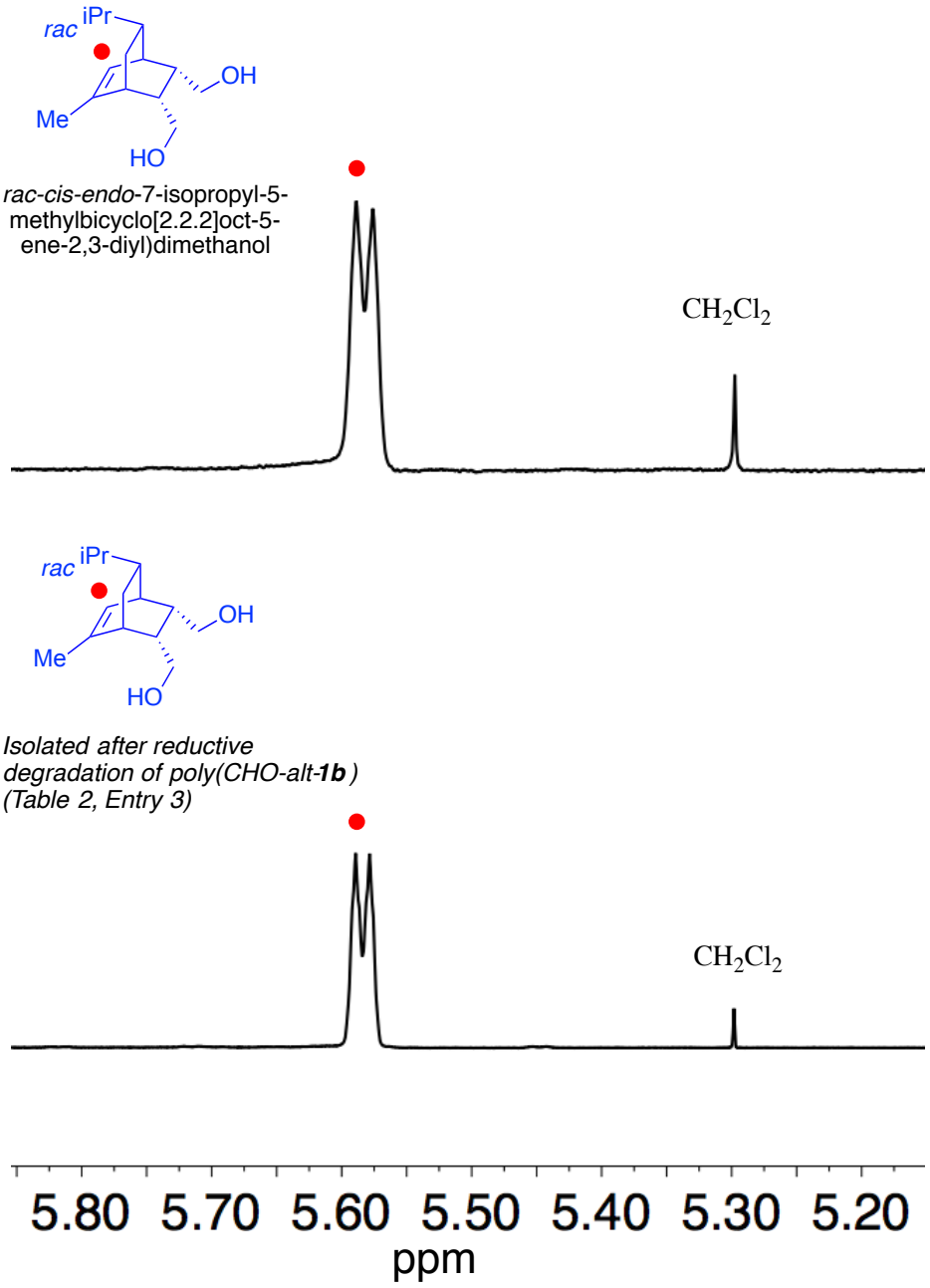

Figure S15. Comparison of vinylic region of ^{1}H NMR spectrum of degraded poly(CHO-*alt*-**1b**) (Table 2, Entry 3) and corresponding *cis* diol.

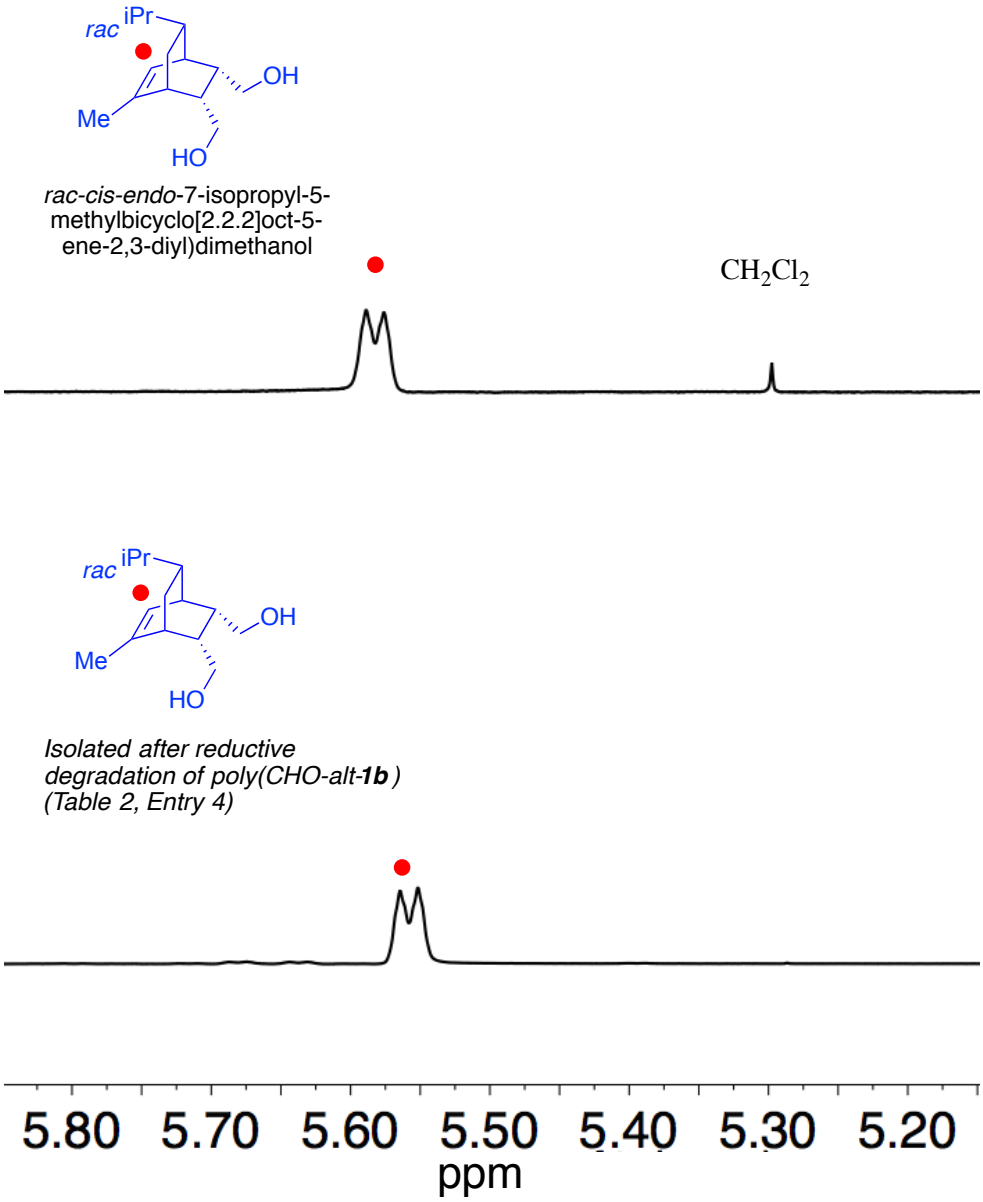

Figure S16. Comparison of vinylic region of ^{1}H NMR spectrum of degraded poly(CHO-*alt*-**1b**) (Table 2, Entry 4) and corresponding *cis* diol.

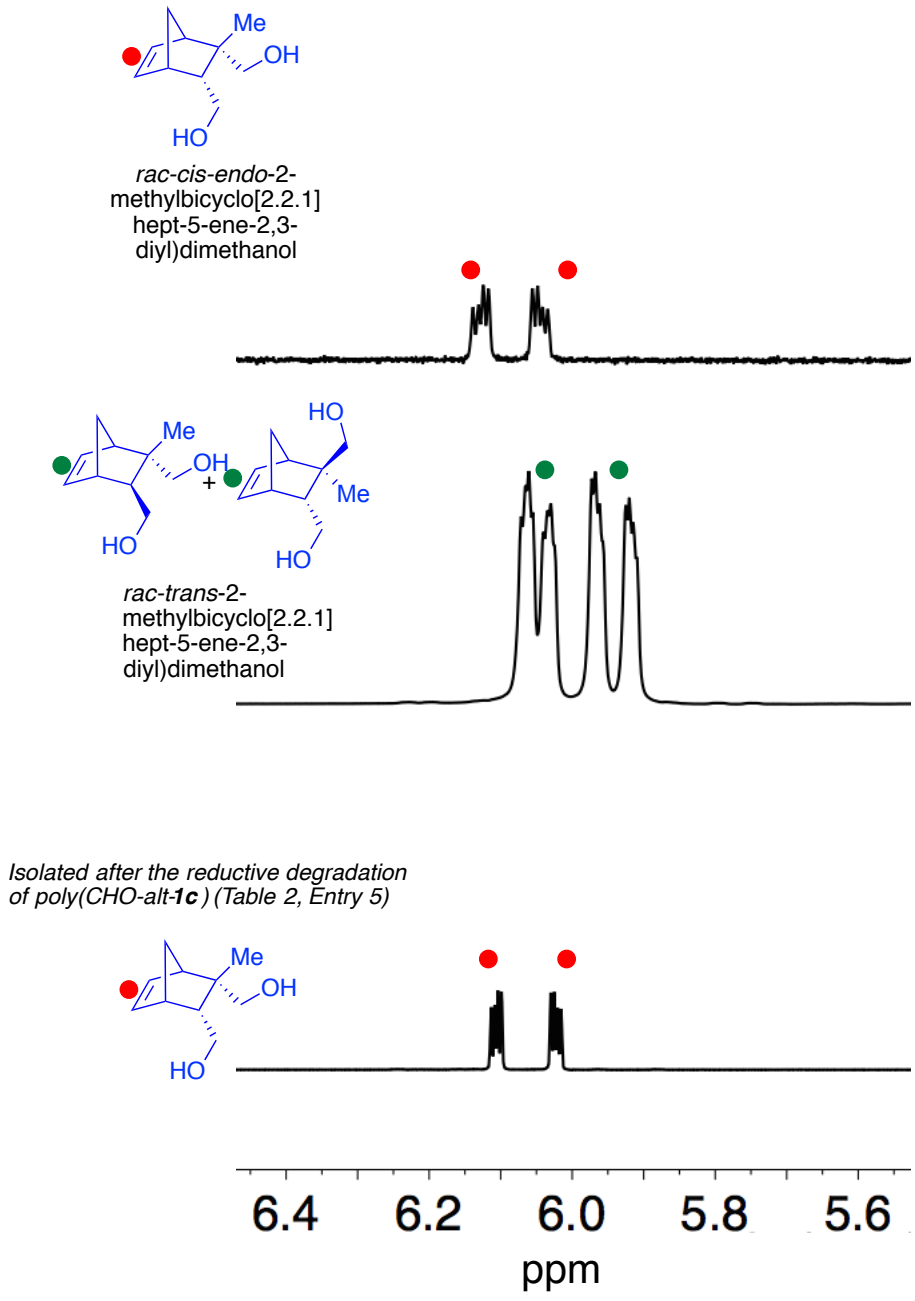

Figure S17. Comparison of vinylic region of ^{1}H NMR spectrum of degraded poly(CHO-*alt*-**1c**) (Table 2, Entry 5) and corresponding *cis* and *trans* diols.

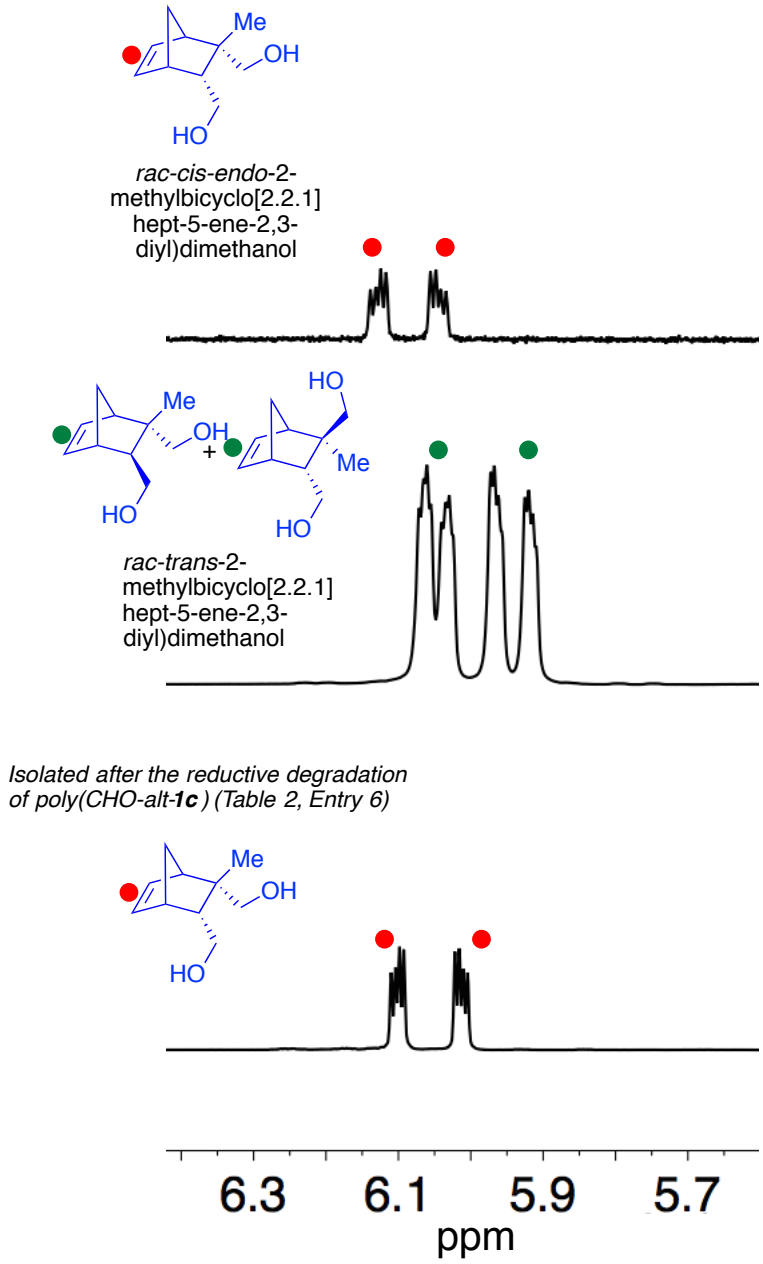

Figure S18. Comparison of vinylic region of ^{1}H NMR spectrum of degraded poly(CHO-*alt*-**1c**) (Table 2, Entry 6) and corresponding *cis* and *trans* diols.

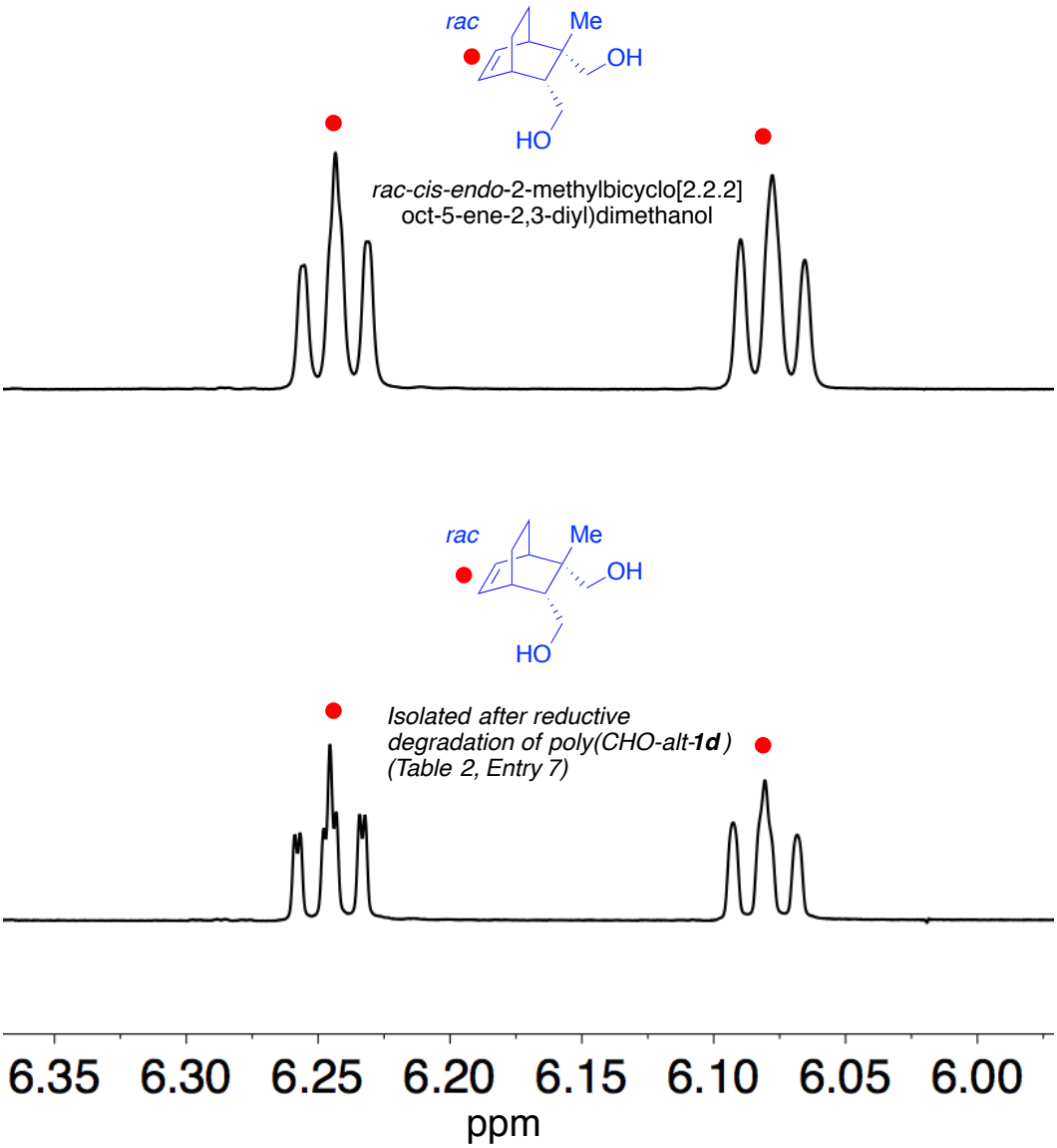

Figure S19. Comparison of vinylic region of ^{1}H NMR spectrum of degraded poly(CHO-*alt*-**1d**) (Table 2, Entry 7) and corresponding *cis* diols.

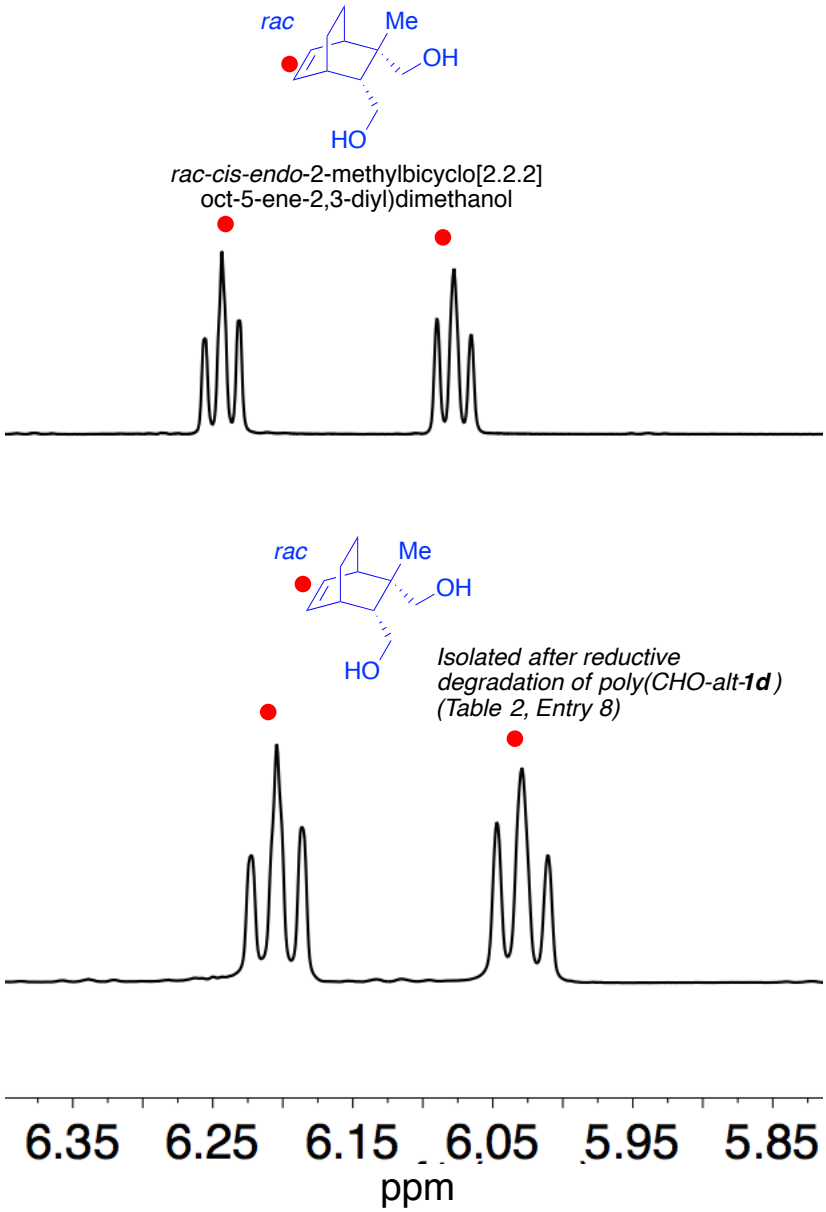

Figure S20. Comparison of vinylic region of ^{1}H NMR spectrum of degraded poly(CHO-*alt*-**1d**) (Table 2, Entry 8) and corresponding *cis* diols.

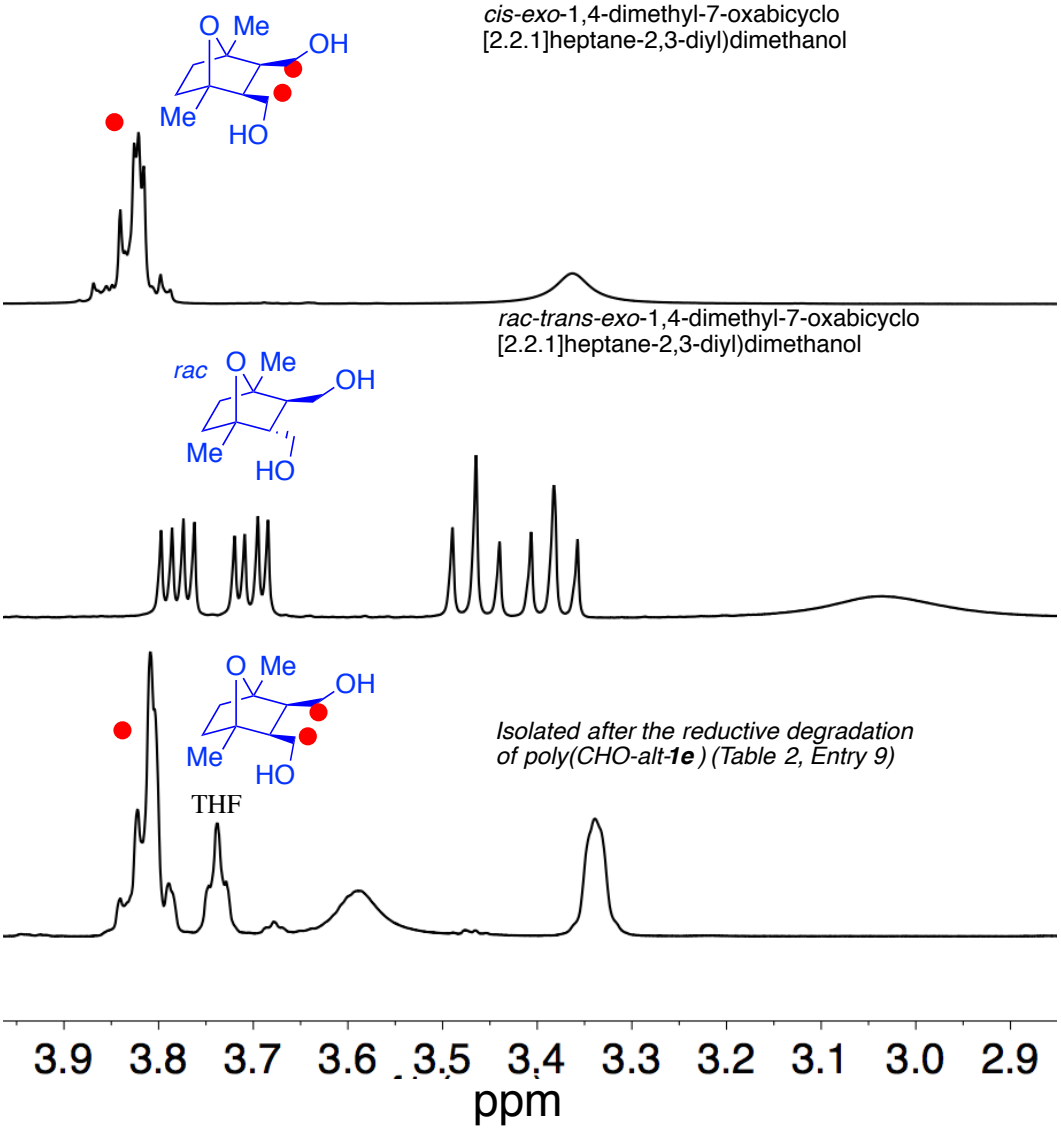

Figure S21. Comparison of diagnostic region of ^{1}H NMR spectrum of degraded poly(CHO-*alt*-**1e**) (Table 2, Entry 9) and corresponding *cis* and *trans* diols.

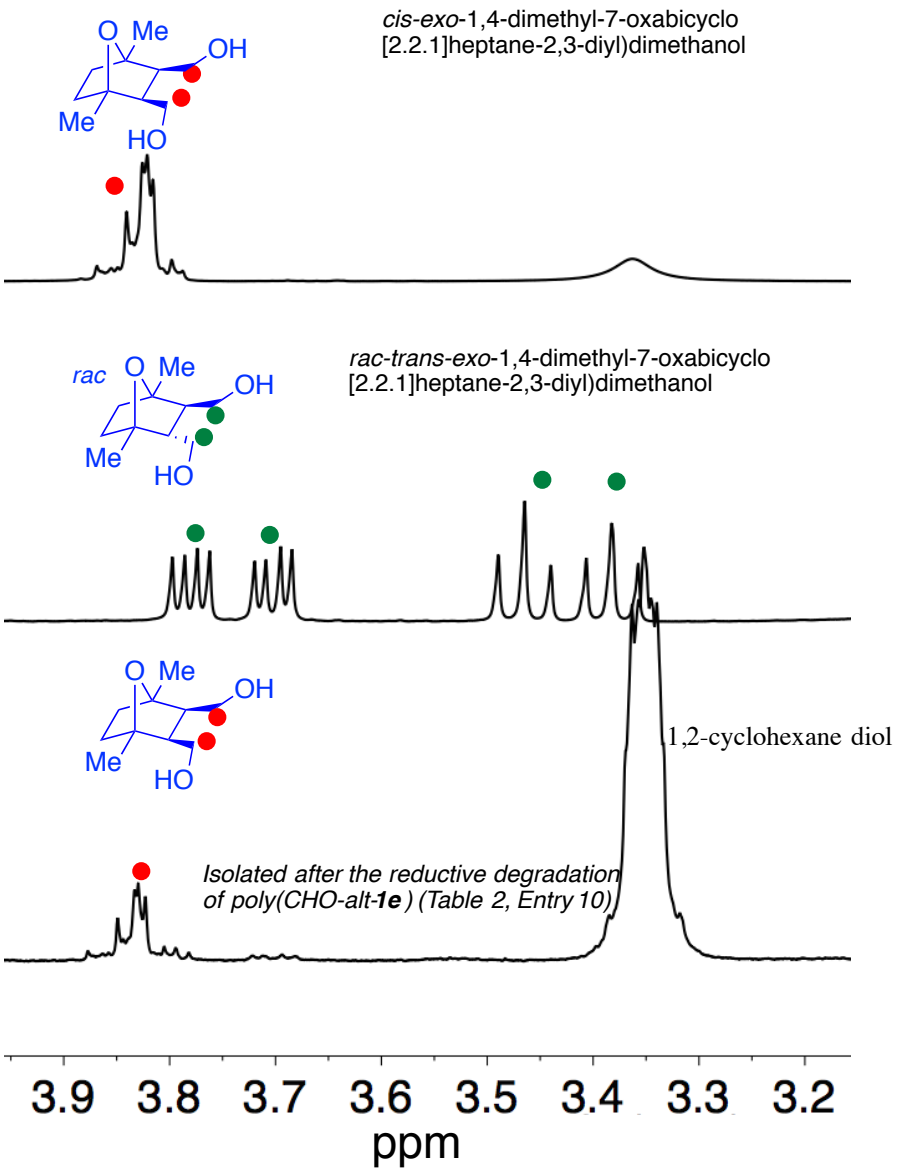

Figure S22. Comparison of diagnostic region of ^{1}H NMR spectrum of degraded poly(CHO-*alt*-**1e**) (Table 2, Entry 10) and corresponding *cis* and *trans* diols.

Mixture of *rac-cis*-7-isopropyl-2,5-dimethylbicyclo[2.2.2]oct-5-ene-2,3-diyl)dimethanol and *rac-cis*-8-isopropyl-2,6-dimethylbicyclo[2.2.2]oct-5-ene-2,3-diyl)dimethanol

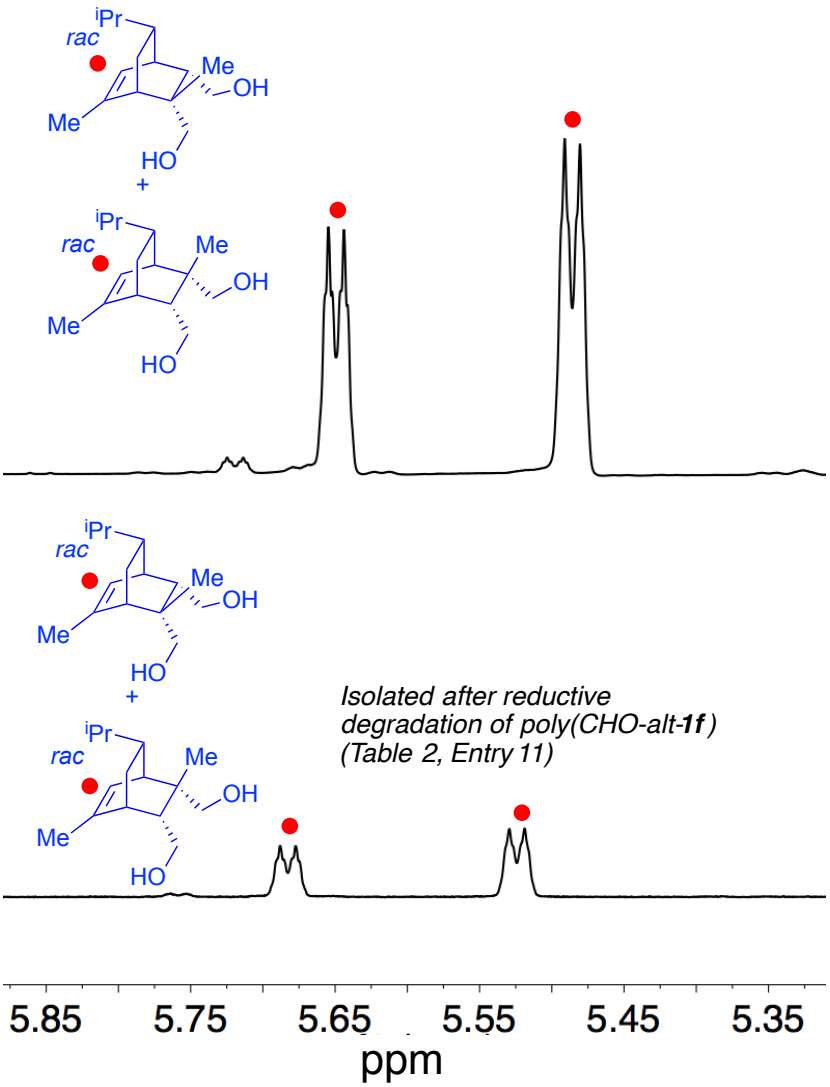

Figure S23. Comparison of vinylic region of ^{1}H NMR spectrum of degraded poly(CHO-*alt*-**1f**) (Table 2, Entry 11) and corresponding *cis* diols.

Mixture of *rac-cis*-7-isopropyl-2,5-dimethylbicyclo[2.2.2]oct-5-ene-2,3-diyl)dimethanol and *rac-cis*-8-isopropyl-2,6-dimethylbicyclo[2.2.2]oct-5-ene-2,3-diyl)dimethanol

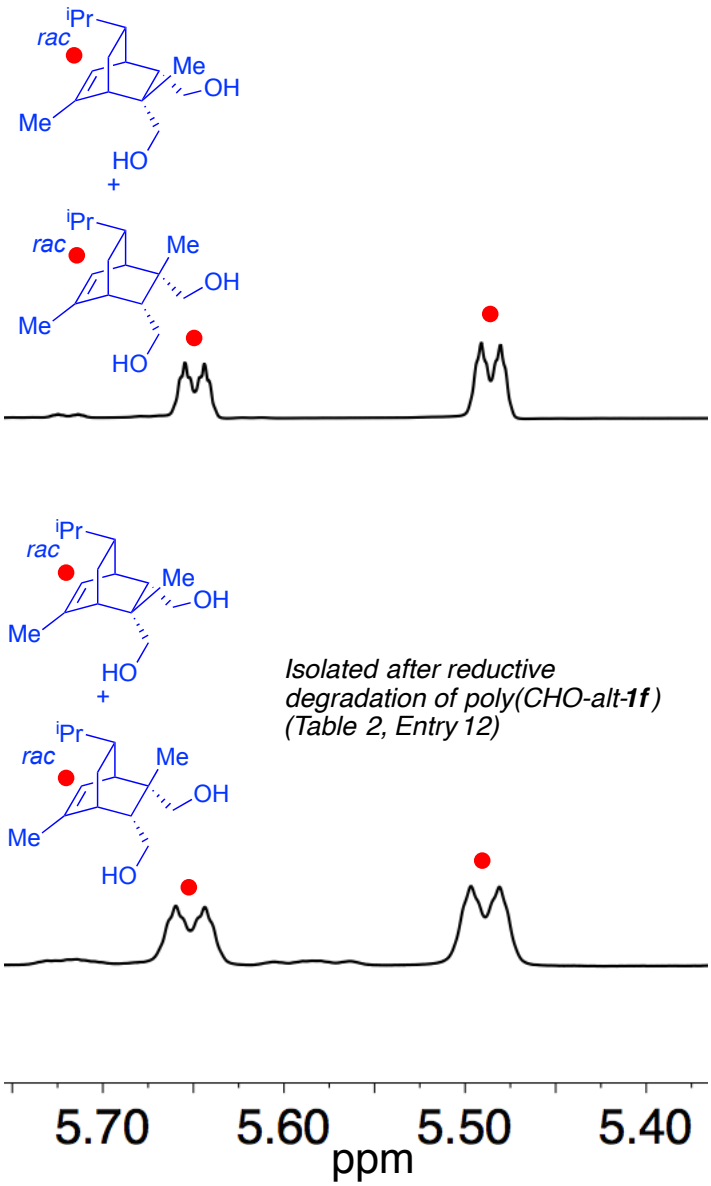

Figure S24. Comparison of vinylic region of ^{1}H NMR spectrum of degraded poly(CHO-*alt*-**1f**) (Table 2, Entry 12) and corresponding *cis* diols.

8. Comparison of GPC traces and Discussion of Initiation by Diacid or Diol

Poly(PO-*alt*-**1**) samples synthesized with complex **2c** had lower molecular weights in general than samples synthesized with **2a** or **2b**. We attribute this to an increased amount of

adventitious water present in samples synthesized with **2c**. This is supported by the different distributions seen in the GPC traces. A representative pair of traces are shown in Figure S25. For Table 1, Entry 3, a sample of poly(PO-*alt*-**1b**) synthesized with **2b,** the major peak in the GPC traces is the lower molecular weight peak attributable to chains intiated by Cl^-. The smaller, high molecuar weight peak is due to chains initiated by adventitious water; by reacting with anhydride to form a diacid, or through chain shuttling, as described in more detail below, it ultimately acts as a bifunctional initatior leading to chains with double the molecuar weight of those initiated by Cl^-. However, for Table 1, Entry 4, a sample of poly(PO-*alt*-**1b**) synthesized with **2c**, the intensities of the two peaks are reversed and the major peak is the higher molecular weight peak, indicating that there was more adventitious water in samples synthesized with **2c** compared to those those synthesized with **2a** or **2b**. It should be noted at the low catalyst loading used in these polymerizations (4.3 μmol catalyst and 3.8 μmol [PPN]Cl) only a very small amount of adventitious water is necessary to significantly affect the molecular weight of the resulting polymers.

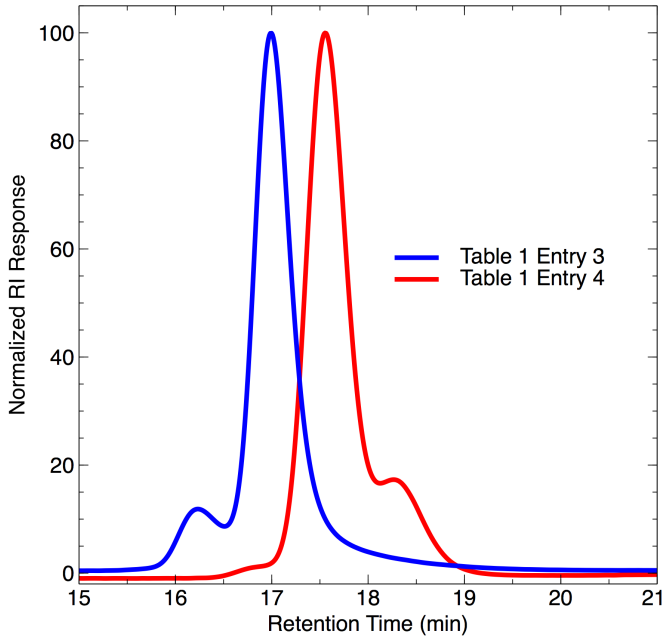

Figure S25. GPC traces of Table 1, Entry 3 and Table 1, Entry 4.

Adventitious water can initiate the polymerization, presumably through ring-opening of an anhydride leading to a diacid (Scheme S1b) or by chain shuttling with a metal-alkoxide followed by reaction with an epoxide to form a diol (Scheme S1c). In the first case, chain shuttling from a growing polymer alkoxide to the diacid allows the diacid to initiate a new polymer chain that can grow from either end leading to a 2X molecular weight distribution, and overall lowering of the molecular weight due to the increased number of initiators. In the second case, a metal alkoxide chain shuttles with water to generate a metal hydroxide species which can either attack an anhydride or react with an epoxide through a bimetallic Jacobsen-type mechanism[8] to generate a diol, which can also grow from either end giving a 2X molecular weight distribution, and overall lowering of the molecular weight due to the increased number of initiators (Scheme S1c). In either case, due to the reversible nature of the proton transfer that gives rise to the chain shuttling, no polymer chains become permanently inactive and the polymerization behaves as an immortal polymerization.[9] For comparison, a proposed mechanism for initiation by Cl^- is also shown (Scheme S1a).

Scheme S1. Initiation by a) Cl^- b) water or diacid and c) chain shuttling to form diol.

a) Initiation with Cl^-

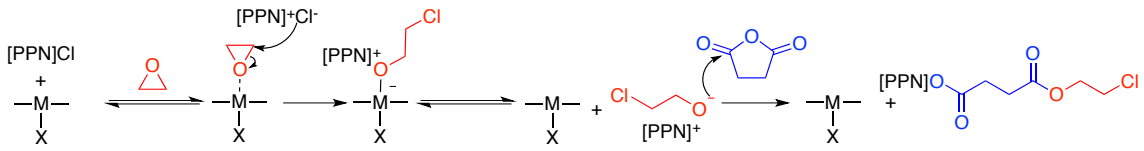

b) Initiation with water or diacid

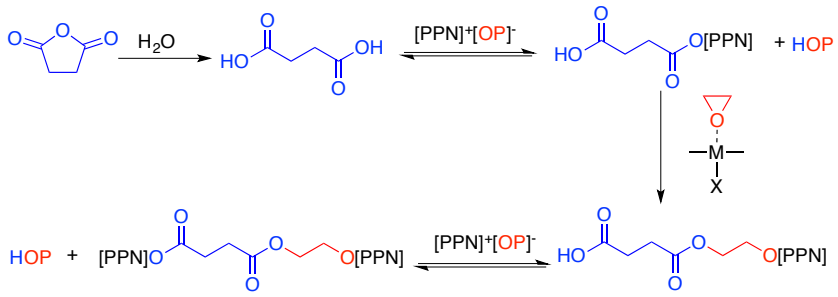

c) Chain shuttling with water to form diol

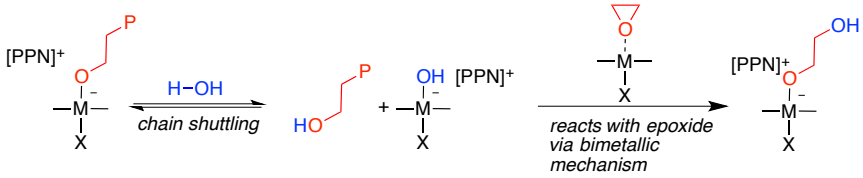

9. MALDI-TOF-MS Analysis

Representative MALDI-TOF-MS spectra are shown in Figure S26 and Figure S27. All spectra showed major distributions attributable to structures A and B. A few spectra contained α,ω-OH,OH terminated signals as a low intensity, high molecular weight distribution. However, because there were no signals due to α,ω-Cl,Cl terminated polymers or cyclic polymers, we do not believe transesterification occurred, and that the α,ω-OH,OH signals were due solely to diacid or diol initiated chains. If transesterification caused the α,ω-OH,OH terminated polymers, then there would have also have to be α,ω-Cl,Cl terminated polymers and cyclic structures as well.[10] It should be noted that based on the work of Duchateau and co-workers, the endgroup in structure B could be either saturated or unsaturated.[11] Due to the small mass difference between these two structures and the lower resolution of the linear mode that had to be used in order to

obtain the MALDI-TOF-MS data, it is not possible to definitively determine if the end group is saturated or unsaturated in structure B.

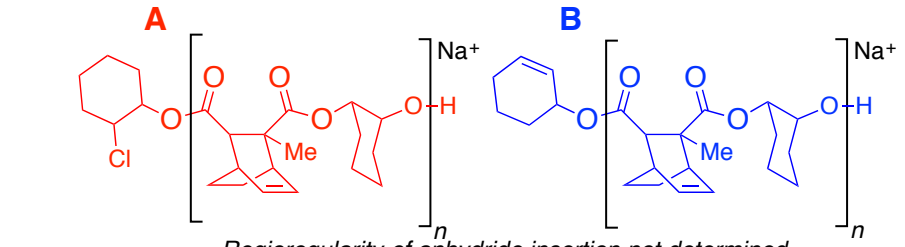

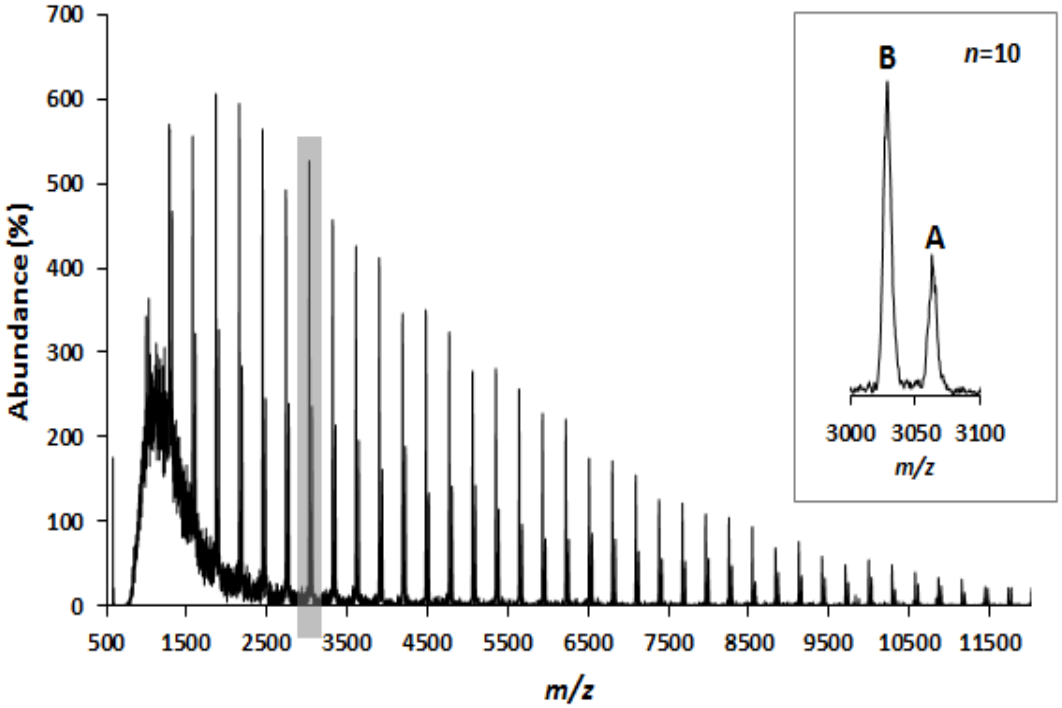

Figure S26. MALDI-TOF-MS Analysis of poly(CHO-*alt*-**1d**) synthesized with **2b**.

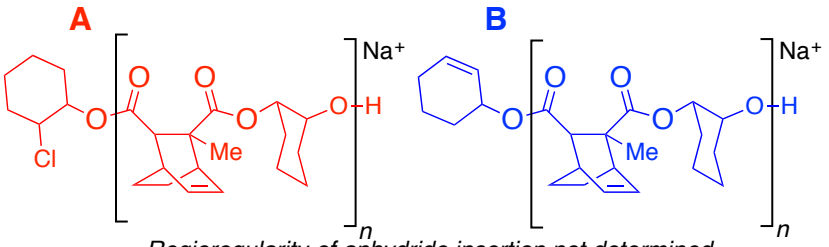

Regioregularity of anhydride insertion not determined.

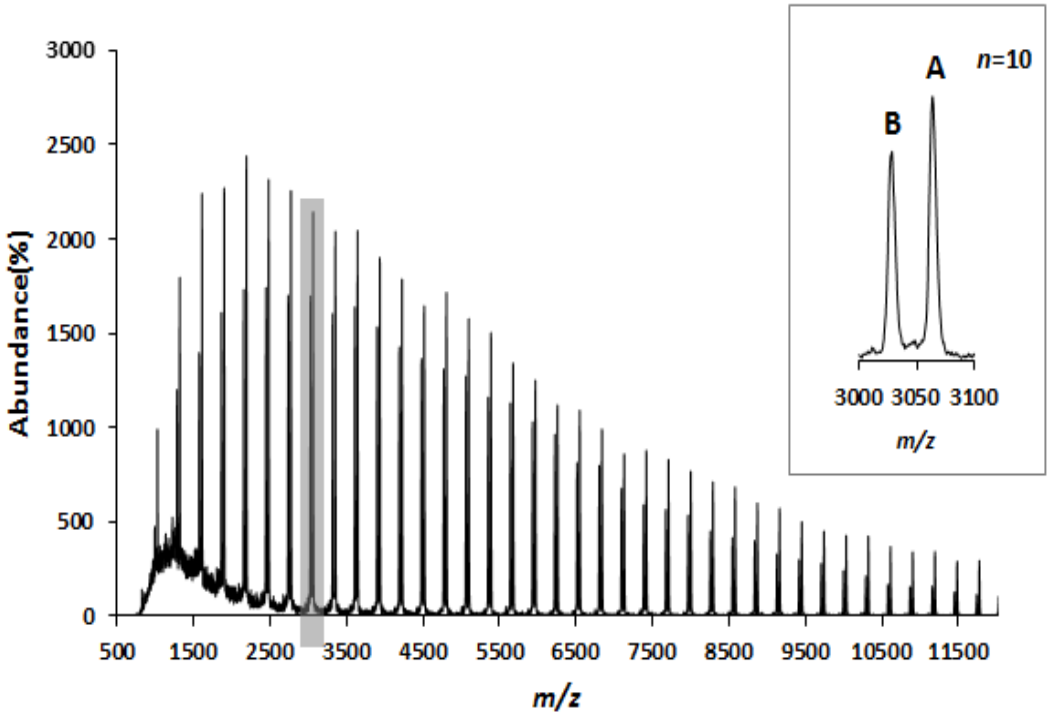

Figure S27. MALDI-TOF-MS Analysis of poly(CHO-*alt*-**1d**) synthesized with **2c**.

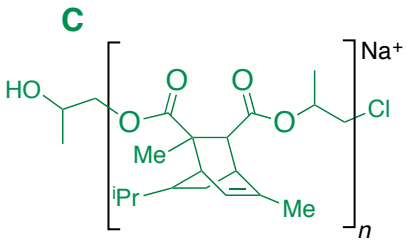

Regioregularity of anhydride insertion not determined.

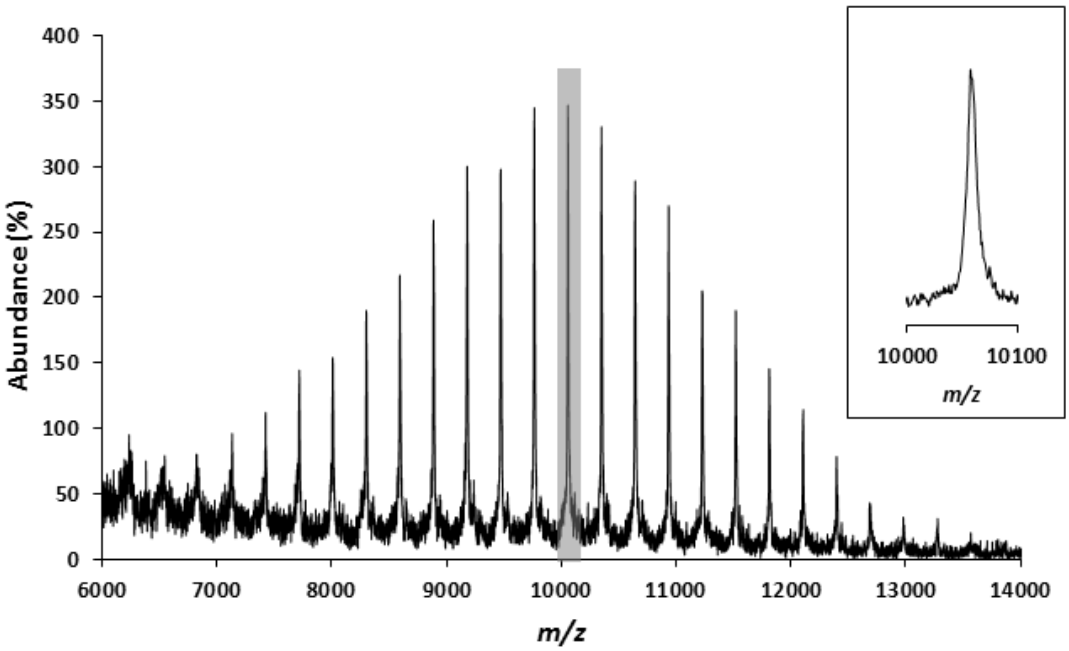

Figure S28. MALDI-TOF-MS Analysis of poly(PO-*alt*-**1b**) synthesized with **2c**.

Scheme S2. a) General MPVO reaction and b) formation of end-groups via MPVO reaction.

a) Meerwein-Ponndorf-Verley-Oppenhauer (MPVO) Reaction

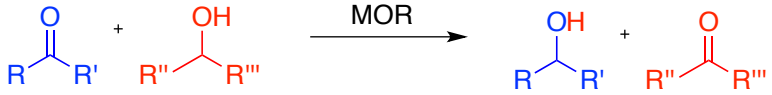

Metal catalyzed hydride shift of α–proton from alcohol to carbonyl

b) Formation of cyclohexanol or cycohexenol end-group via MPVO reaction

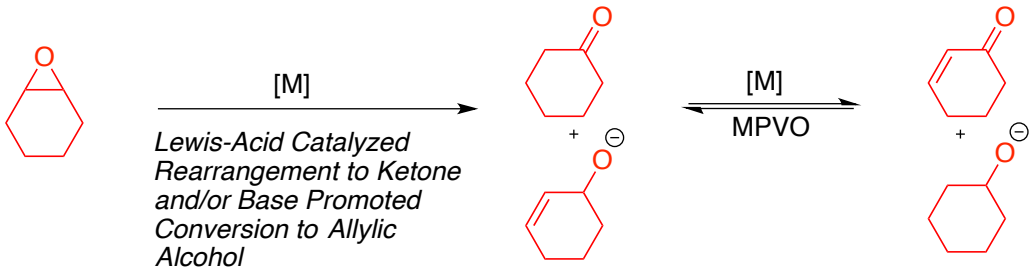

A general reaction scheme for the MPVO reaction is shown in Scheme S2a, and the formation of the cyclohexenol or cyclohexanol end-groups are shown in Scheme S2b. It should be noted that another possibility exists for the formation of the cyclohexenol end-group. Elimination of Cl^- from α,ω-Cl,OH polymers by a polymer alkoxide could also generate this end group. While we have been unable to definitively rule out this possibility we believe that the MPVO reaction is the more likely cause of these end-groups. First, when a polymer sample was resubmitted to a mixture of CHO, **2a**, and [PPN]Cl – conditions which should generate alkoxides and which mimic conditions near the end of the polymerization – the ratio of end groups remained unchanged by MALDI-TOF-MS analysis. If Cl^- elimination was the cause of the cyclohexenol end-groups then under those conditions, the number of cyclohexenol end groups should have increased. Second, if Cl^- elimination was occuring, the ratio of α,ω-Cl,OH end-groups to cyclohexenol end-groups should increase with decreasing molecular weight as new Cl^- initiators would be slowly generated over the course of the polmyerization, resulting in a bias towards low molecular chains having α,ω-Cl,OH end-groups. As seen in Figure S27, this is not the case. Finally, we do not believe that reducing the amount of CHO present from 1500 eq to 900 eq would have had as great an impact on the polymerization (see Table S1 and associated discussion) as it did if Cl^- elimination was the source of the cyclohexenol end-groups. While we are still working on confirming the exact source of the cyclohexenol end groups, in either case

the net effect is the same on the polymerization – slow introduction of new initiators over the course of the polymerization leads to lowered M_n values and increased $Đ$ values.

10. Thermogravimetric Analysis of Polymers

Samples made under the conditions given in Table 1 and Table 2 were analyzed using a Mettler Toledo Thermogravimetric Analyzer (TGA), model TGA/SDTA851. The heating program was 30 °C to 500 °C at 10 °C/min under a nitrogen atmosphere. Onset thermal decomposition temperatures are reported in Table S2.

Table S2. Thermal degradation data for all polymers.

Polymer	Catalyst	T_d (°C)[a]
Poly(PO-*alt*-**1a**)	**2a**	309
	2c	315
Poly(PO-*alt*-**1b**)	**2b**	316
	2c	328
Poly(PO-*alt*-**1c**)	**2a**	242
	2c	245
Poly(PO-*alt*-**1d**)	**2a**	290
	2c	313
Poly(PO-*alt*-**1e**)	**2b**	261
	2c	325
Poly(PO-*alt*-**1f**)	**2a**	305
	2c	326
Poly(CHO-*alt*-**1a**)	**2a**	272
	2c	316
Poly(CHO-*alt*-**1b**)	**2a**	314
	2c	324
Poly(CHO-*alt*-**1c**)	**2a**	236
	2c	252
Poly(CHO-*alt*-**1d**)	**2a**	272
	2c	324
Poly(CHO-*alt*-**1e**)	**2a**	280
	2c	286
Poly(CHO-*alt*-**1f**)	**2a**	300
	2c	323

[a] Reported T_d is the onset temperature.

11. Copies of DSC Thermograms

All polyesters were analyzed using the following heating program: −70 °C to 200 °C at 25 °C/min, 200 to −70 °C at 10°C/min, and then −70 °C to 200 °C at 25 °C/min. All reported glass transition temperatures were observed on the second heating cycle and the second heating cycle for each sample is shown below.

Table 1 Entry 1: poly(PO-*alt*-**1a**) prepared with complex **2a**

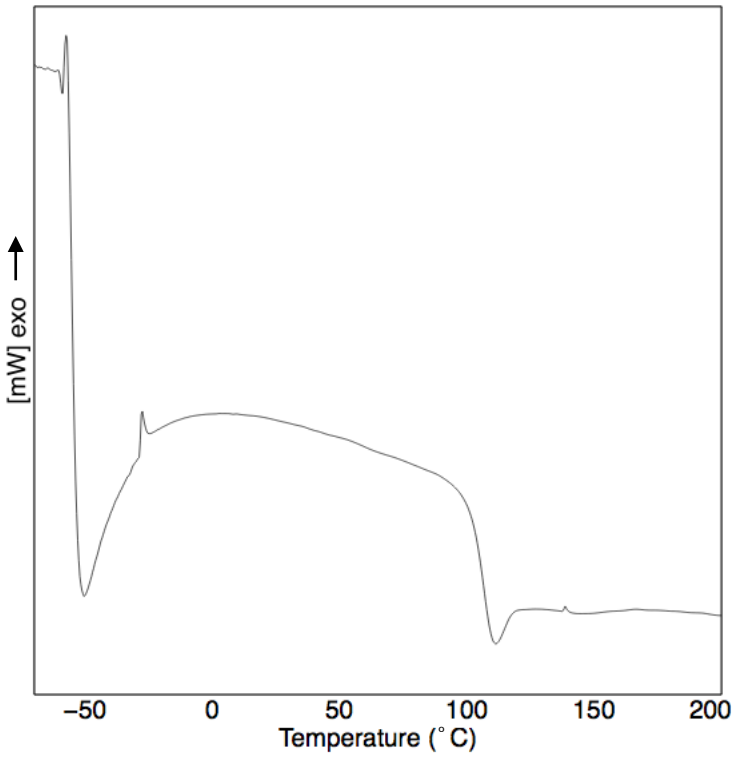

Table 1 Entry 2: poly(PO-*alt*-**1a**) prepared with complex **2c**

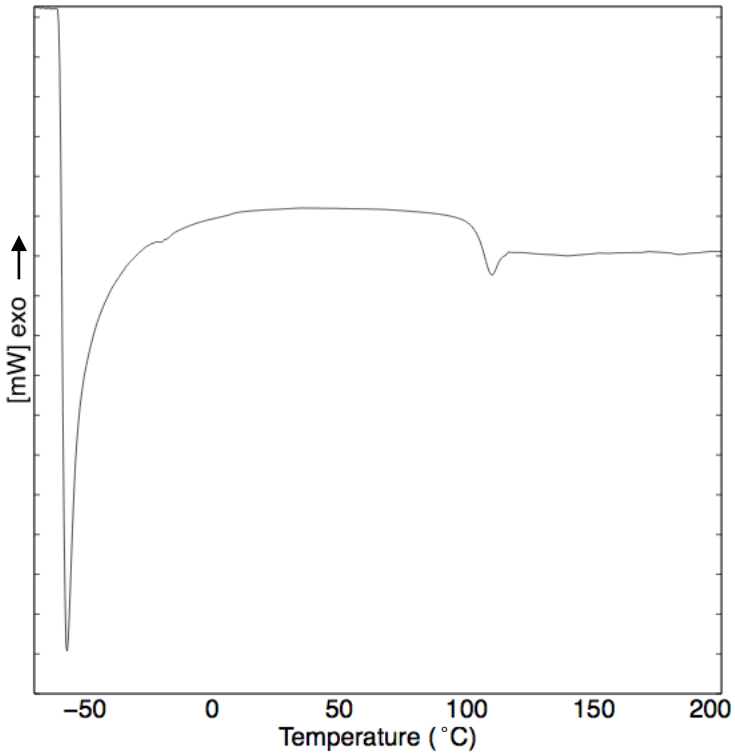

Table 1 Entry 3: poly(PO-*alt*-**1b**) prepared with complex **2b**

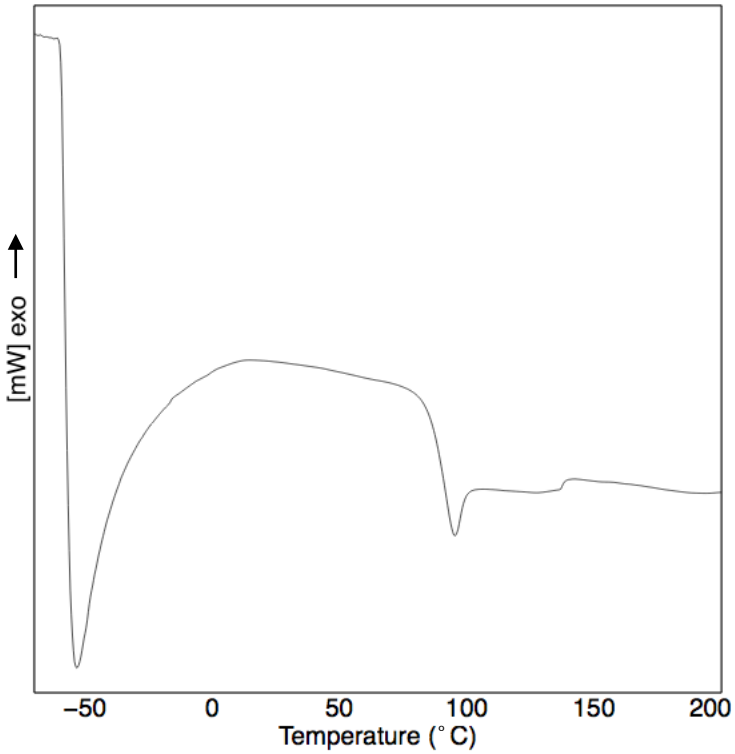

Table 1 Entry 4: poly(PO-*alt*-**1b**) prepared with complex **2c**

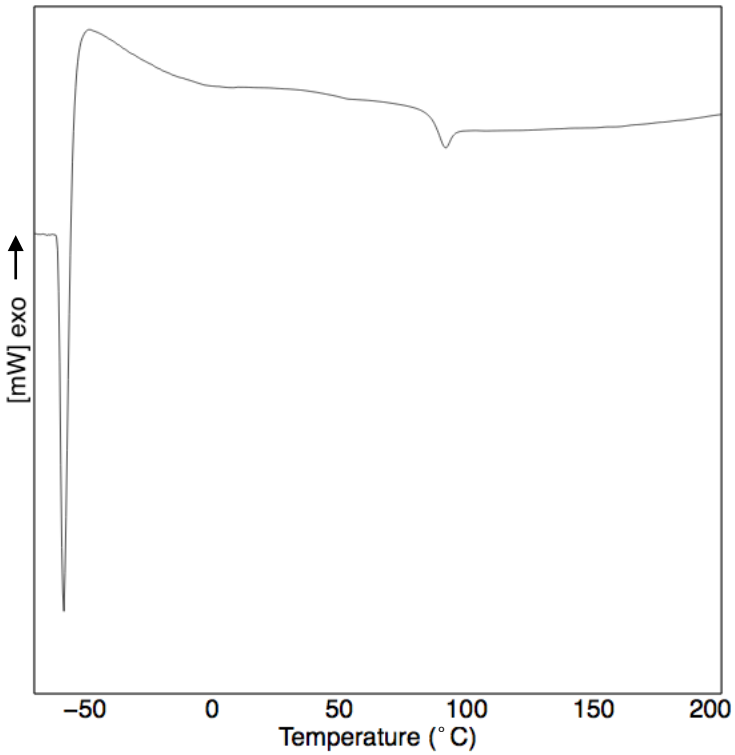

Table 1 Entry 5: poly(PO-*alt*-**1c**) prepared with complex **2a**

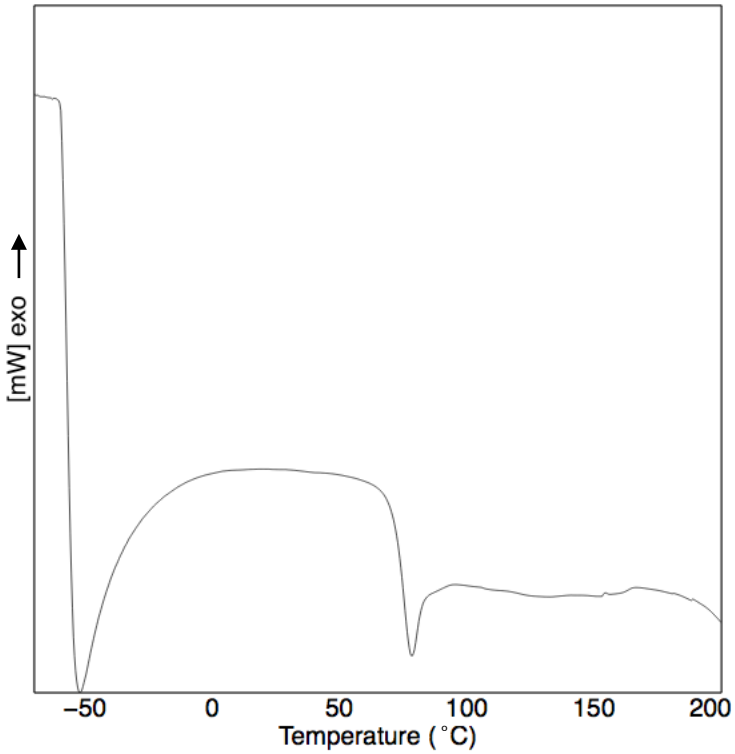

Table 1 Entry 6: poly(PO-*alt*-**1c**) prepared with complex **2c**

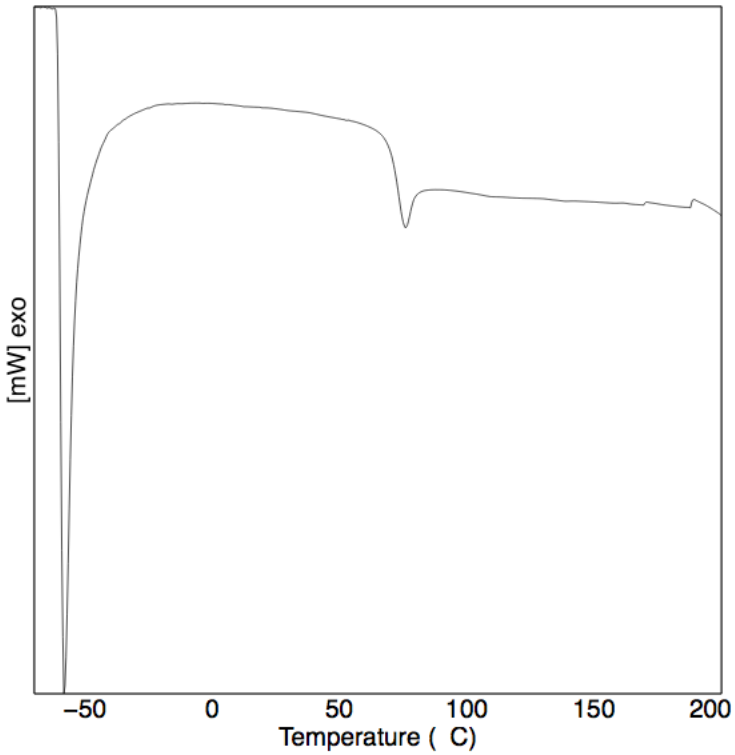

Table 1 Entry 7: poly(PO-*alt*-**1d**) prepared with complex **2a**

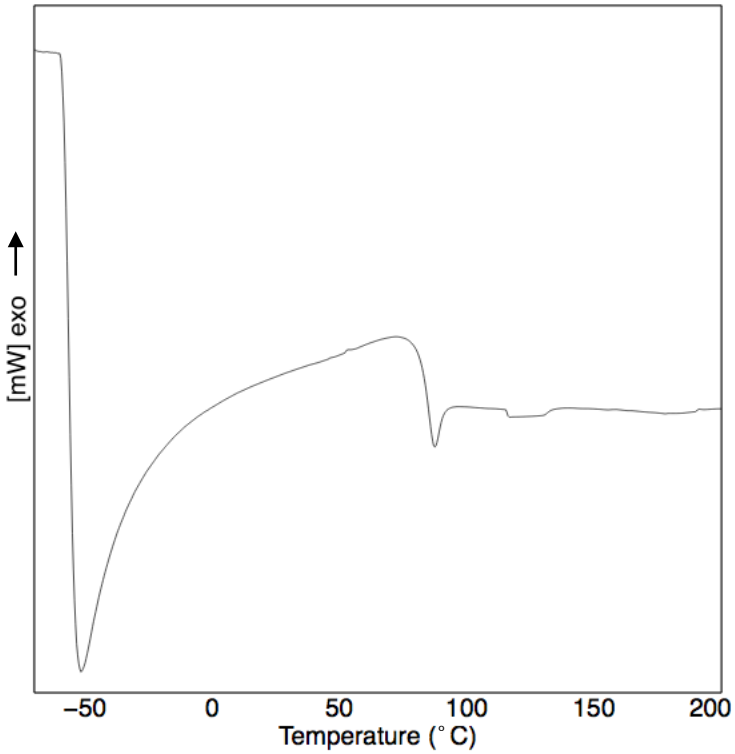

Table 1 Entry 8: poly(PO-*alt*-**1d**) prepared with complex **2c**

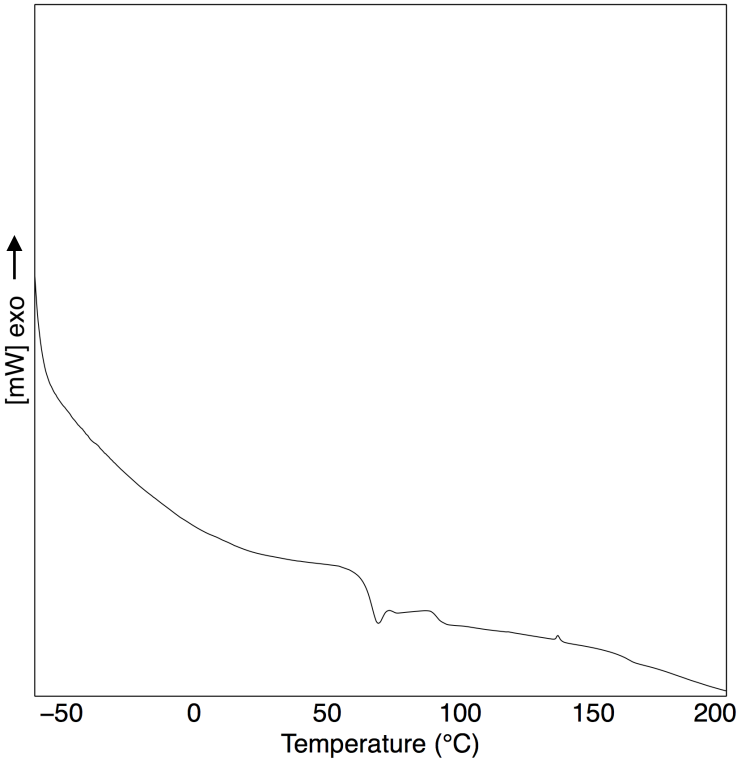

Table 1 Entry 9: poly(PO-*alt*-**1e**) prepared with complex **2b**

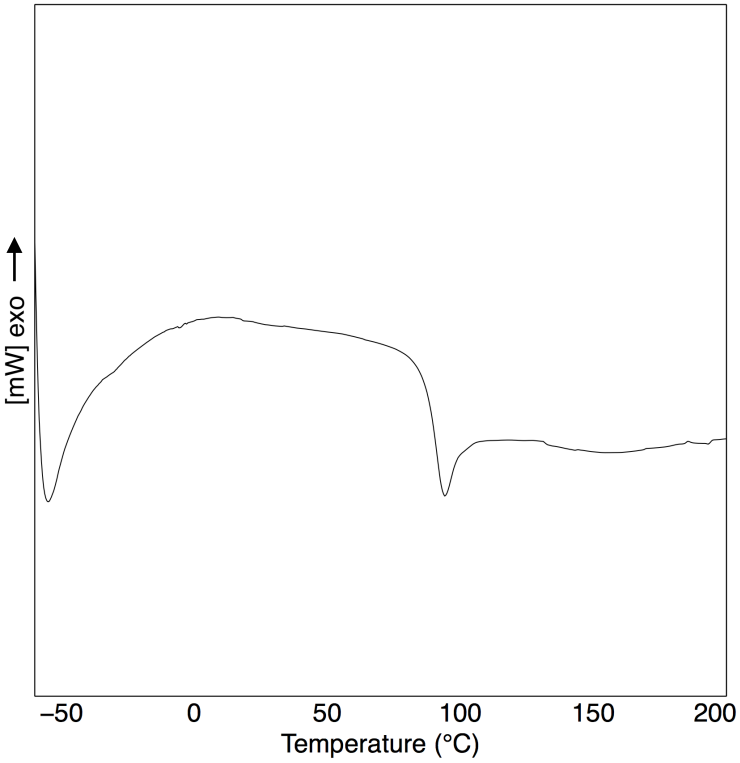

Table 1 Entry 10: poly(PO-*alt*-**1e**)prepared with complex **2c**

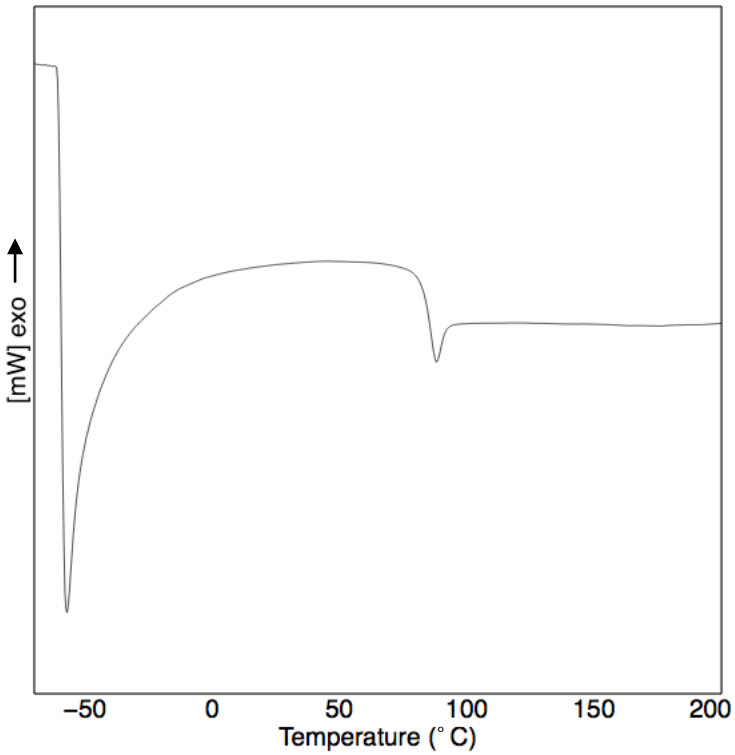

Table 1 Entry 11: poly(PO-*alt*-**1f**) prepared with complex **2a**

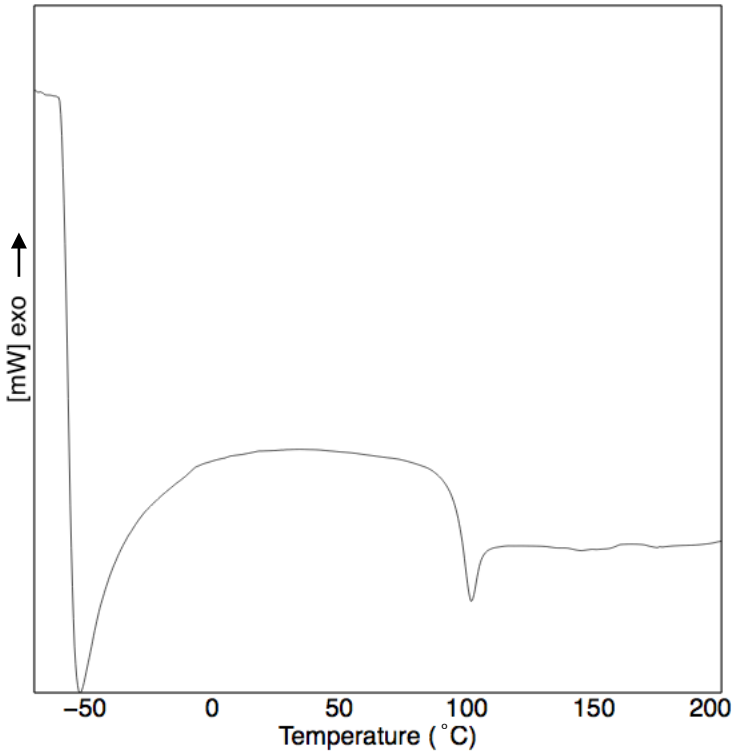

Table 1 Entry 12: poly(PO-*alt*-**1f**) prepared with complex **2c**

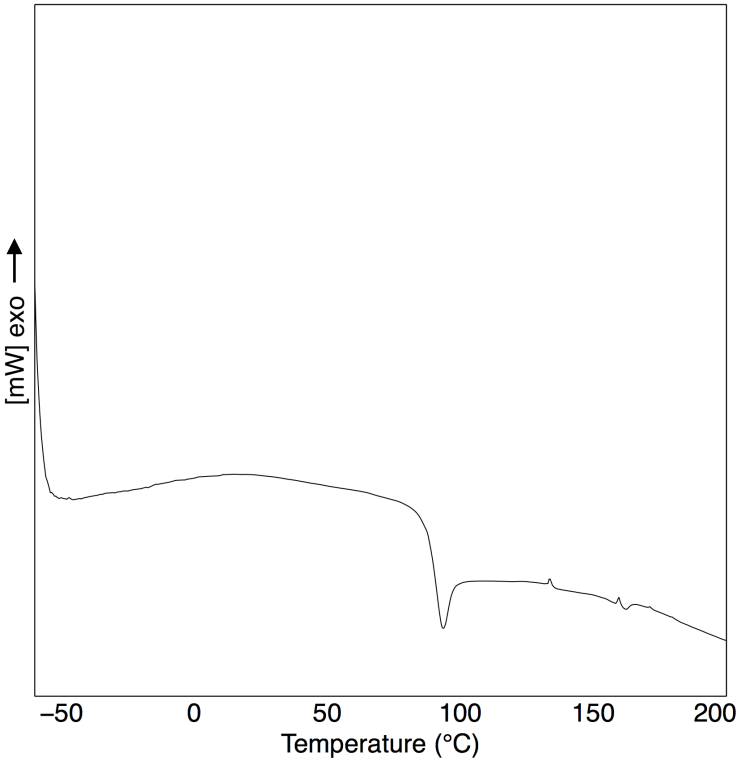

Table 2 Entry 1: poly(CHO-*alt*-**1a**) prepared with complex **2a**

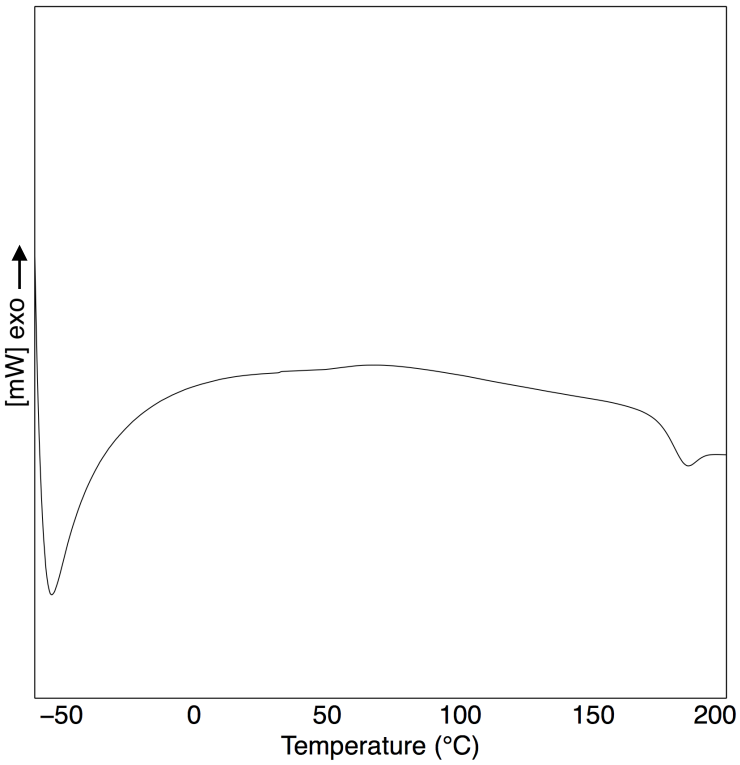

Table 2 Entry 2: poly(CHO-*alt*-**1a**) prepared with complex **2c**

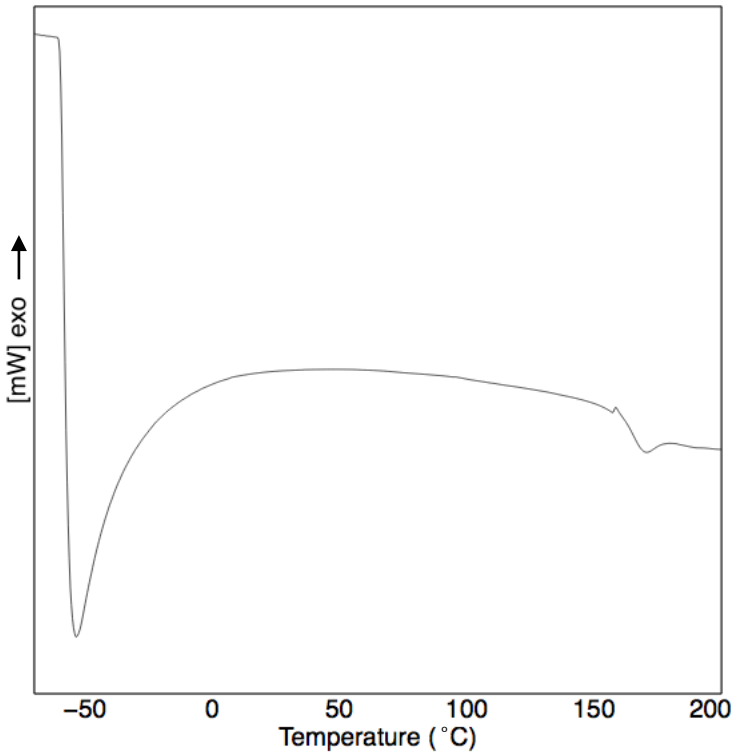

Table 2 Entry 3: poly(CHO-*alt*-**1b**) prepared with complex **2a**

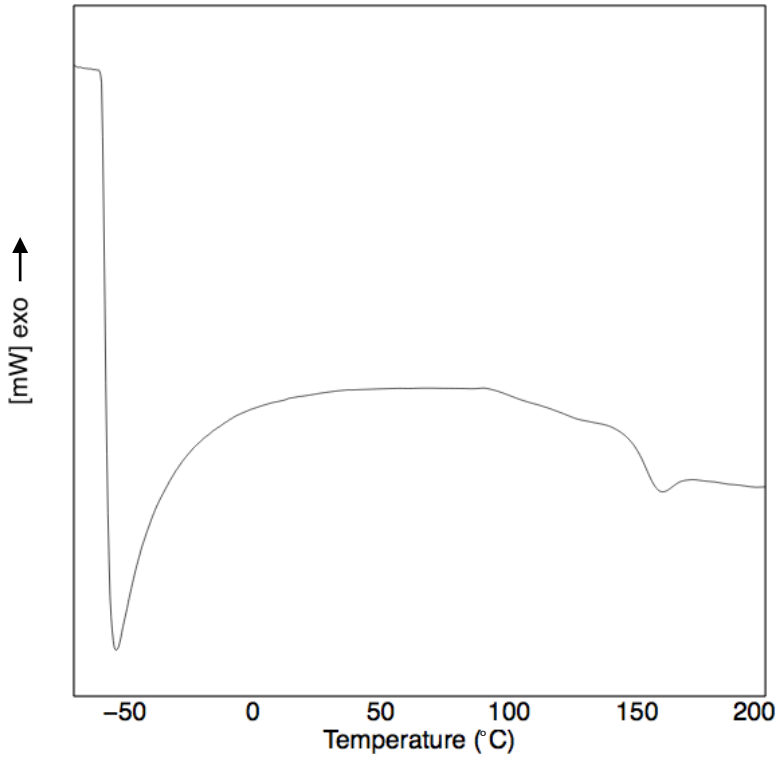

Table 2 Entry 4: poly(CHO-*alt*-**1b**) prepared with complex **2c**

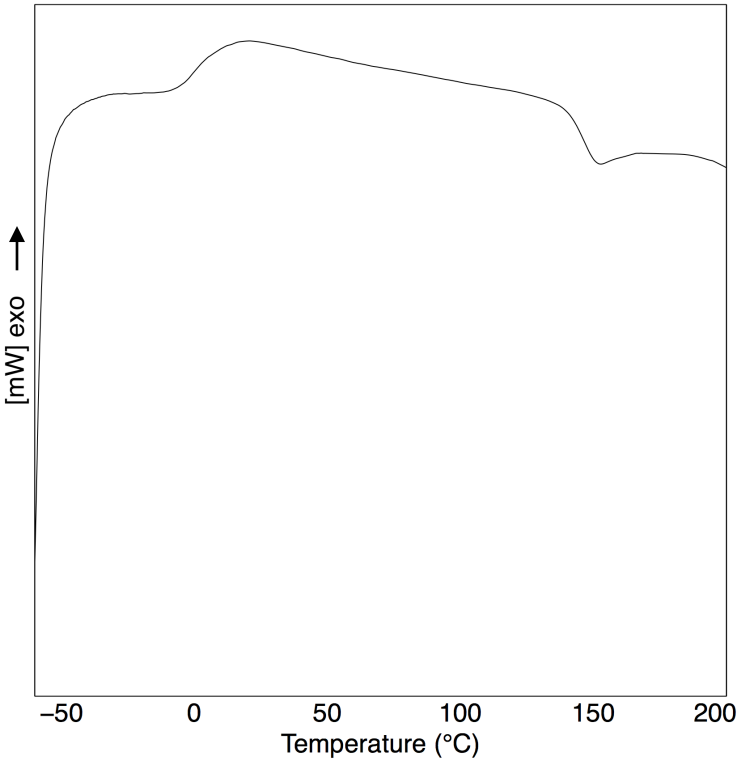

Table 2 Entry 5: poly(CHO-*alt*-**1c**) prepared with complex **2a**

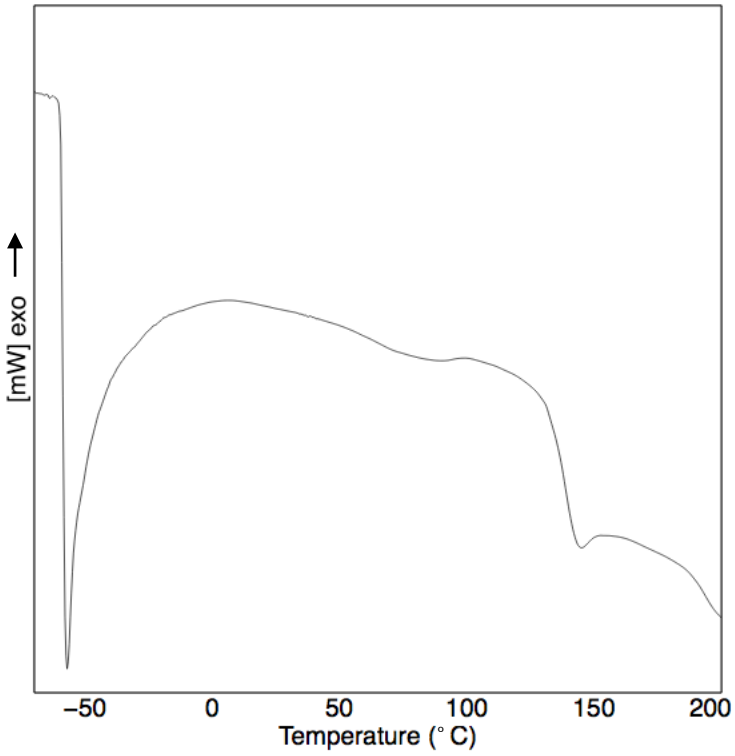

Table 2 Entry 6: poly(CHO-*alt*-**1c**) prepared with complex **2c**

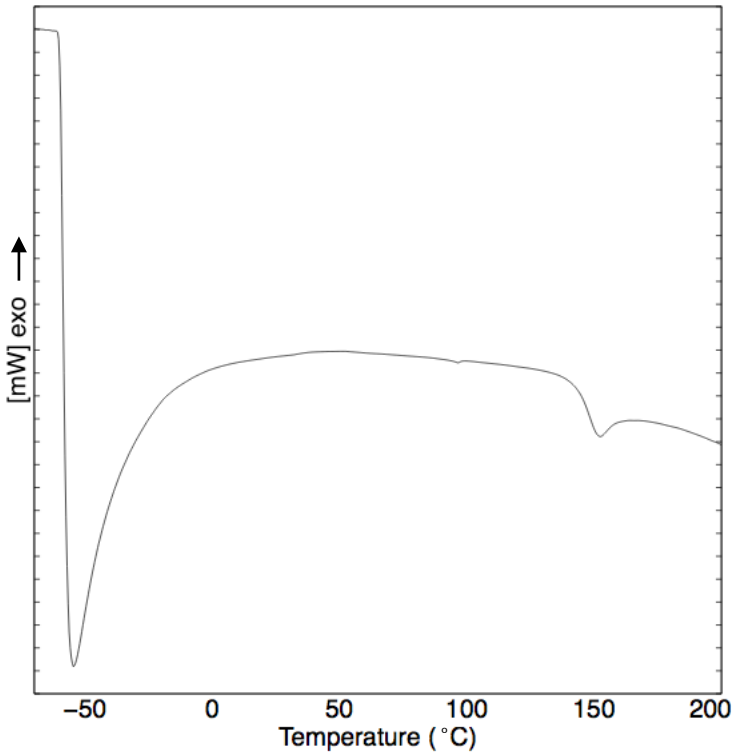

Table 2 Entry 7: poly(CHO-*alt*-**1d**) prepared with complex **2a**

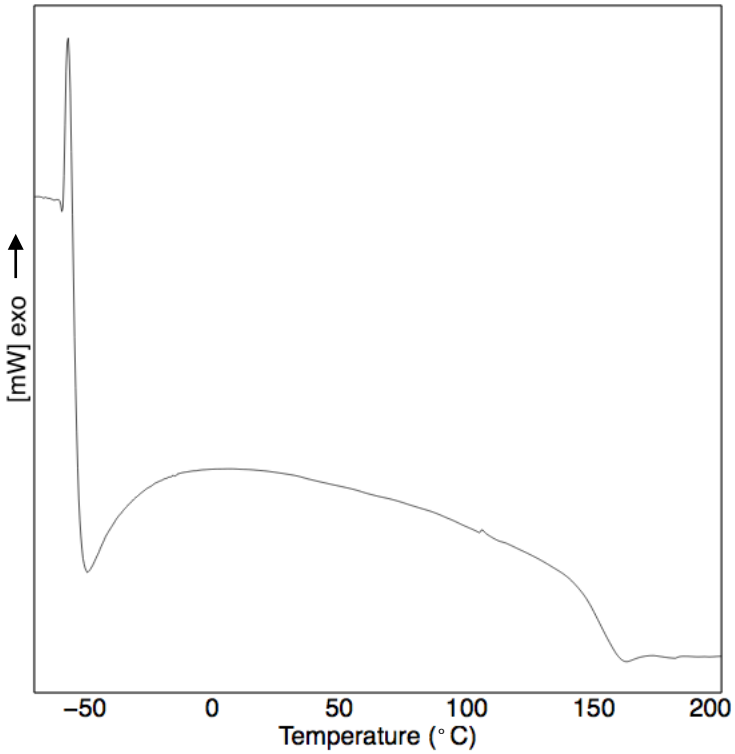

Table 2 Entry 8: poly(CHO-*alt*-**1d**) prepared with complex **2c**

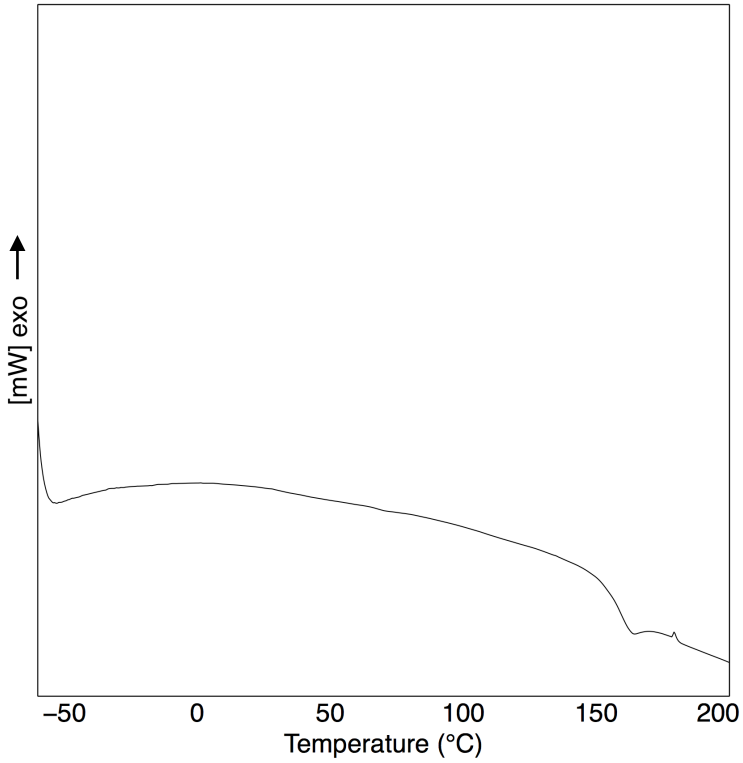

Table 2 Entry 9: poly(CHO-*alt*-**1e**) prepared with complex **2a**

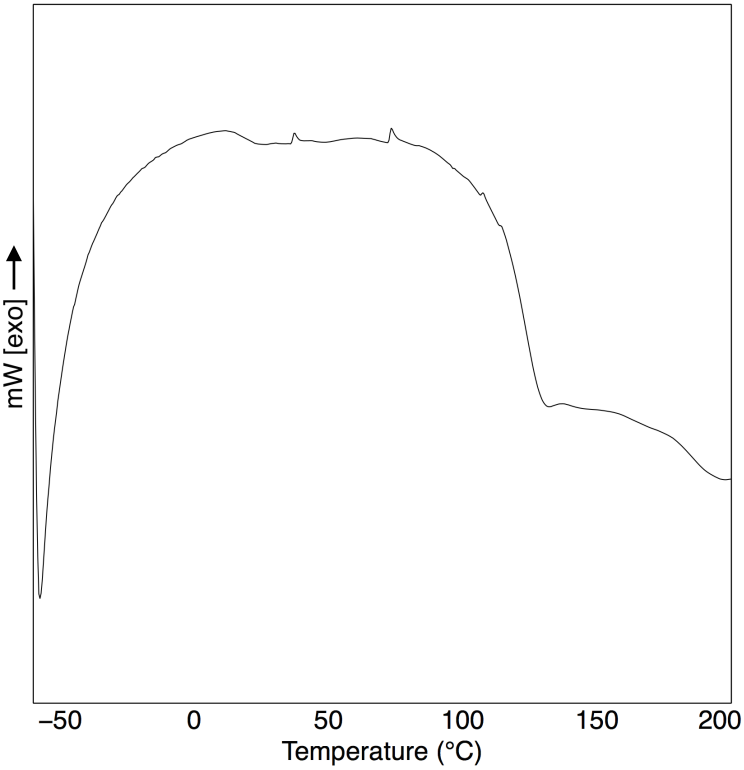

Table 2 Entry 10: poly(CHO-*alt*-**1e**) prepared with complex **2c**

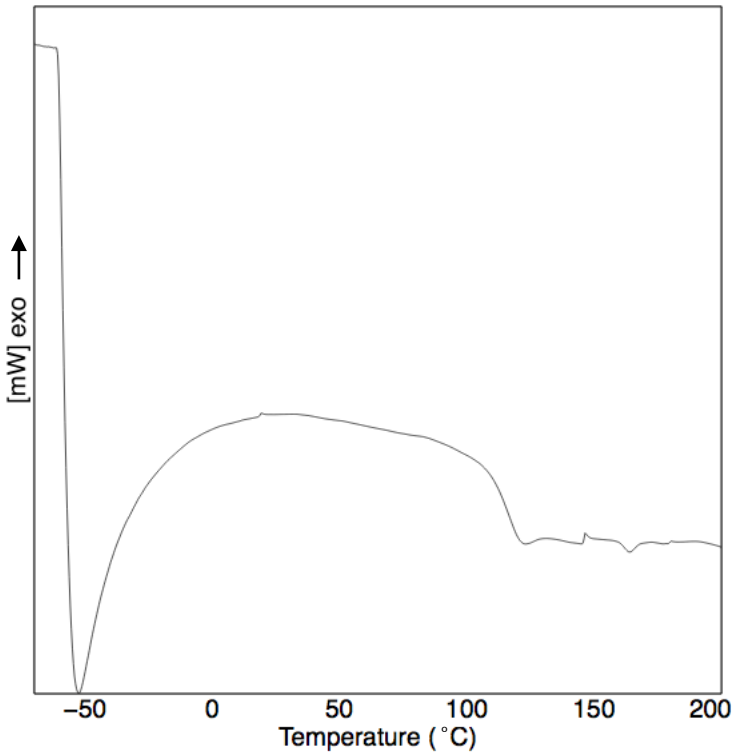

Table 2 Entry 11: poly(CHO-*alt*-**1f**) prepared with complex **2a**

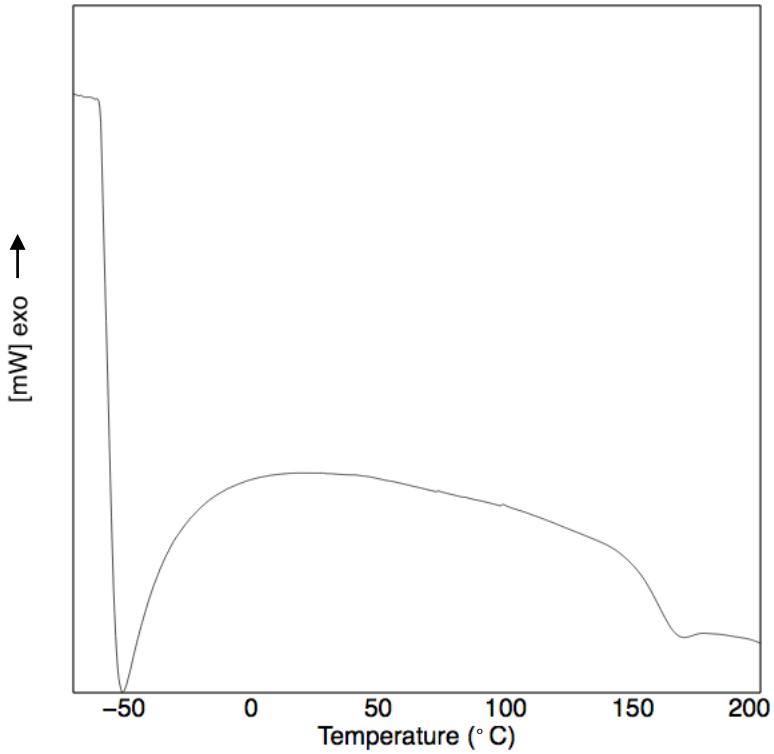

Table 2 Entry 12: poly(CHO-*alt*-**1f**) prepared with complex **2c**

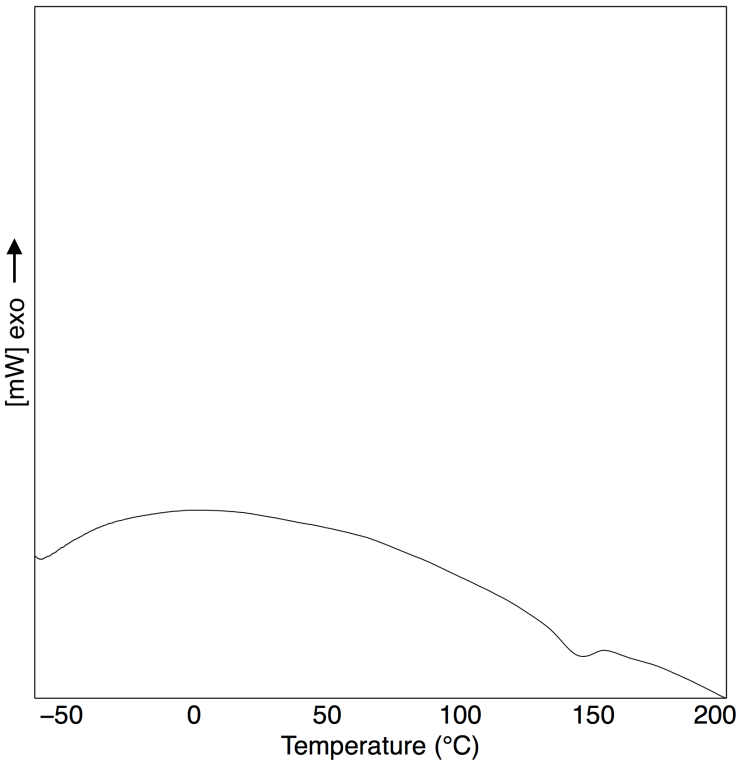

12. Copies of ^{1}H and ^{13}C NMR Spectra for Cyclic Anhydrides and Diols

3-*tert*-butyl-5-chlorosalicylaldehyde (SA-**Cl**)

^{1}H NMR (400 MHz, $CDCl_3$)

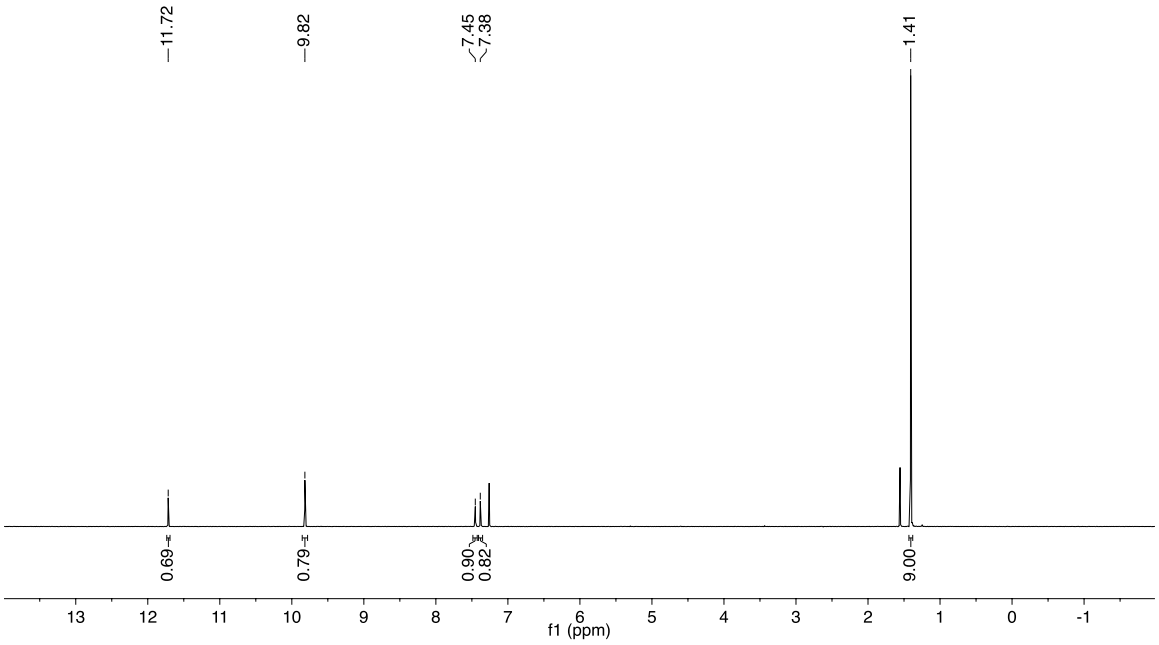

N,N'-bis(3-*tert*-butyl-5-chlorosalicylidene)-1,2-diaminobenzene [(salph-**Cl**)H_2]

^{1}H NMR (600 MHz, $CDCl_3$)

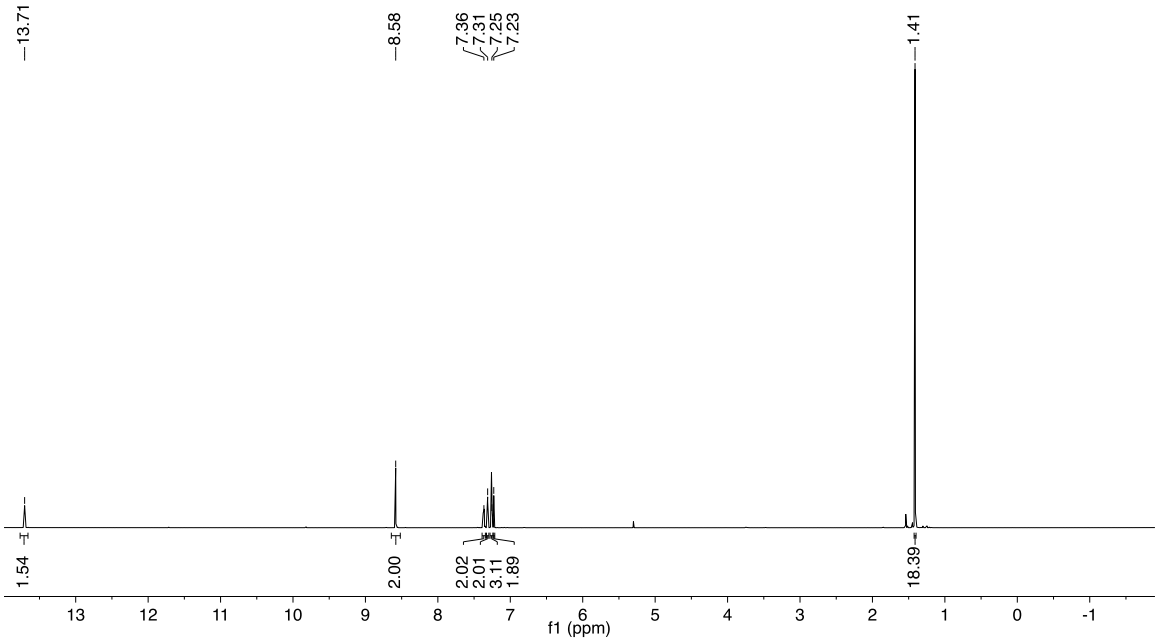

N,N'-bis(3-*tert*-butyl-5-chlorosalicylidene)-1,2-diaminobenzene [(salph-**Cl**)H_2]

^{13}C NMR (125 MHz, $CDCl_3$)

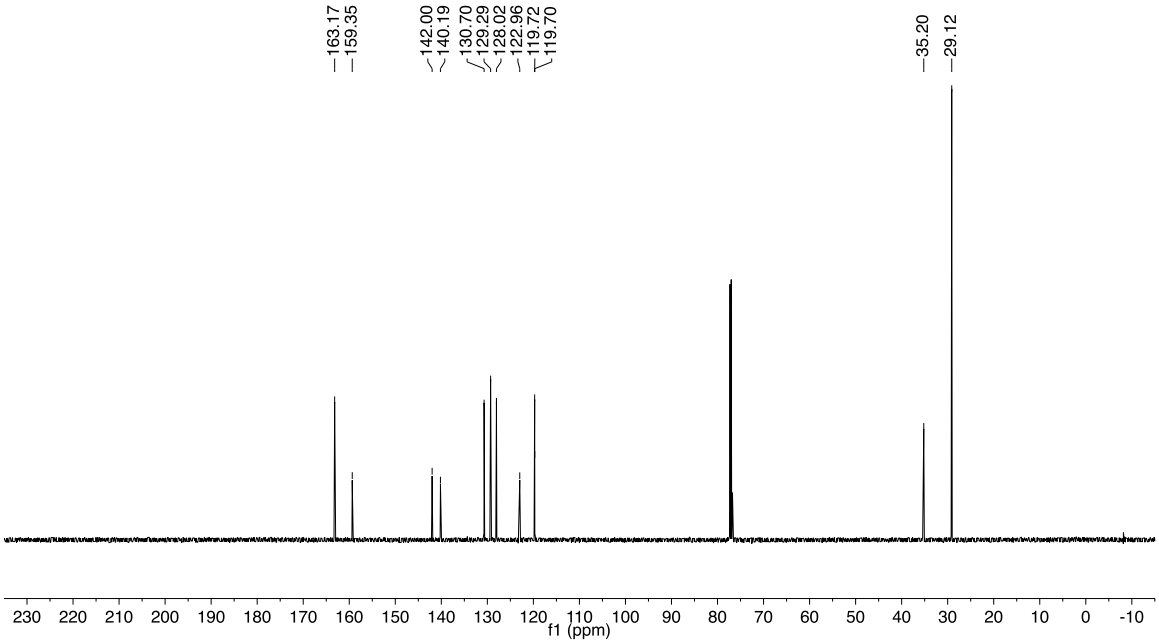

(salph-Cl)AlCl (2b)

^{1}H NMR (500 MHz, DMSO-d_6)

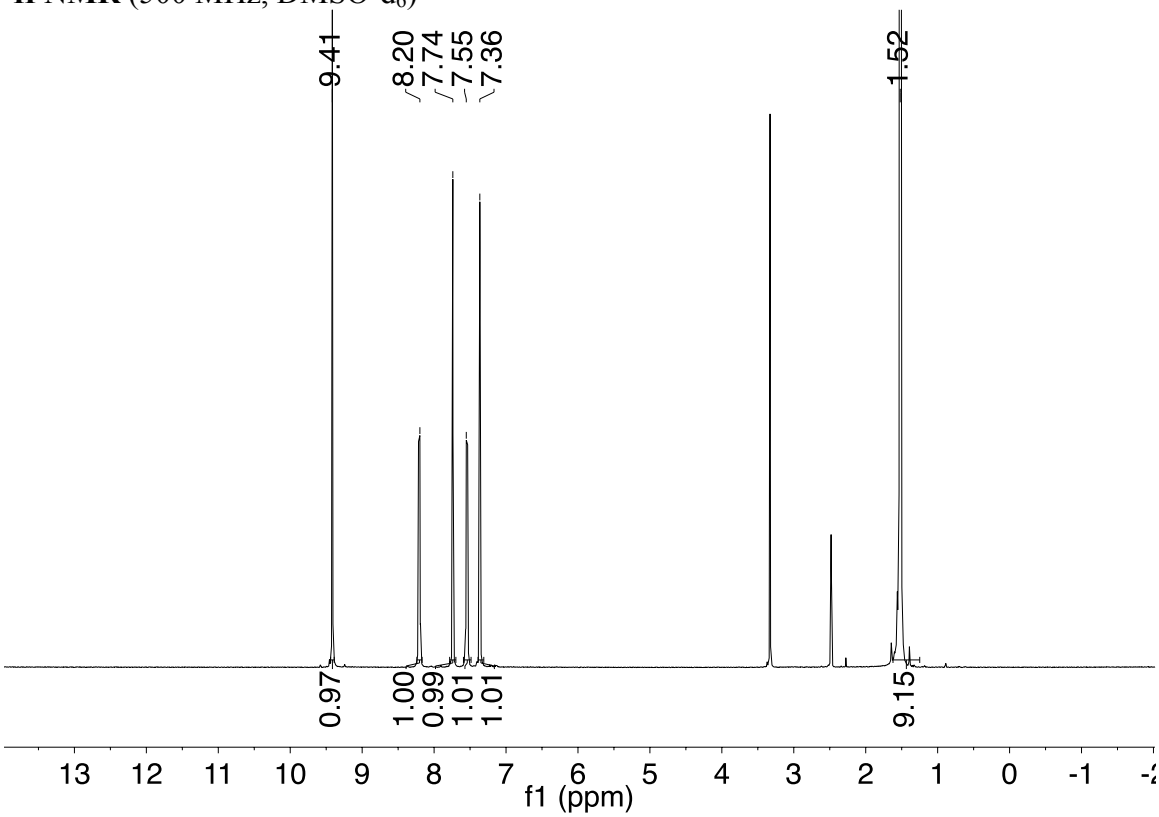

(salph-Cl)AlCl (2b)

^{13}C NMR (125 MHz, DMSO-d_6)

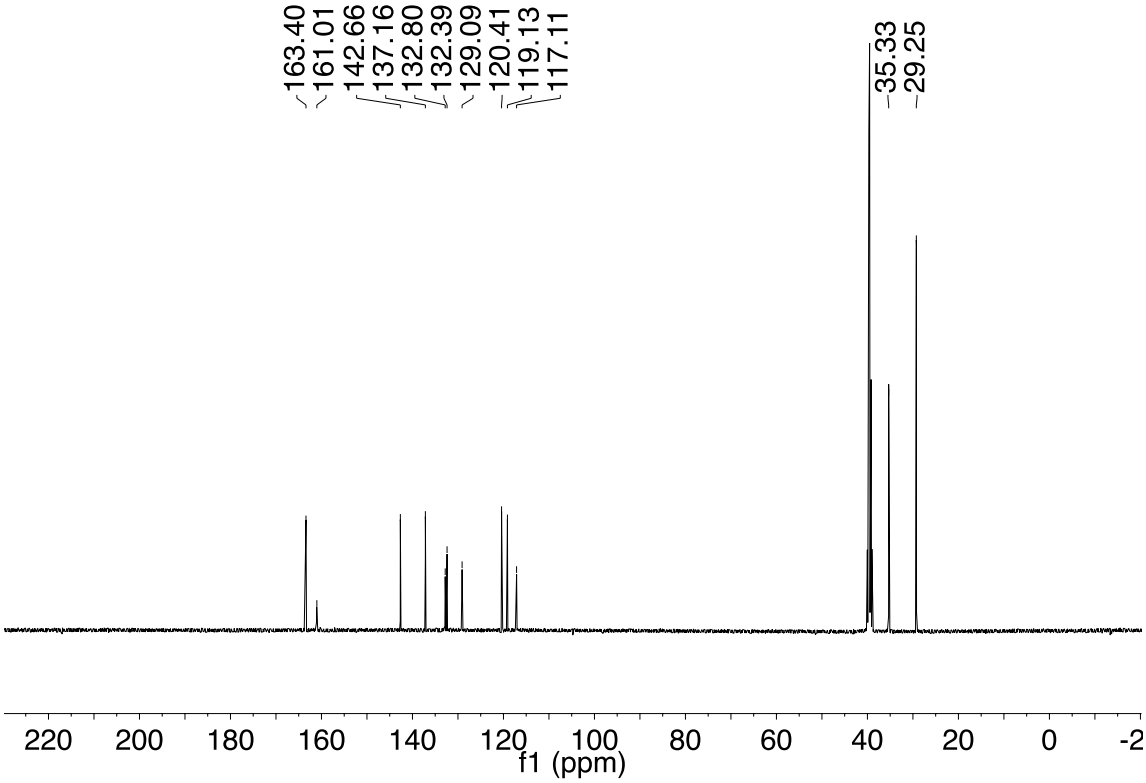

***rac-cis-endo*-2-methyl-bicyclo[2.2.2]hept-5-ene-2,3-dicarboxylic anhydride [1d]**

^{1}H NMR (500 MHz, $CDCl_3$)

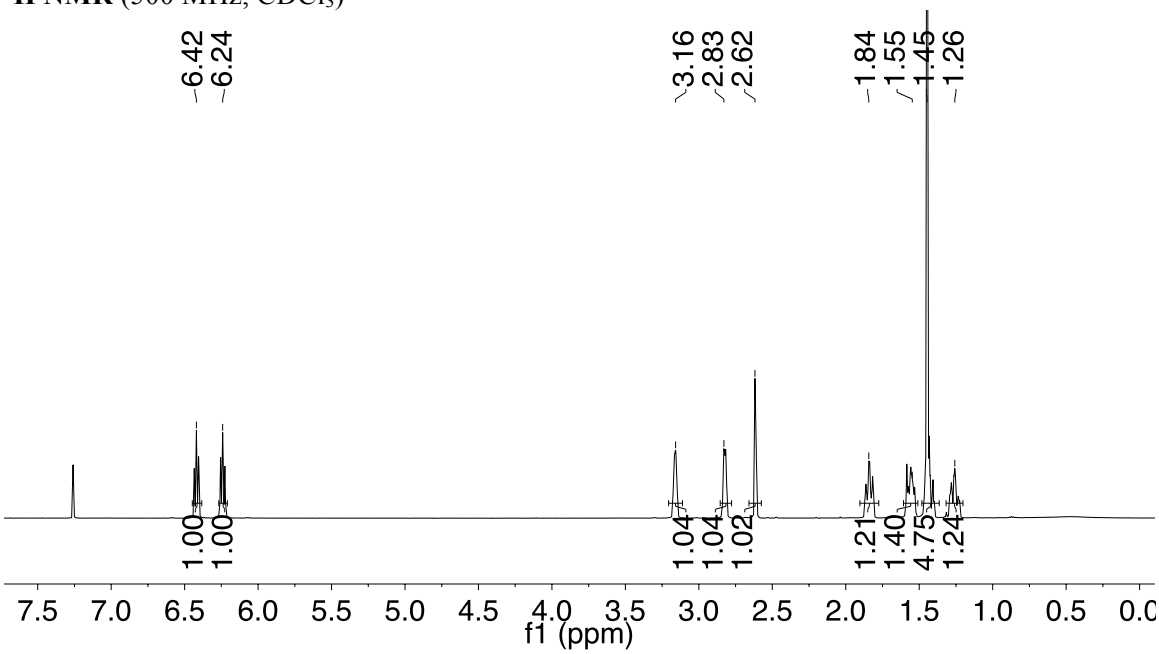

***rac-cis-endo*-2-methyl-bicyclo[2.2.2]hept-5-ene-2,3-dicarboxylic anhydride [1d]**
^{13}C NMR (125 MHz, $CDCl_3$)

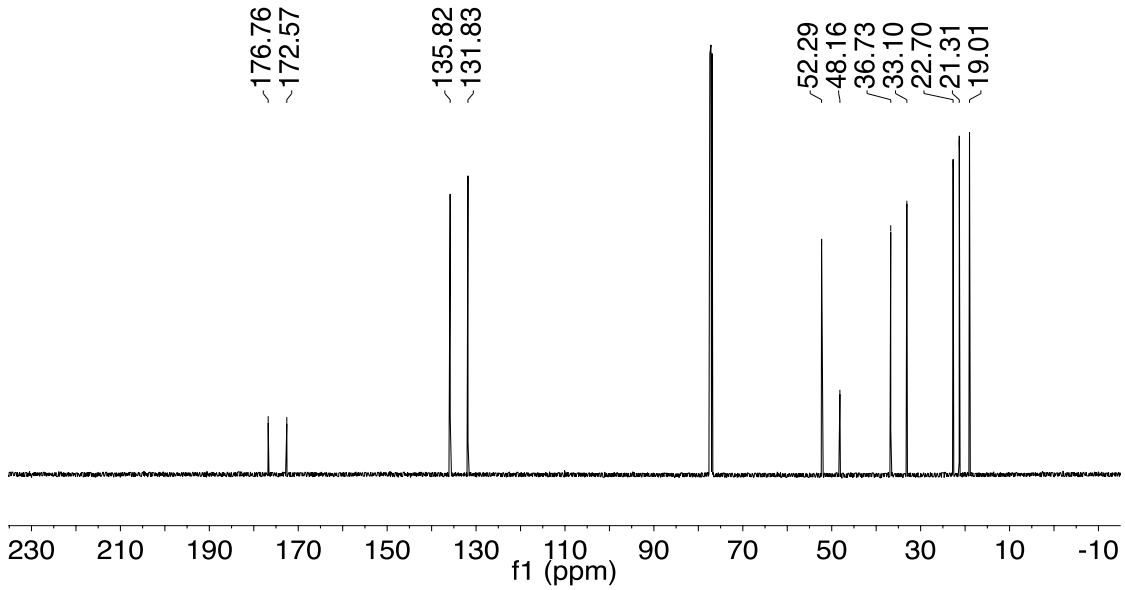

***cis-exo*-1,4-dimethyl-7-oxabicyclo[2.2.1]heptane-2,3-dicarboxylic anhydride [1e]**
^{1}H NMR (500 MHz, $CDCl_3$)

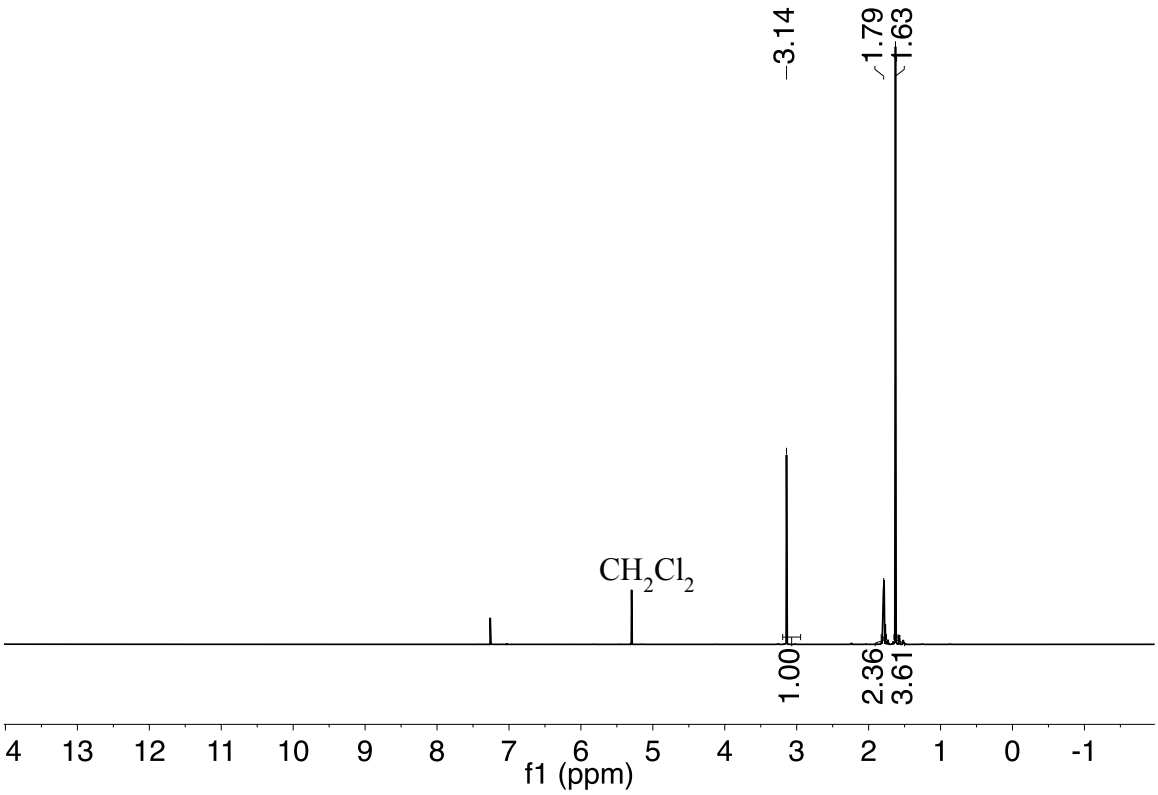

***cis-exo*-1,4-dimethyl-7-oxabicyclo[2.2.1]heptane-2,3-dicarboxylic anhydride [1e]**
^{13}C NMR (125 MHz, $CDCl_3$)

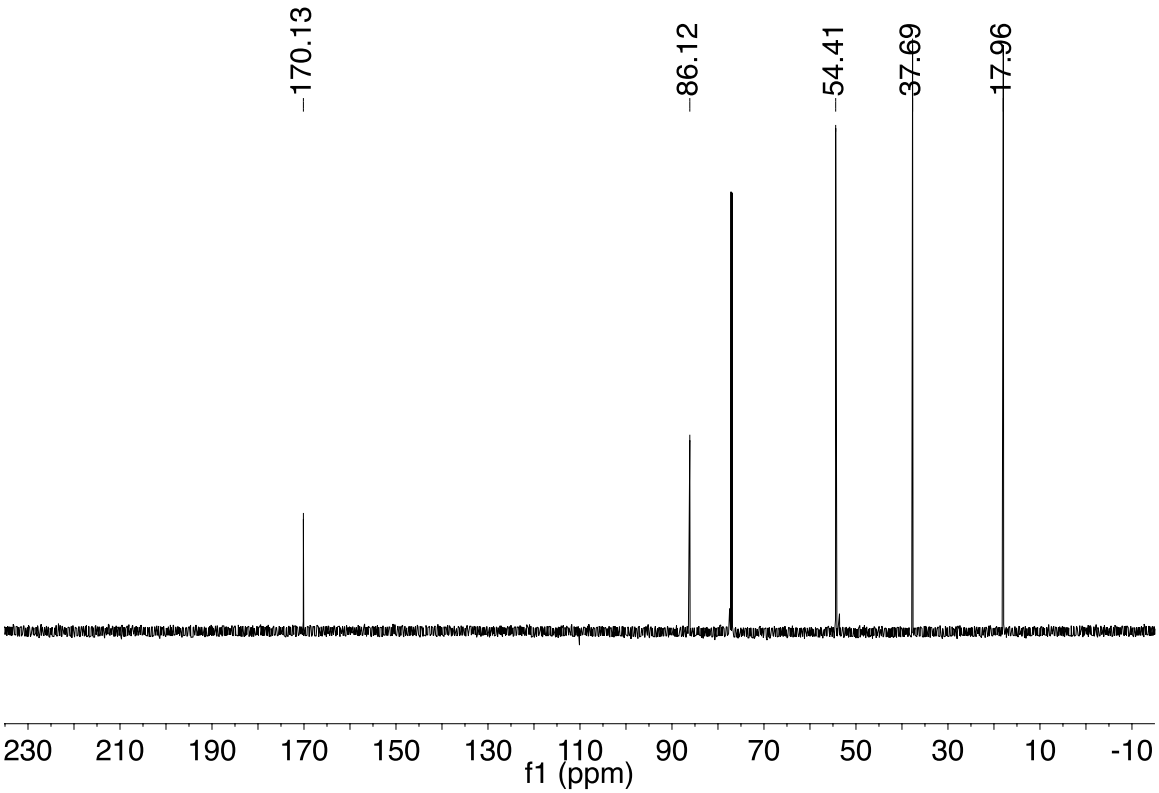

Mixture of *rac*-7-isopropyl-2,5-dimethylbicyclo[2.2.2]oct-5-ene-2,3-dicarboxylic anhydride and *rac*-8-isopropyl-2,6-dimethylbicyclo[2.2.2]oct-5-ene-2,3-dicarboxylic anhydride [1f]

^{1}H NMR (600 MHz, $CDCl_3$)

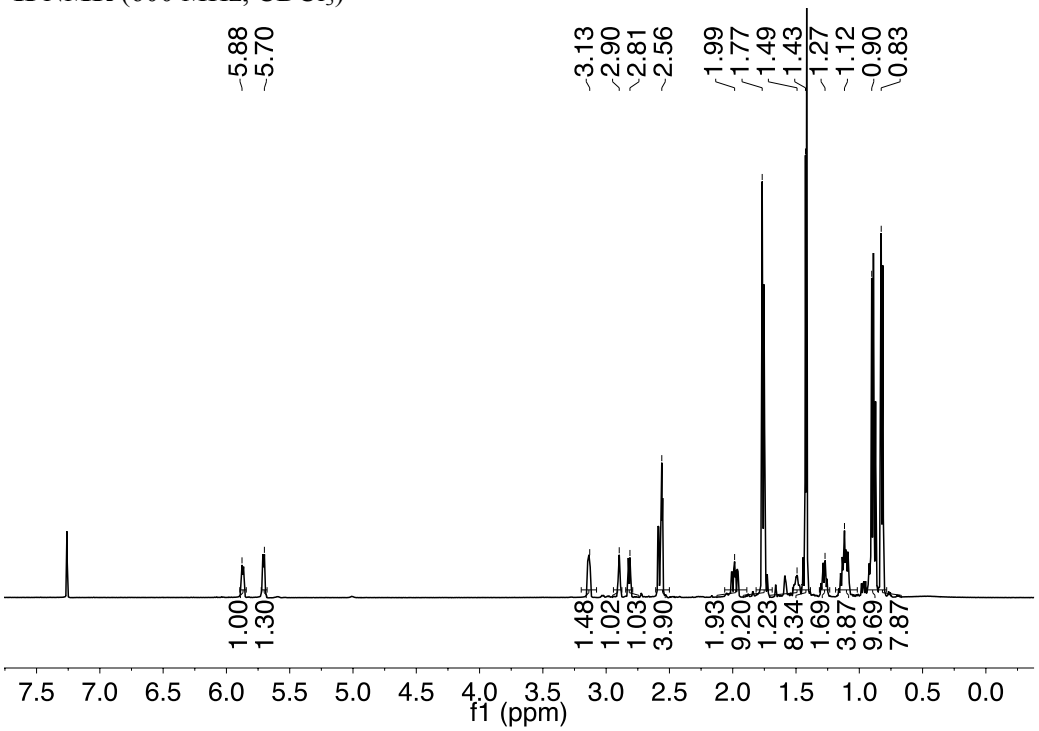

Mixture of *rac*-7-isopropyl-2,5-dimethylbicyclo[2.2.2]oct-5-ene-2,3-dicarboxylic anhydride and *rac*-8-isopropyl-2,6-dimethylbicyclo[2.2.2]oct-5-ene-2,3-dicarboxylic anhydride [1f]

^{13}C NMR (125 MHz, $CDCl_3$)

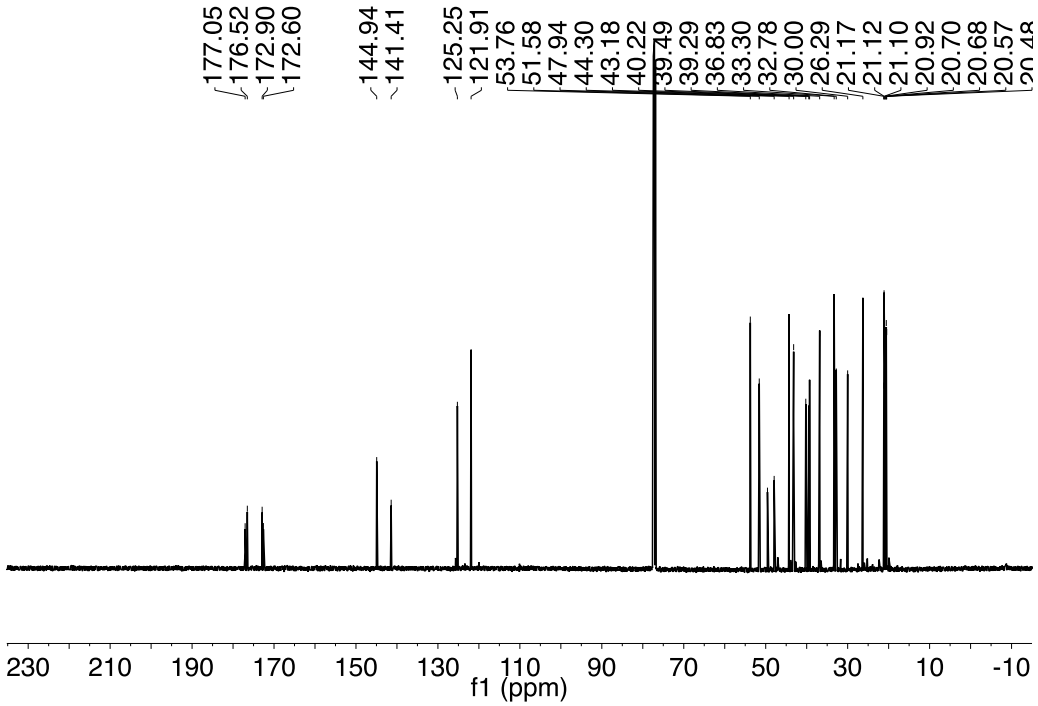

***Rac-cis-endo*-7-isopropyl-5-methylbicyclo[2.2.2]oct-5-ene-2,3-diyl)dimethanol**
^{1}H NMR (400 MHz, $CDCl_3$)

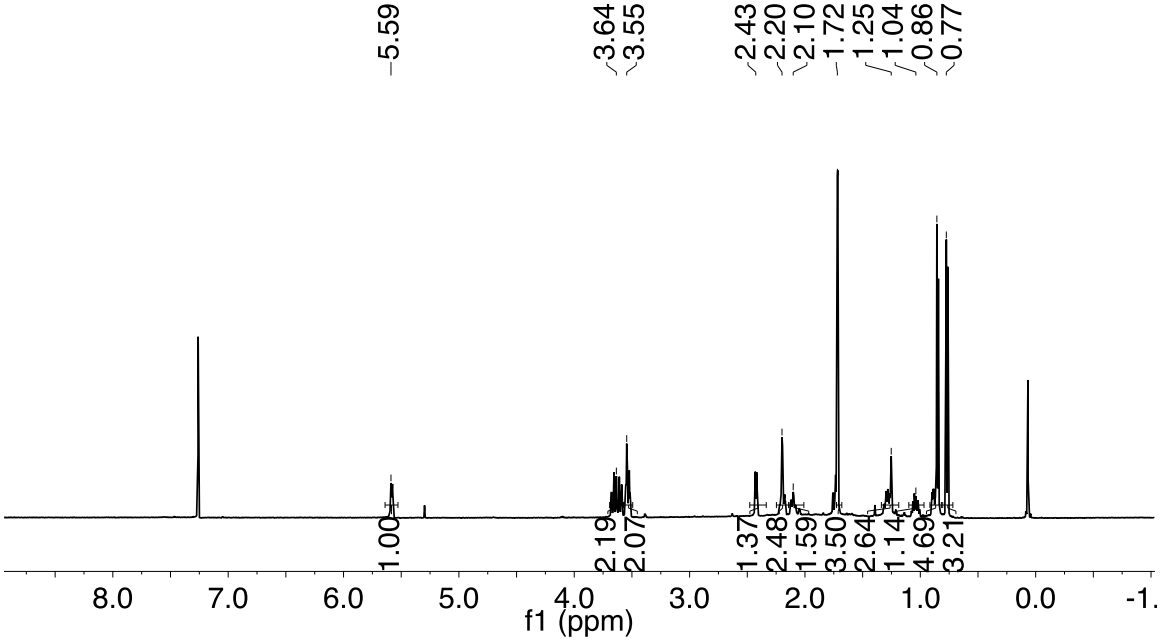

***Rac-cis-endo*-7-isopropyl-5-methylbicyclo[2.2.2]oct-5-ene-2,3-diyl)dimethanol**
^{13}C NMR (125 MHz, $CDCl_3$)

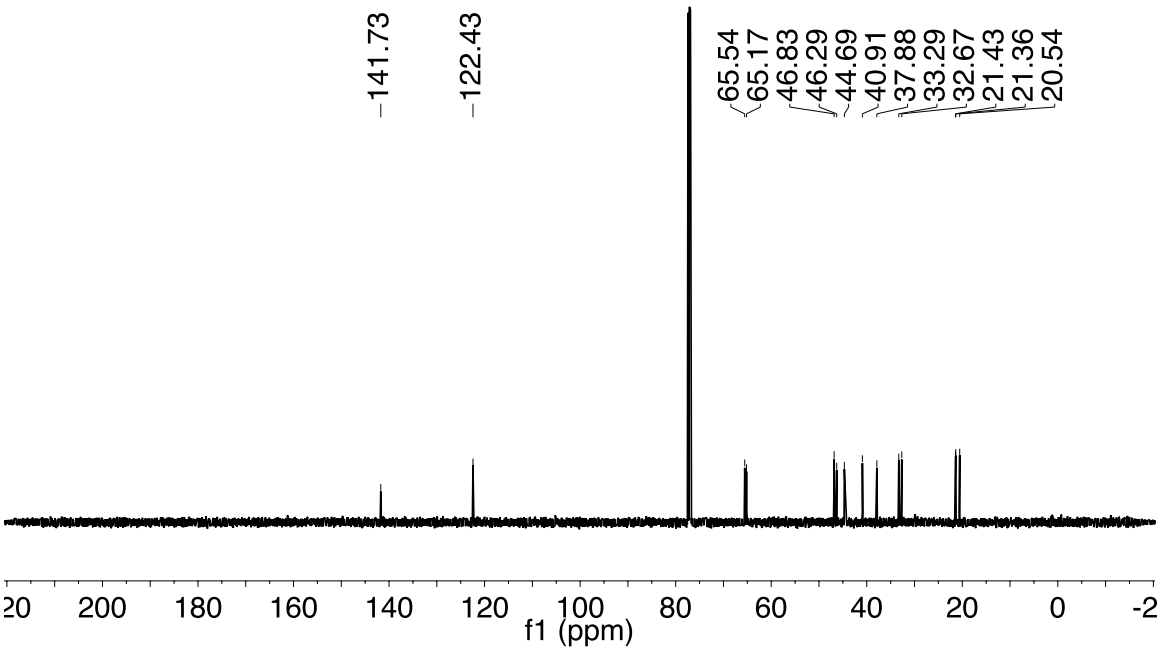

***Rac-cis-endo*-2-methylbicyclo[2.2.1]hept-5-ene-2,3-diyl)dimethanol**
^{1}H NMR (400 MHz, $CDCl_3$)

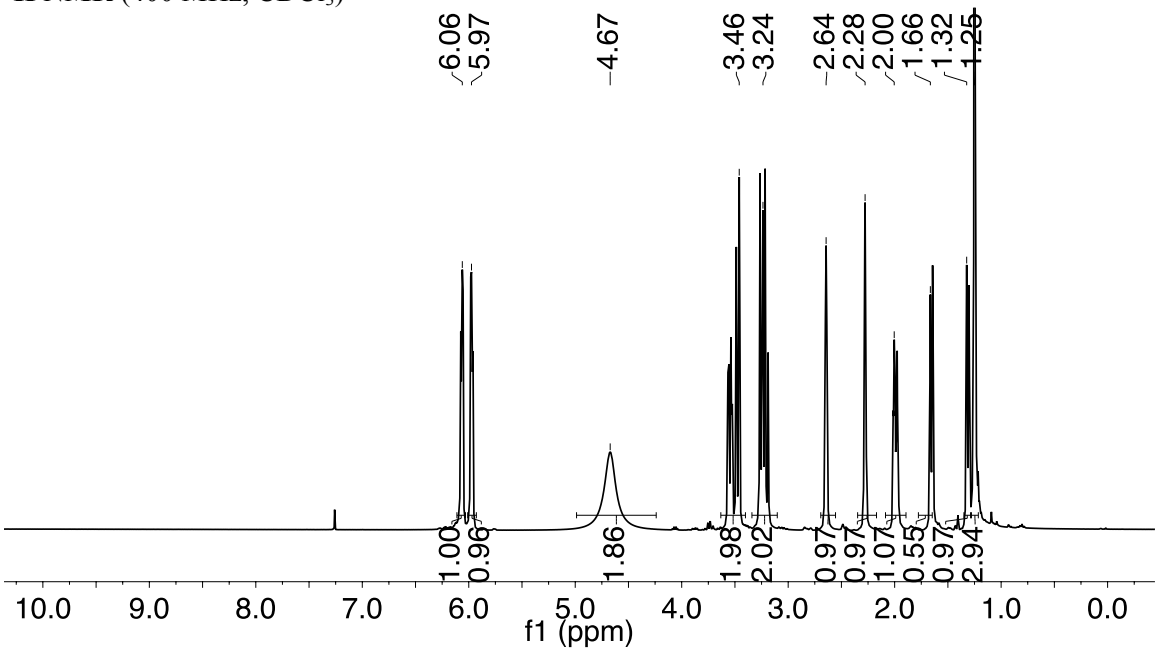

***Rac-cis-endo*-2-methylbicyclo[2.2.1]hept-5-ene-2,3-diyl)dimethanol**
^{13}C NMR (125 MHz, $CDCl_3$)

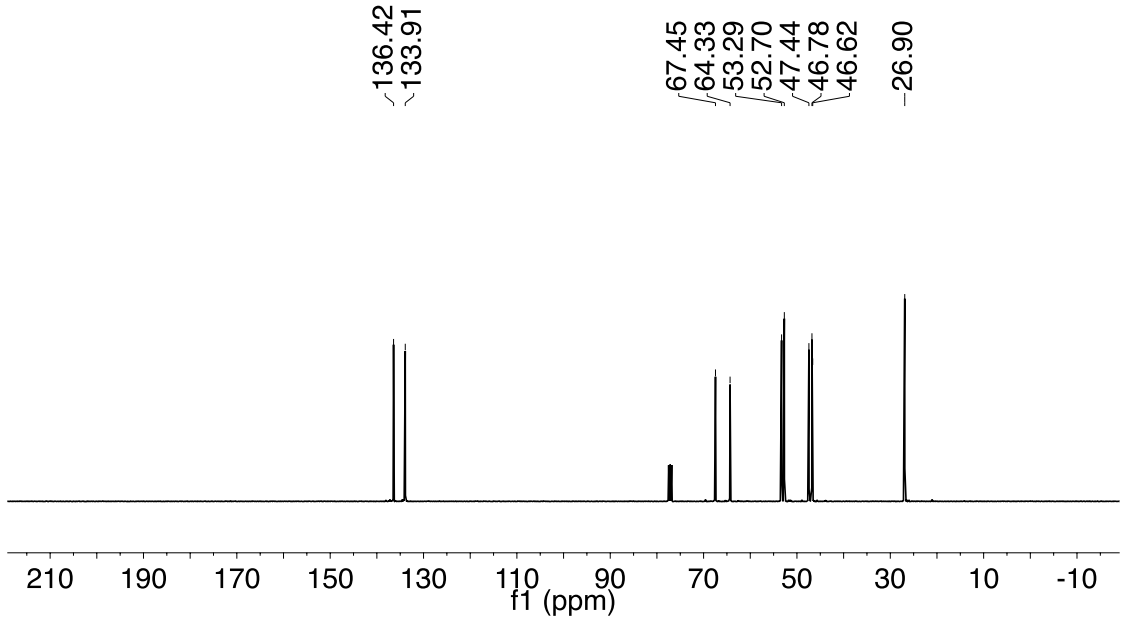

***Rac-trans* -2-methylbicyclo[2.2.1]hept-5-ene-2,3-diyl)dimethanol**

^{1}H NMR (400 MHz, $CDCl_3$)

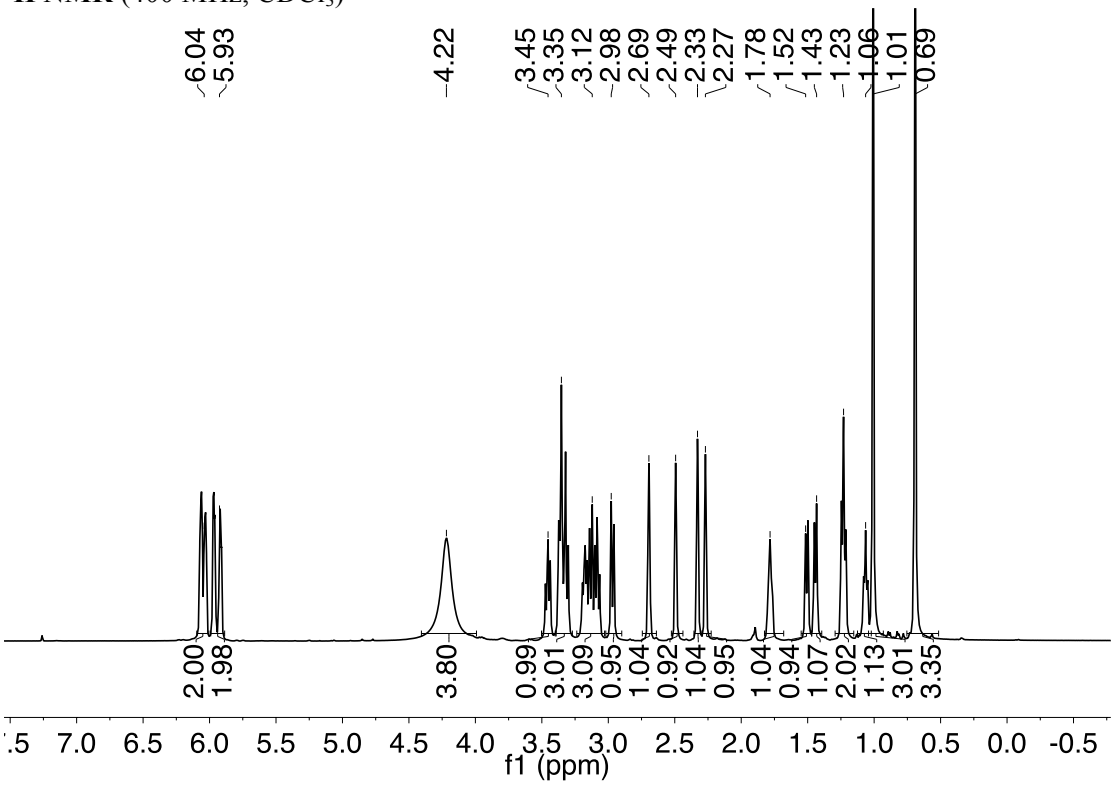

***Rac-trans* -2-methylbicyclo[2.2.1]hept-5-ene-2,3-diyl)dimethanol**

^{13}C NMR (125 MHz, $CDCl_3$)

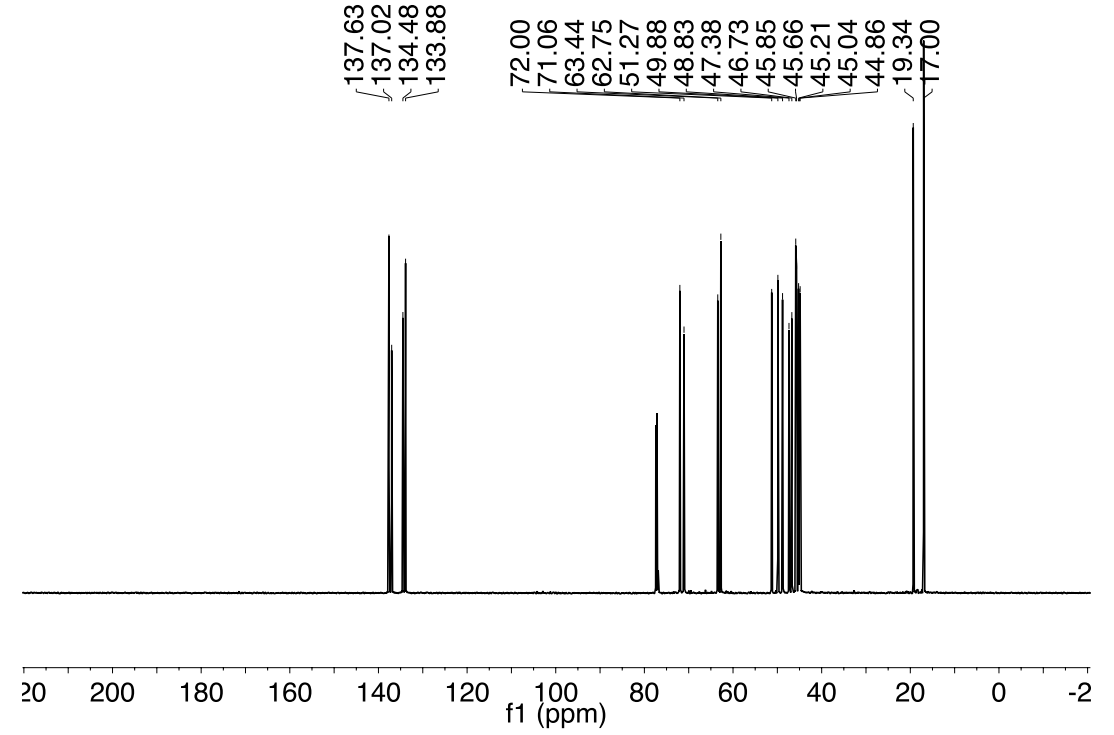

***Rac*-2-methylbicyclo[2.2.2]oct-5-ene-2,3-diyl)dimethanol**

^{1}H NMR (600 MHz, $CDCl_3$)

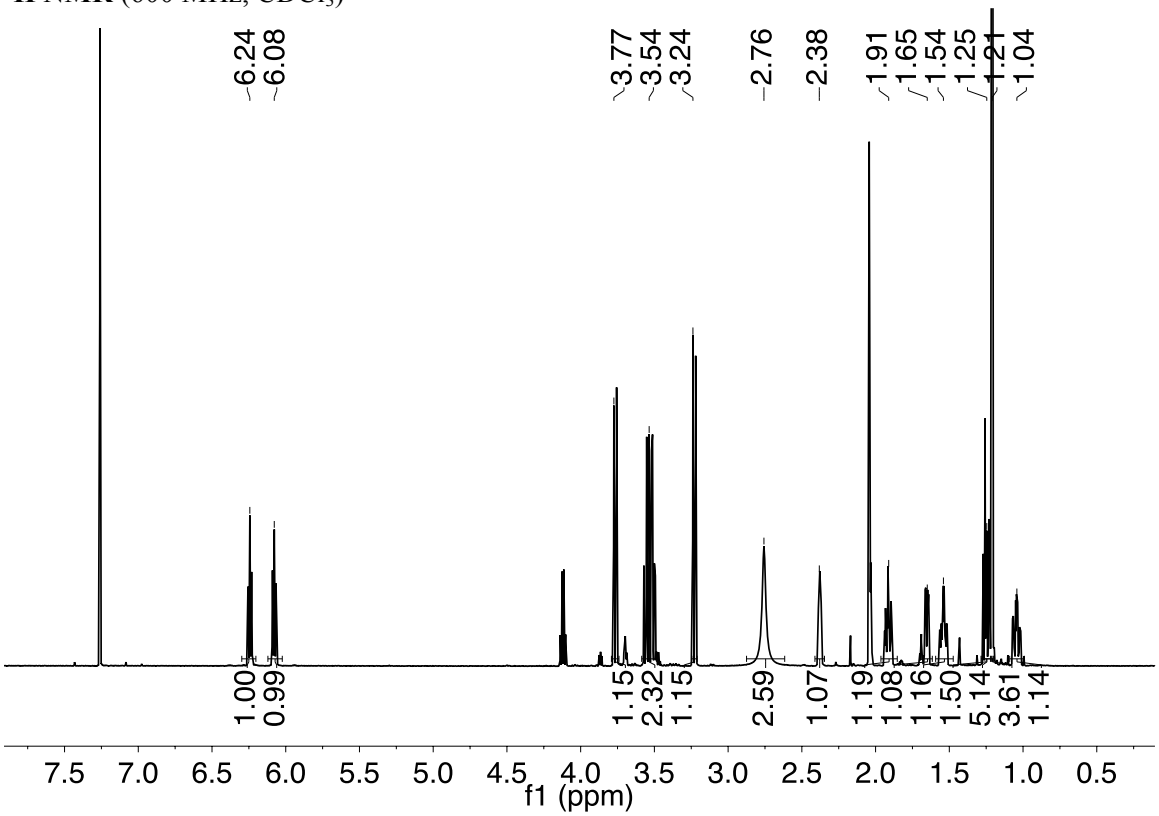

***Rac*-2-methylbicyclo[2.2.2]oct-5-ene-2,3-diyl)dimethanol**

^{13}C NMR (125 MHz, $CDCl_3$

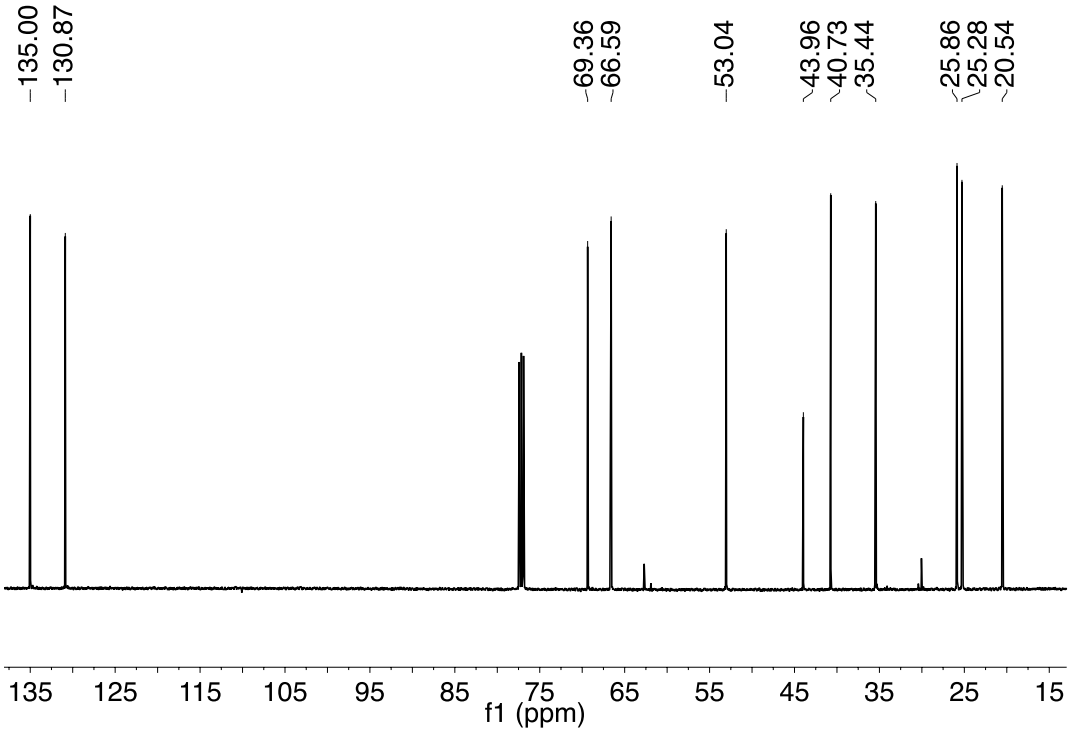

***Rac-cis-endo*-1,4-dimethyl-7-oxabicyclo[2.2.1]heptane-2,3-diyl)dimethanol**
^{1}H NMR (400 MHz, $CDCl_3$)

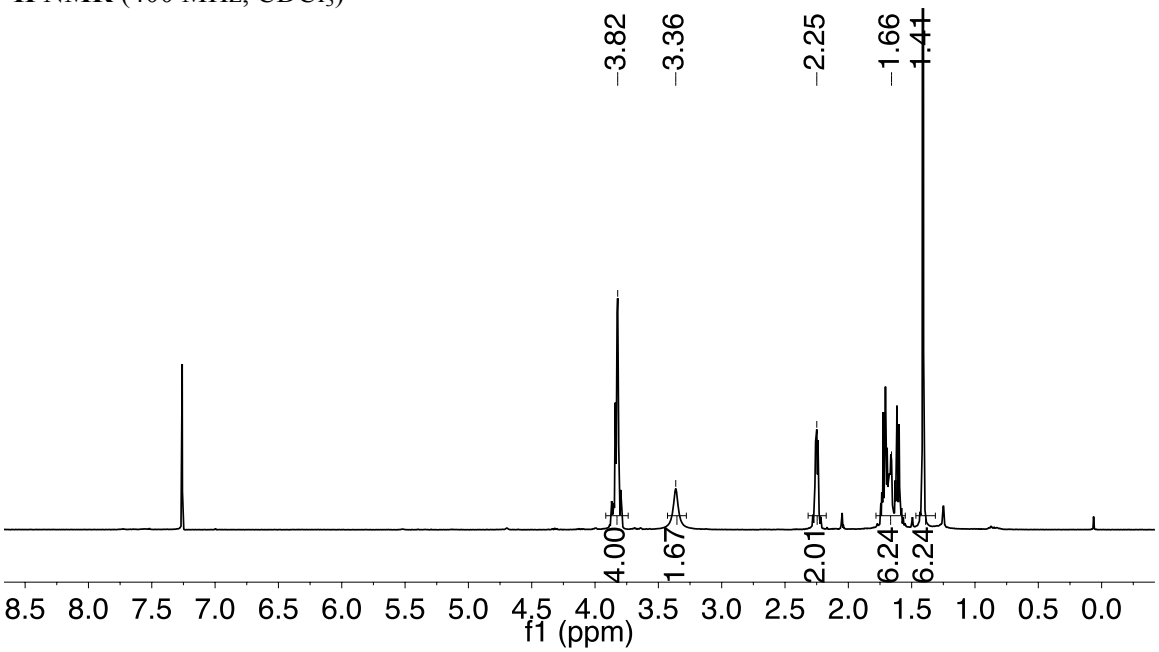

***Rac-cis-endo*-1,4-dimethyl-7-oxabicyclo[2.2.1]heptane-2,3-diyl)dimethanol**
^{13}C NMR (125 MHz, $CDCl_3$)

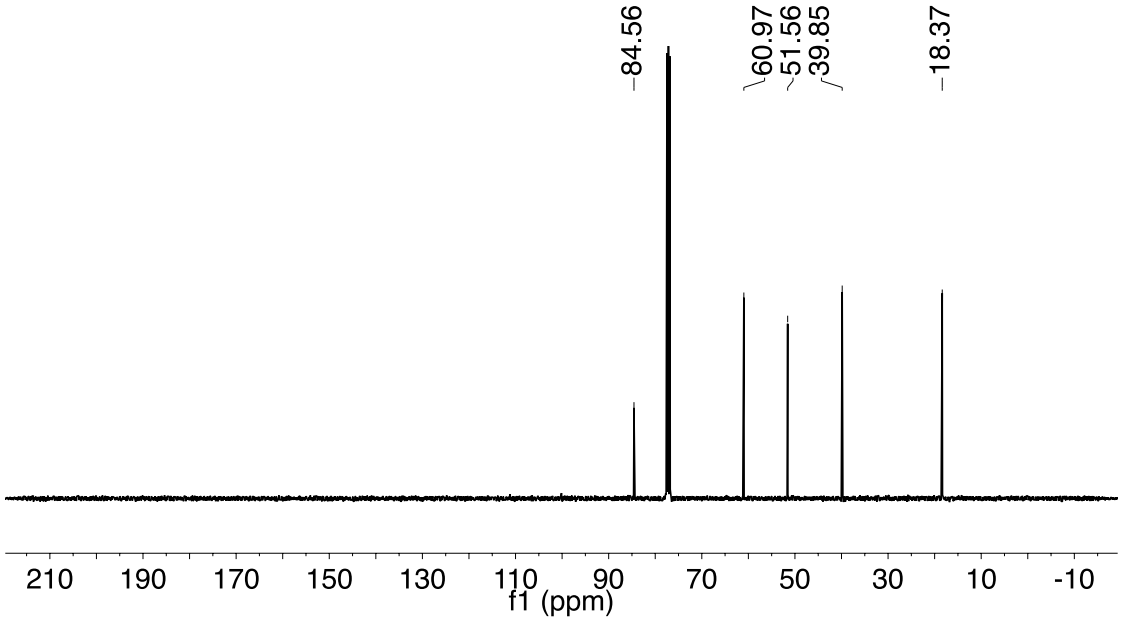

***Rac-trans*-1,4-dimethyl-7-oxabicyclo[2.2.1]heptane-2,3-diyl)dimethanol**
^{1}H NMR (400 MHz, $CDCl_3$)

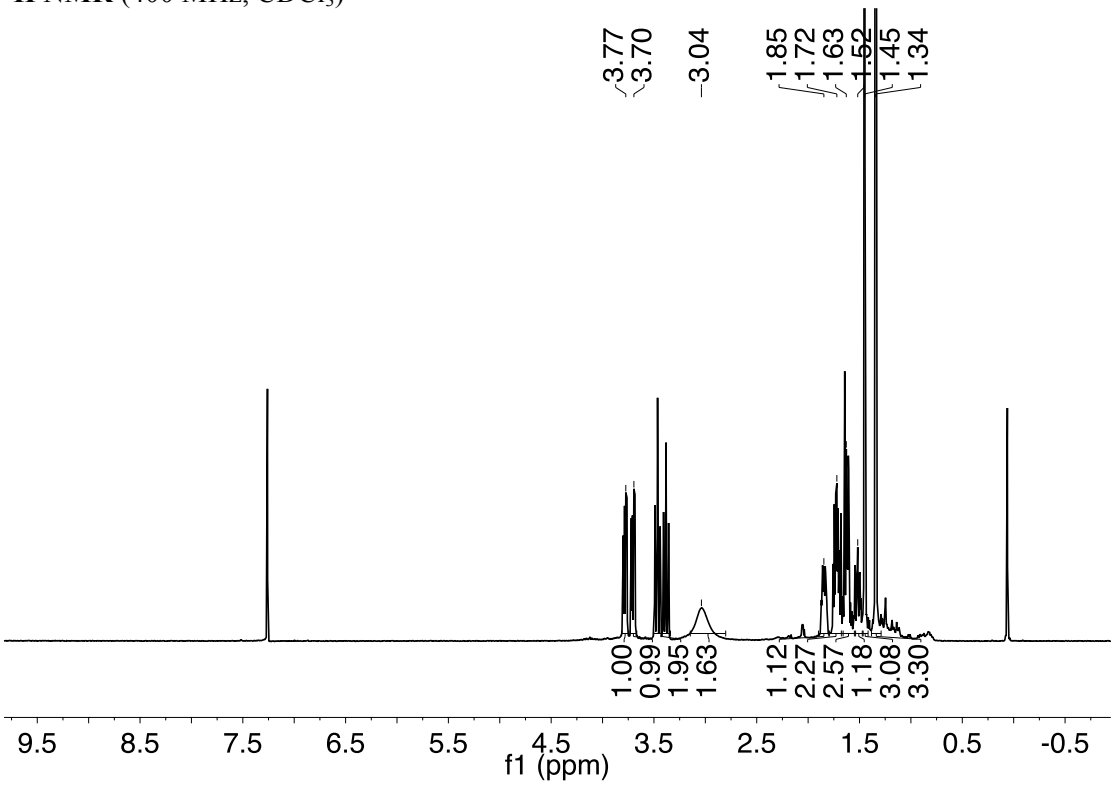

***Rac-trans*-1,4-dimethyl-7-oxabicyclo[2.2.1]heptane-2,3-diyl)dimethanol**
^{13}C NMR (125 MHz, $CDCl_3$)

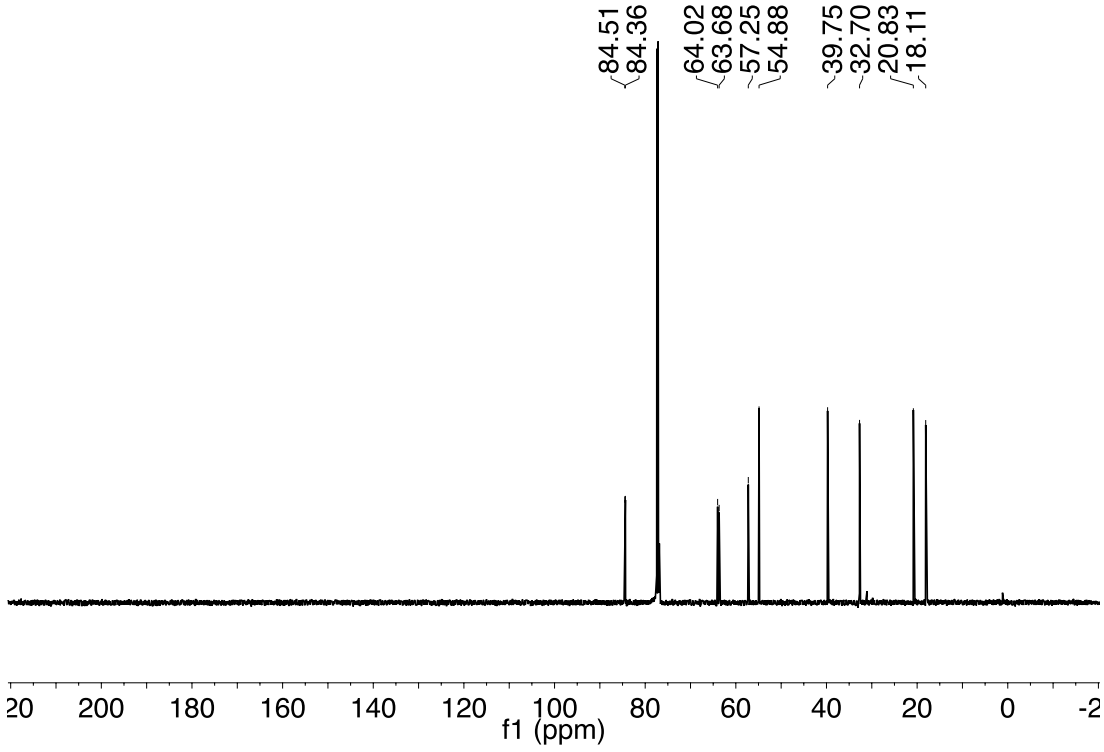

Mixture of *rac-cis*-7-isopropyl-2,5-dimethylbicyclo[2.2.2]oct-5-ene-2,3-diyl)dimethanol and *rac-cis*-8-isopropyl-2,6-dimethylbicyclo[2.2.2]oct-5-ene-2,3-diyl)dimethanol
^{1}H NMR (600 MHz, $CDCl_3$)

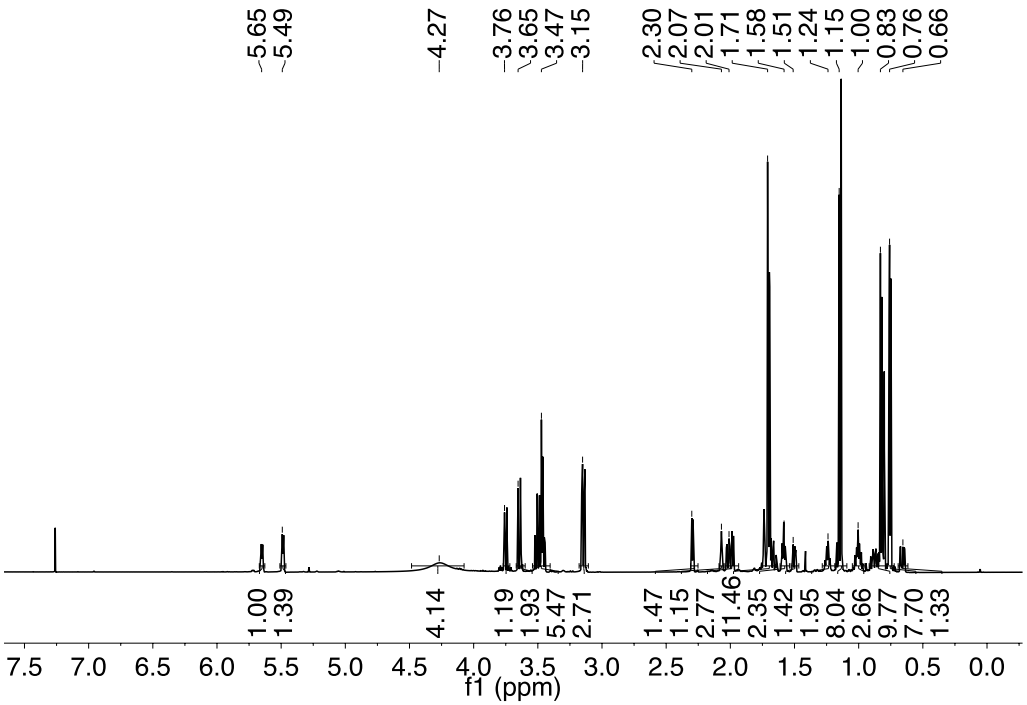

Mixture of *rac-cis*-7-isopropyl-2,5-dimethylbicyclo[2.2.2]oct-5-ene-2,3-diyl)dimethanol and *rac-cis*-8-isopropyl-2,6-dimethylbicyclo[2.2.2]oct-5-ene-2,3-diyl)dimethanol
^{13}C NMR (125 MHz, $CDCl_3$)

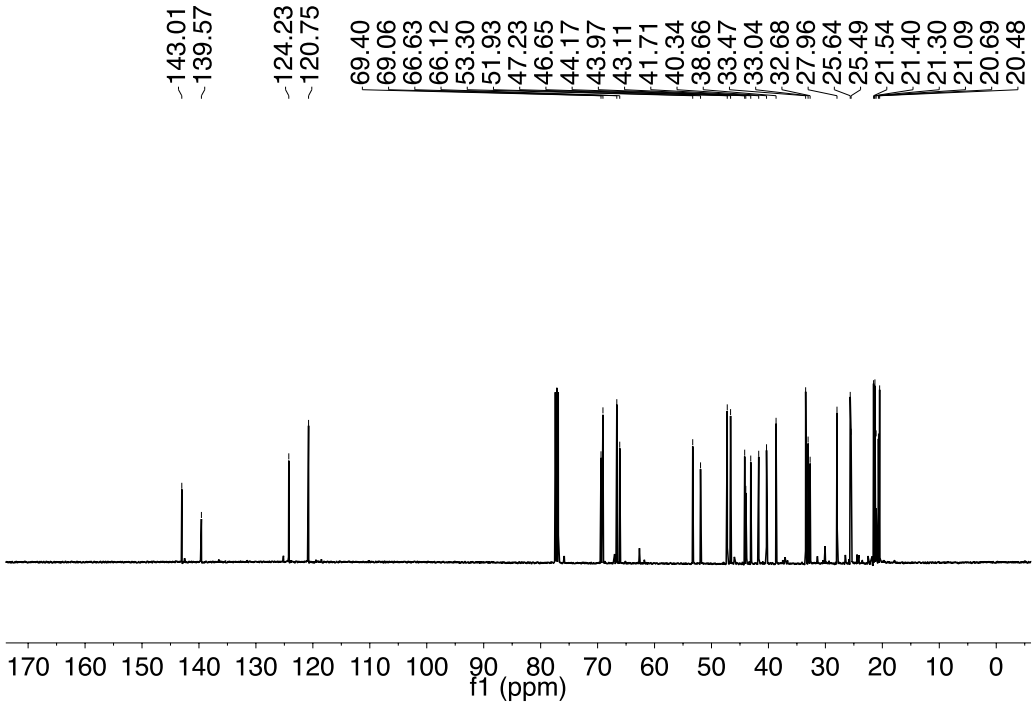

13. Assigned ^{1}H and ^{13}C NMR Spectra of Polymers

All ^{1}H NMR spectra were acquired at 400 MHz in $CDCl_3$; ^{13}C NMR spectra were acquired at 125 MHz in $CDCl_3$. Assignments were made on the basis of 2D NMR.

Figure S29. a)^{1}H NMR of poly(PO-*alt*-**1a**) and b) ^{13}C NMR of poly(PO-*alt*-**1a**)

a)

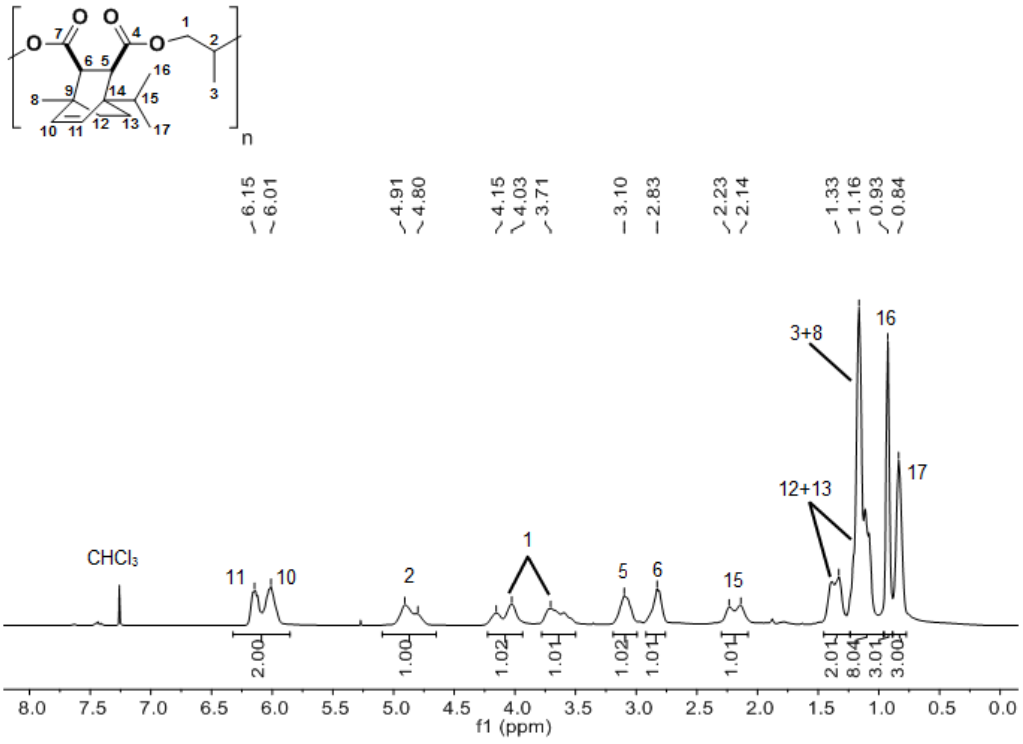

b)

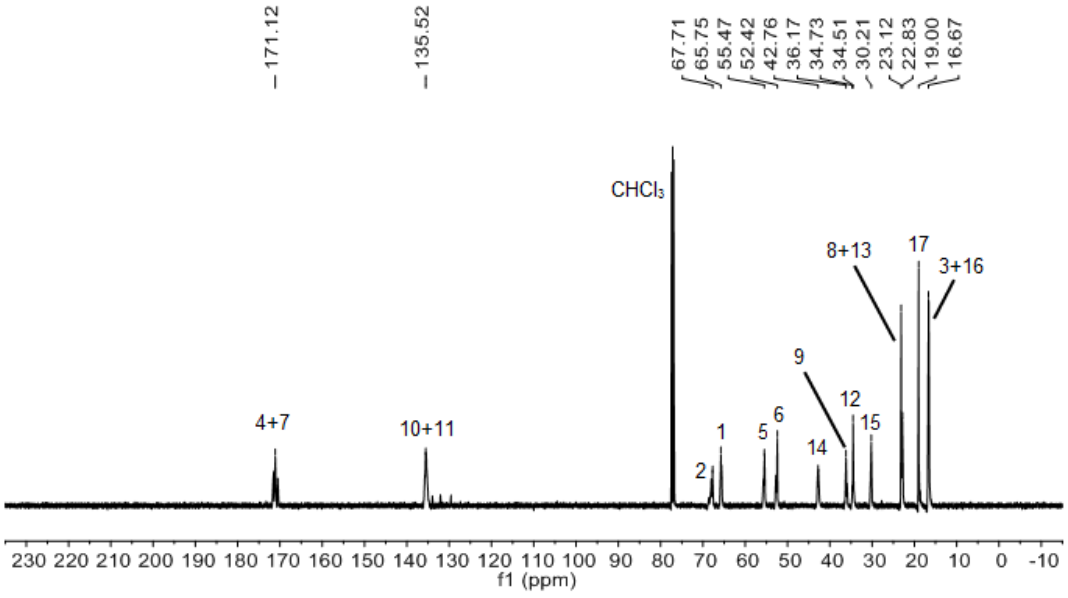

Figure S30. a)[1]H NMR of poly(PO-*alt*-**1b**) and b) [13]C NMR of poly(PO-*alt*-**1b**)

a)

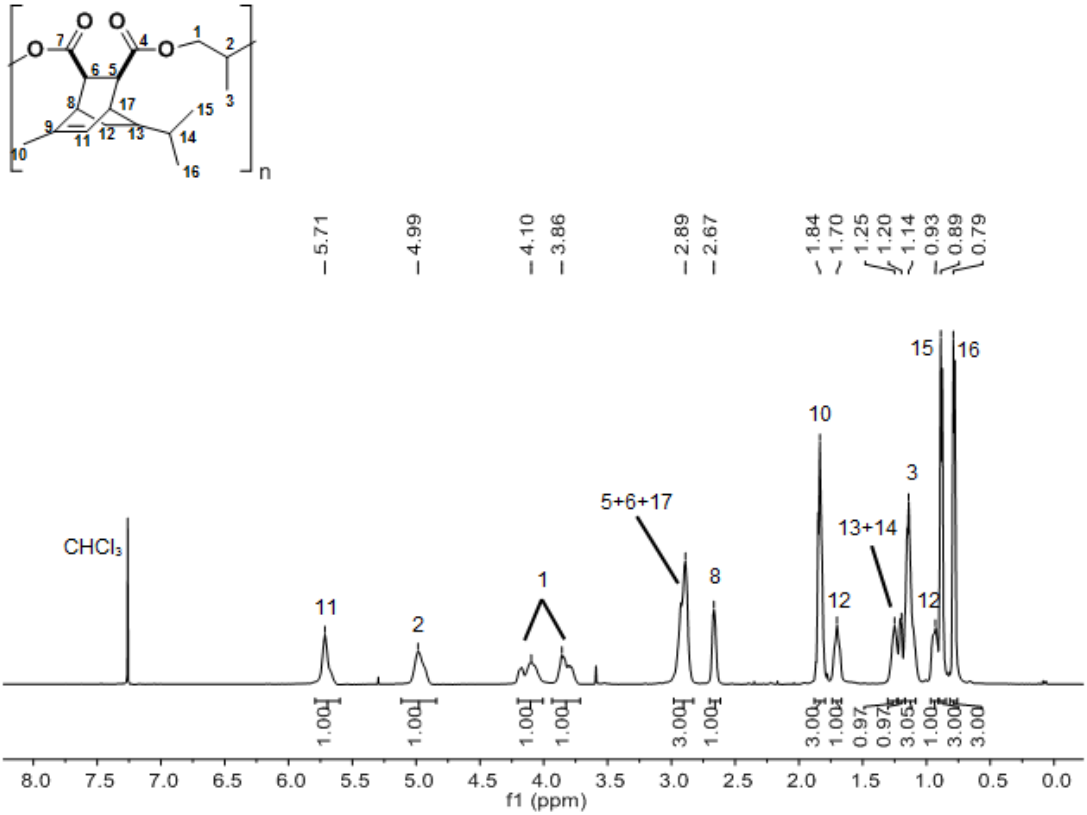

b)

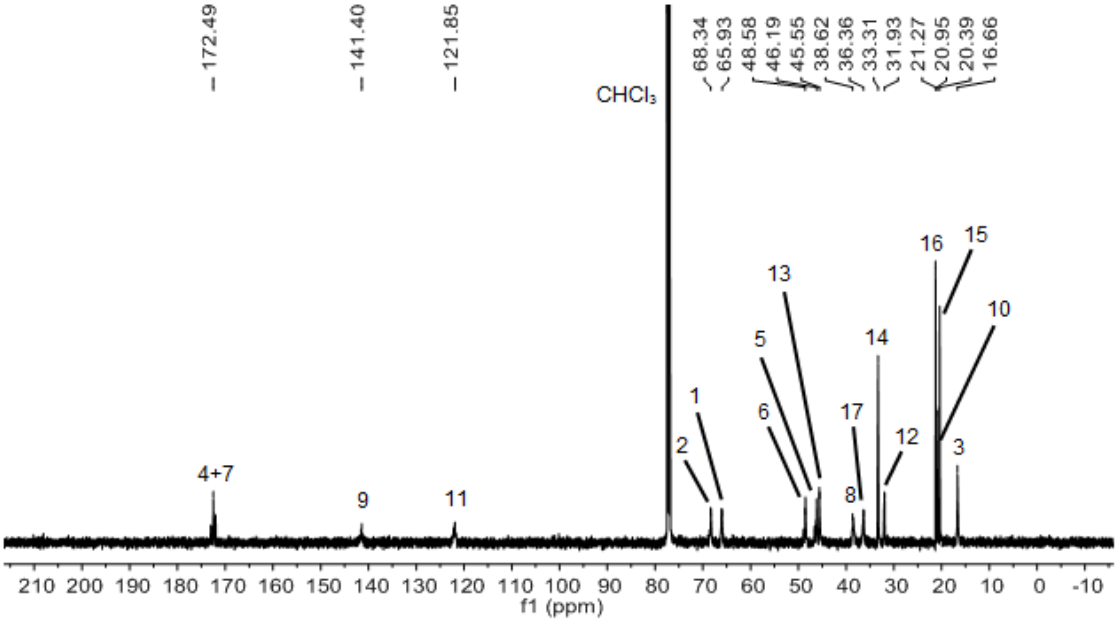

Figure S31. a)[1]H NMR of poly(PO-*alt*-**1c**) and b) [13]C NMR of poly(PO-*alt*-**1c**)

a)

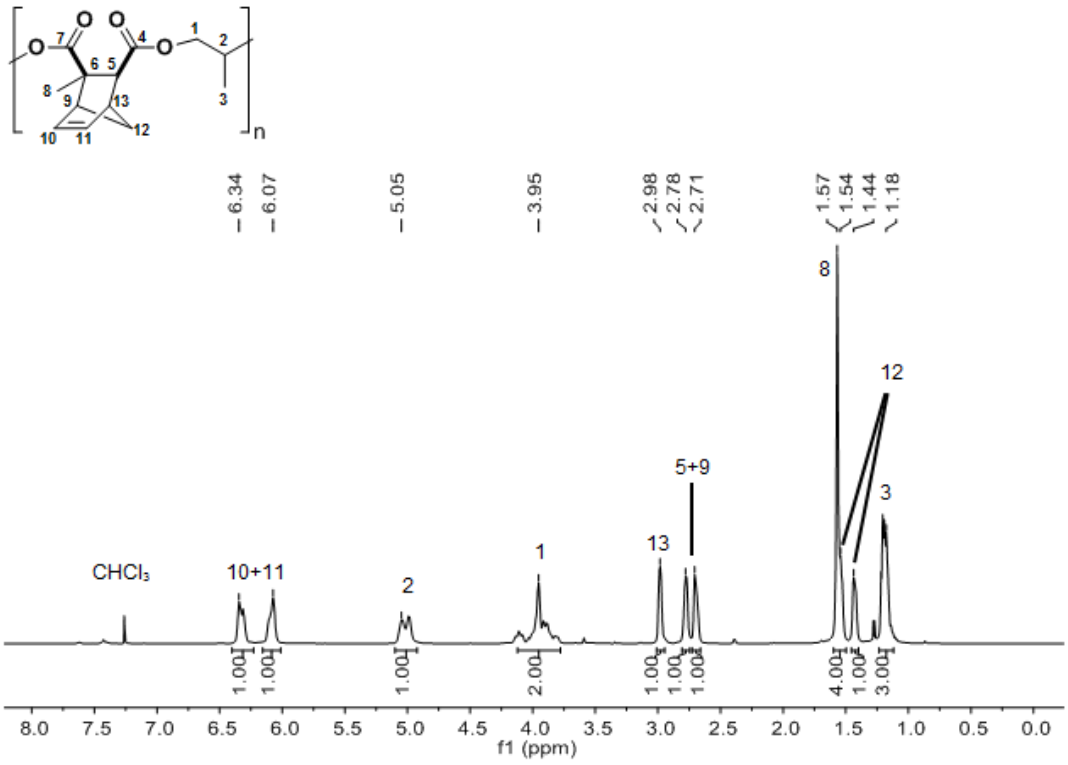

b)

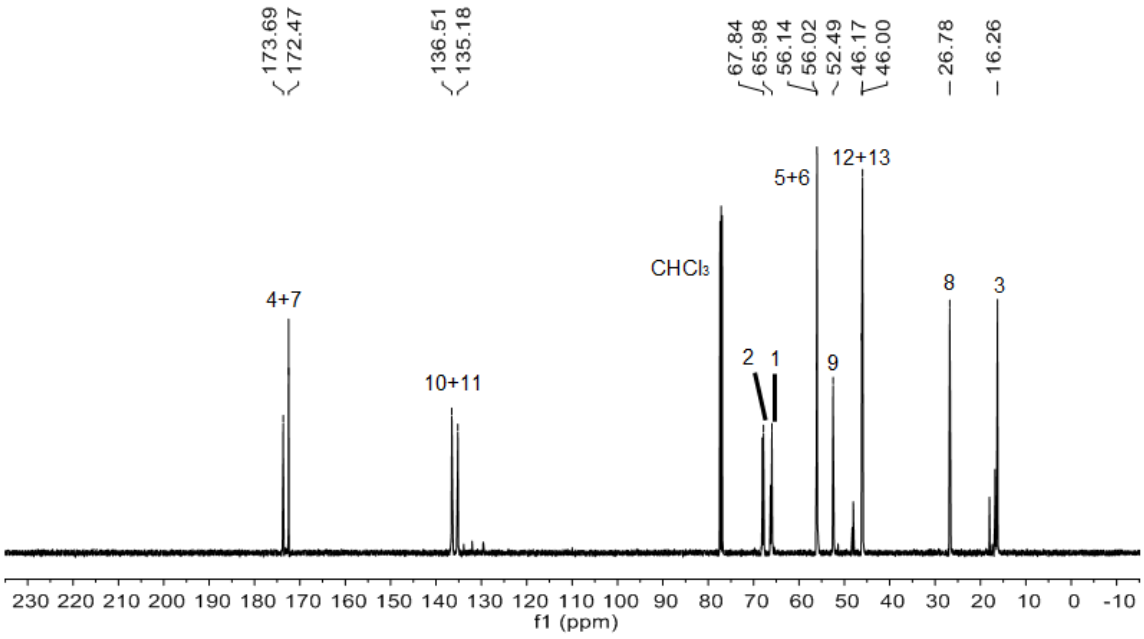

Figure S32. a)[1]H NMR of poly(PO-*alt*-**1d**) and b) [13]C NMR of poly(PO-*alt*-**1d**)

a)

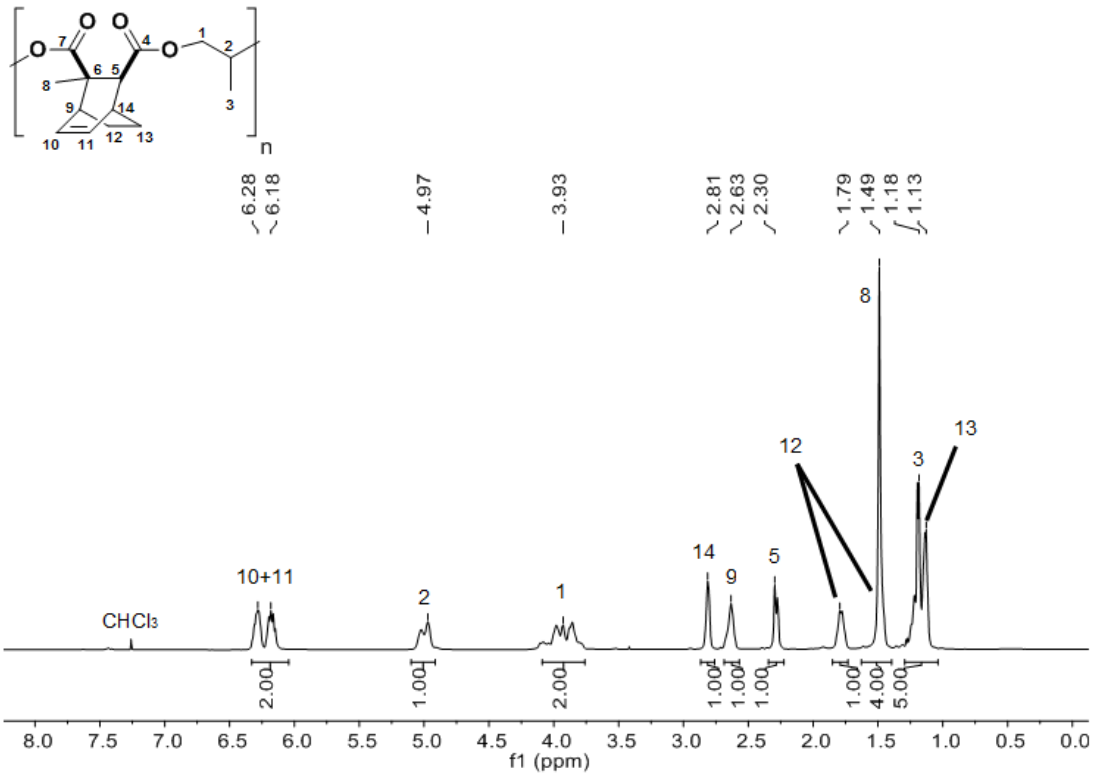

b)

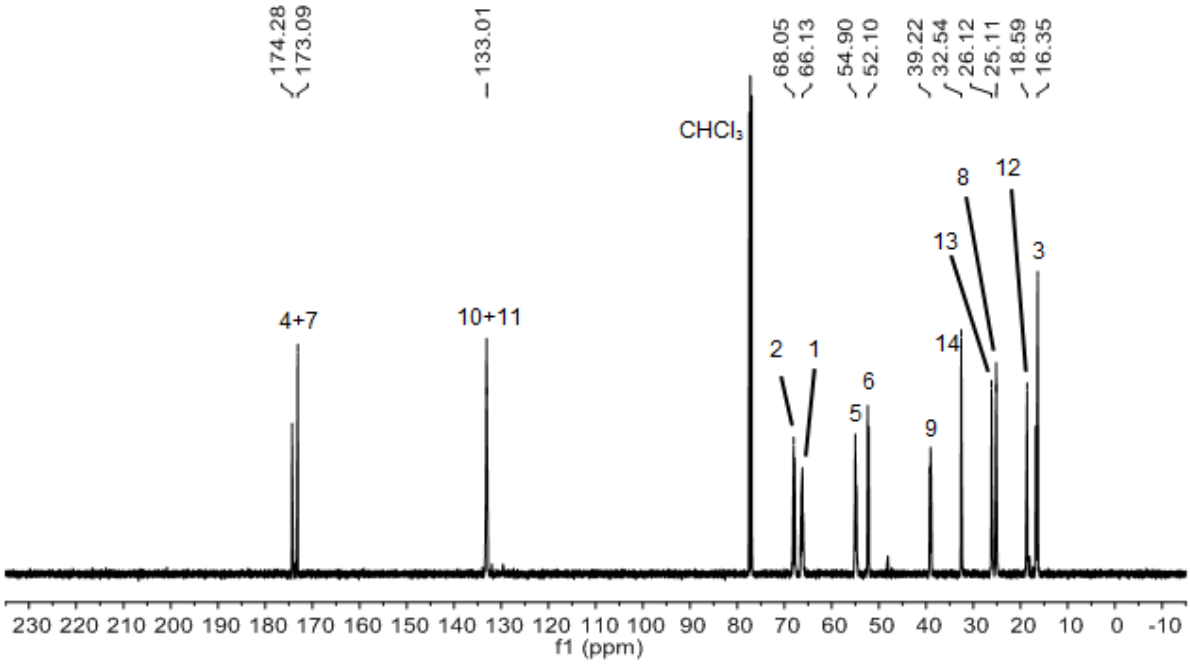

Figure S33. a)[1]H NMR of poly(PO-*alt*-**1e**) and b) [13]C NMR of poly(PO-*alt*-**1e**)

a)

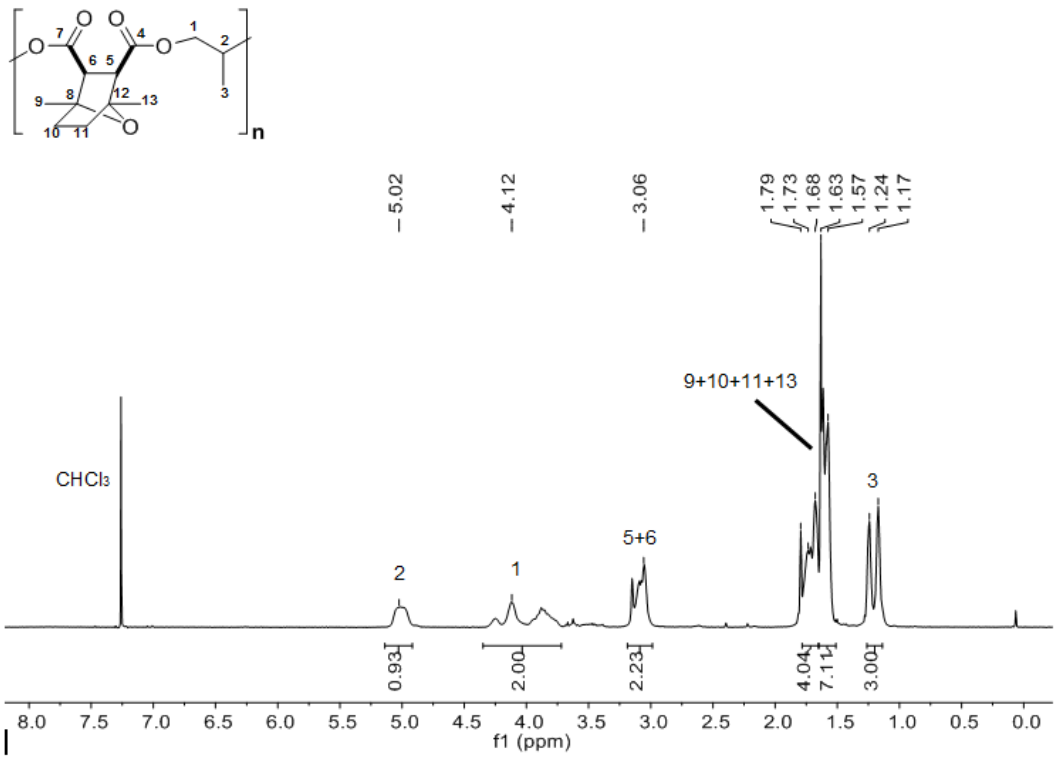

b)

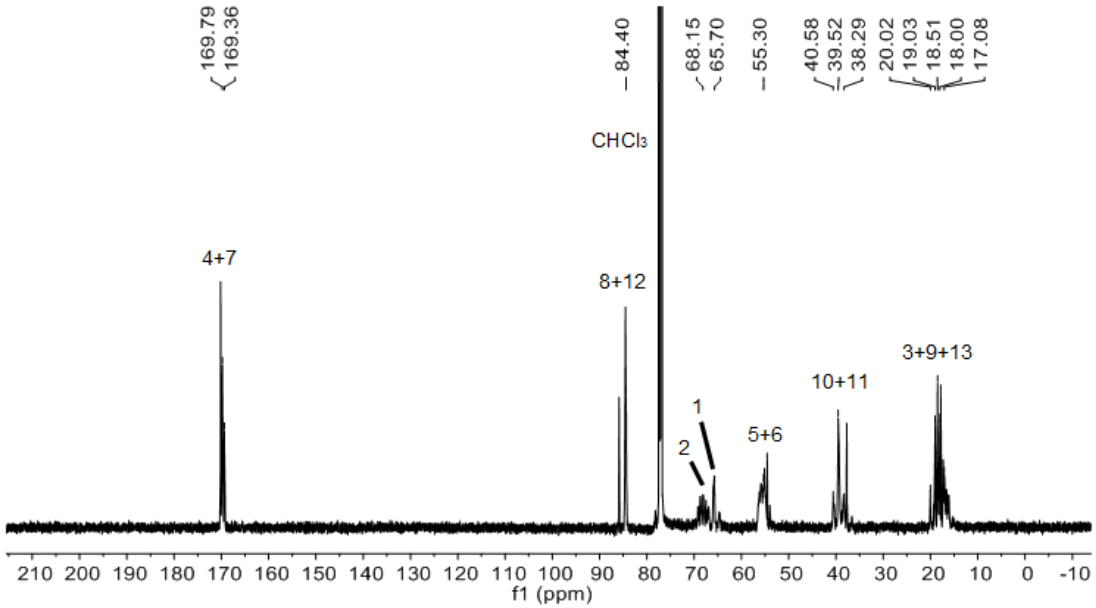

Figure S34. a)[1]H NMR of poly(PO-*alt*-**1f**) and b) [13]C NMR of poly(PO-*alt*-**1f** (Note that while there are multiple possible isomers, the peaks are overlapping and for simplicity's sake only one isomer is drawn.)

a)

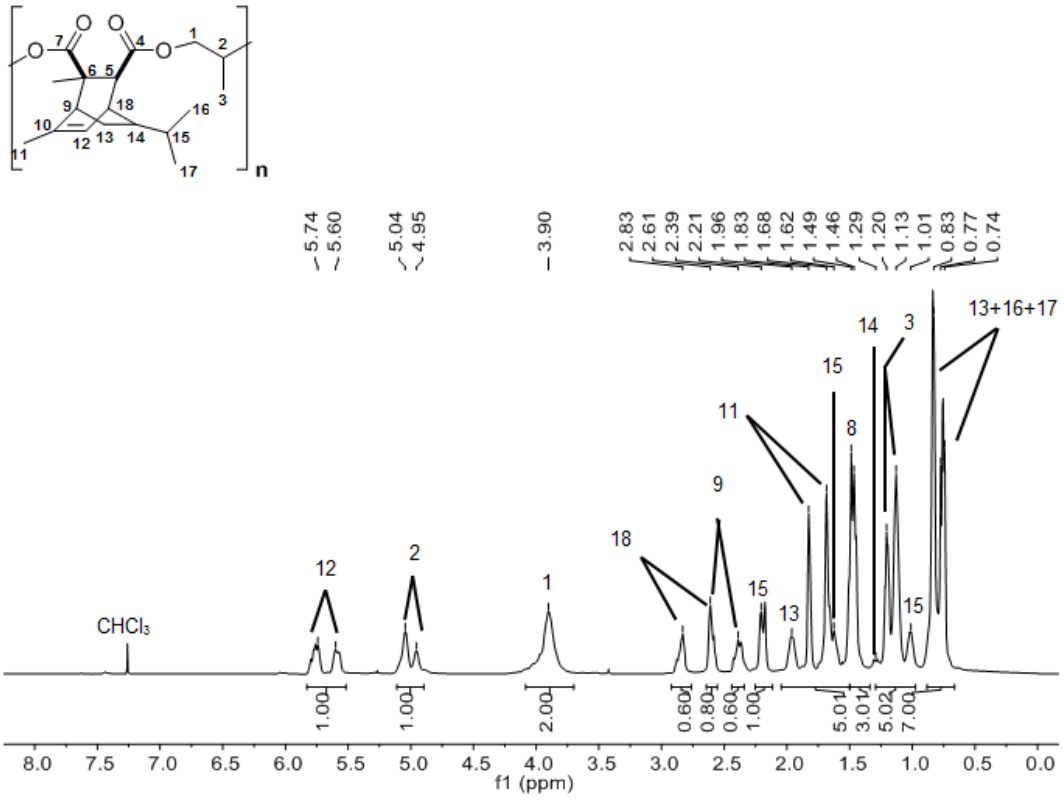

b)

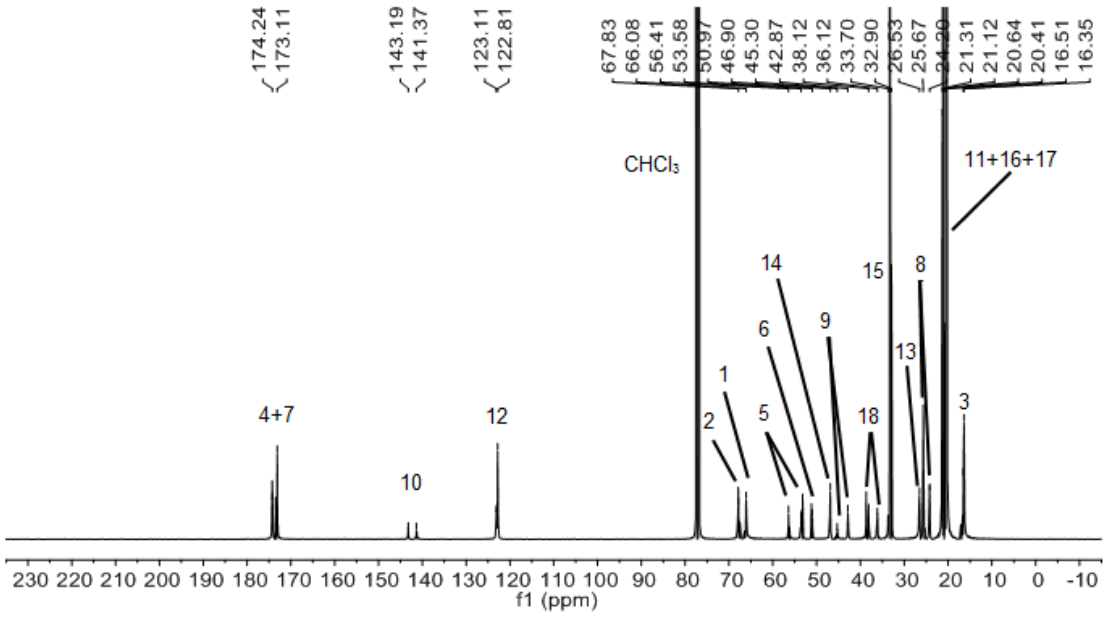

Figure S35. a)[1]H NMR of poly(CHO-*alt*-**1a**) and b) [13]C NMR of poly(CHO-*alt*-**1a**)

a)

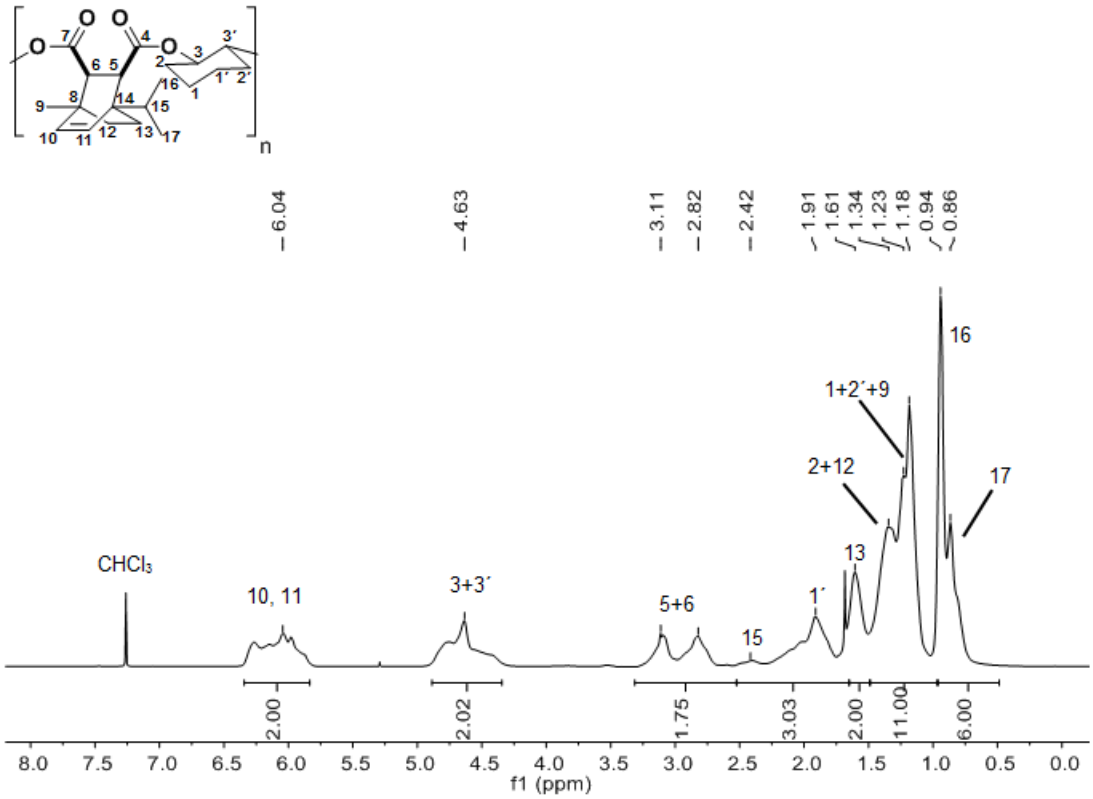

b)

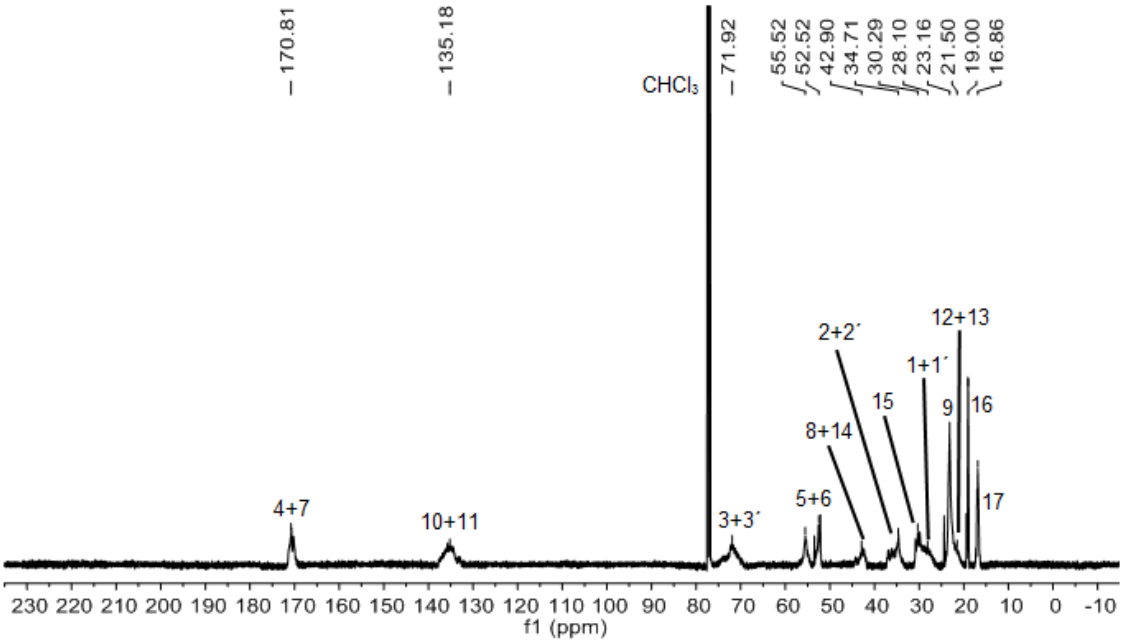

Figure S36. a)[1]H NMR of poly(CHO-*alt*-**1b**) and b) [13]C NMR of poly(CHO-*alt*-**1b**)

a)

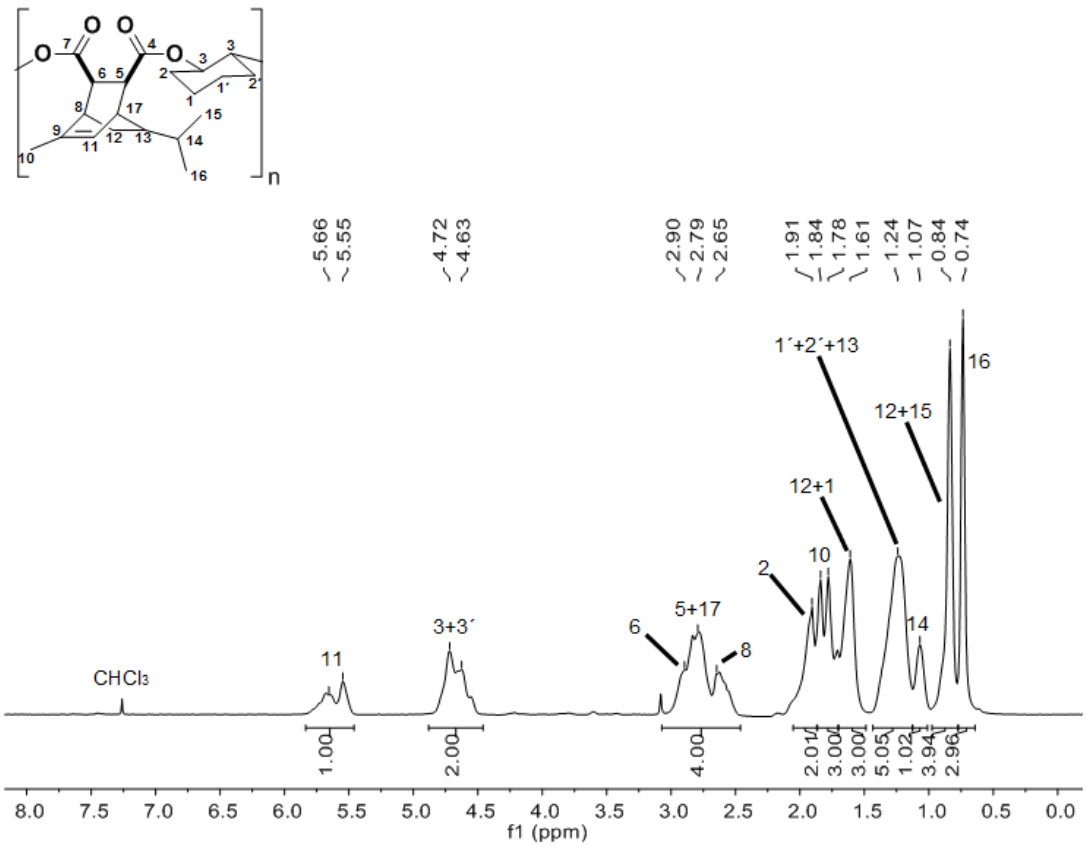

b)

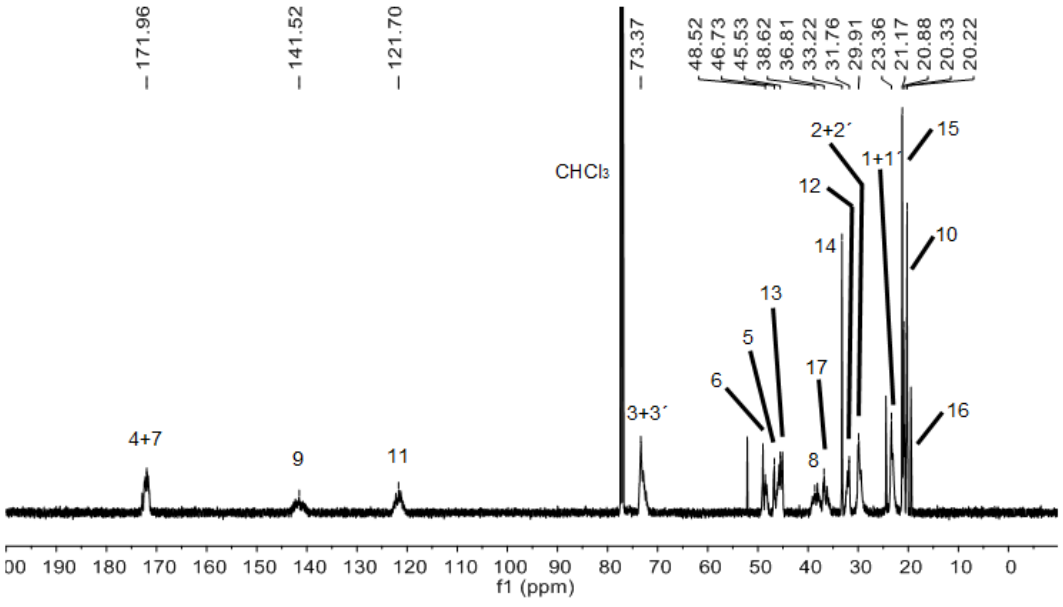

Figure S37. a)[1]H NMR of poly(CHO-*alt*-**1c**) and b) [13]C NMR of poly(CHO-*alt*-**1c**)

a)

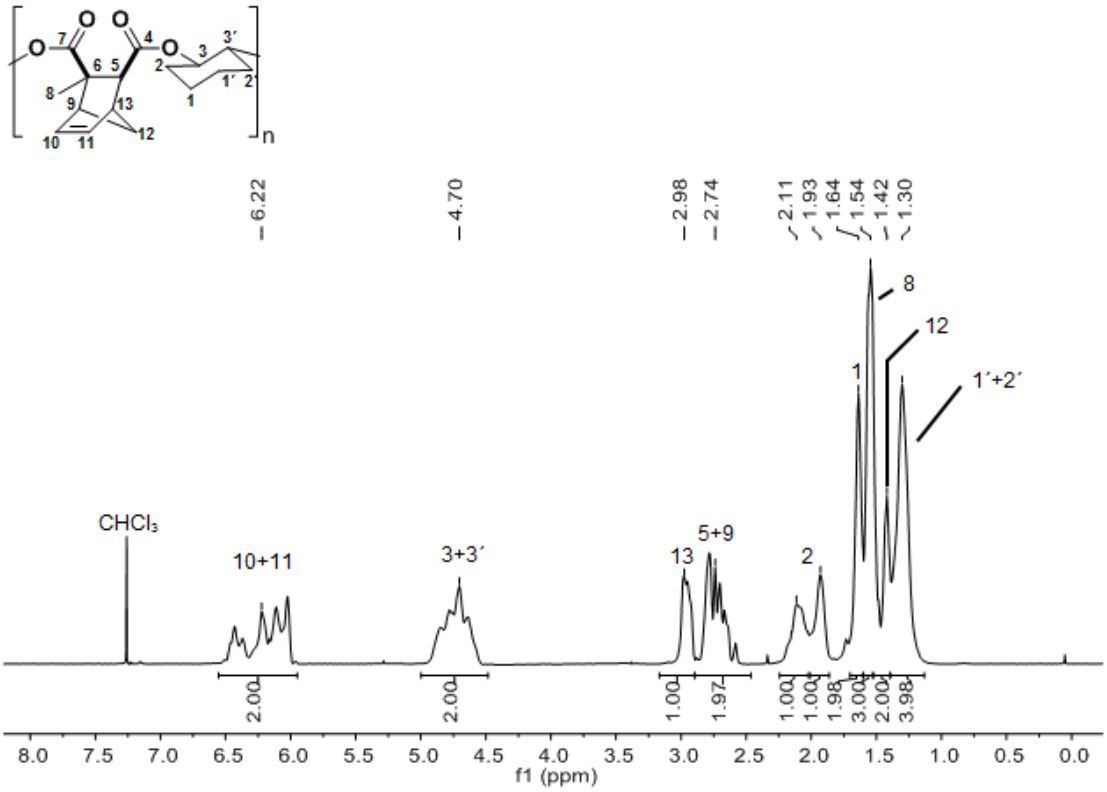

b)

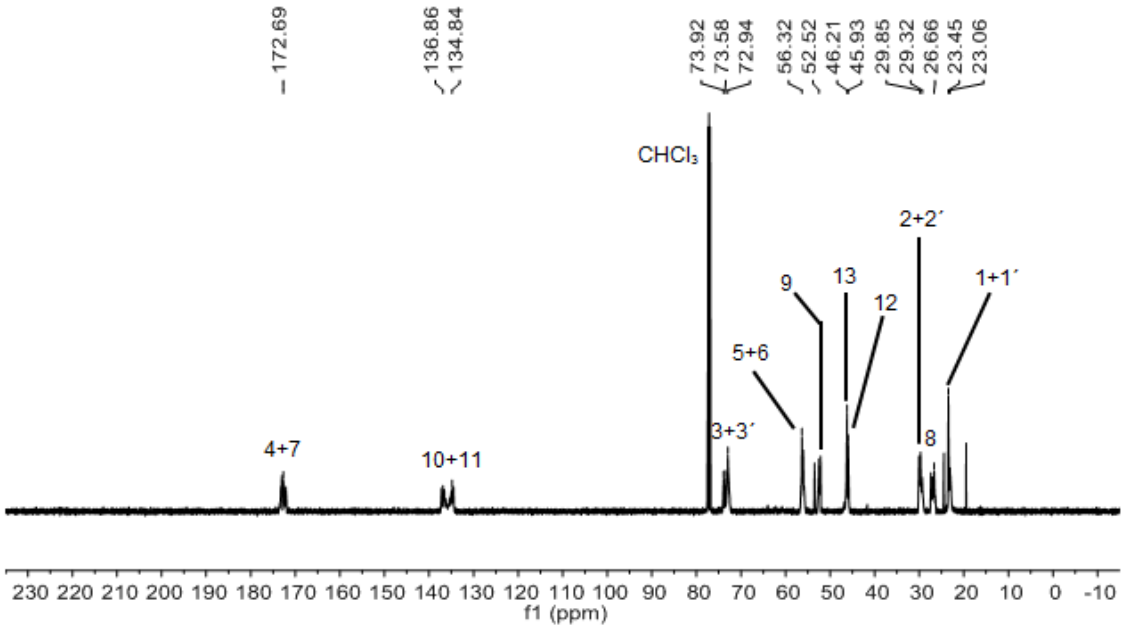

Figure S38. a)[1]H NMR of poly(CHO-*alt*-**1d**) and b) [13]C NMR of poly(CHO-*alt*-**1d**)

a)

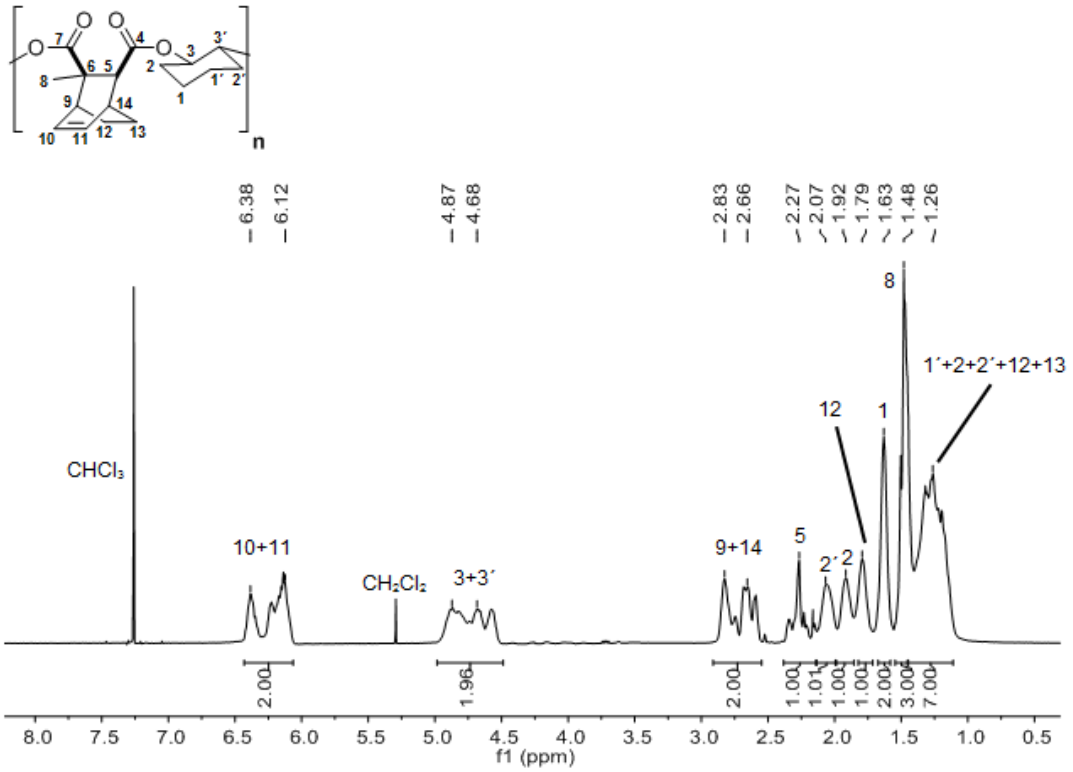

b)

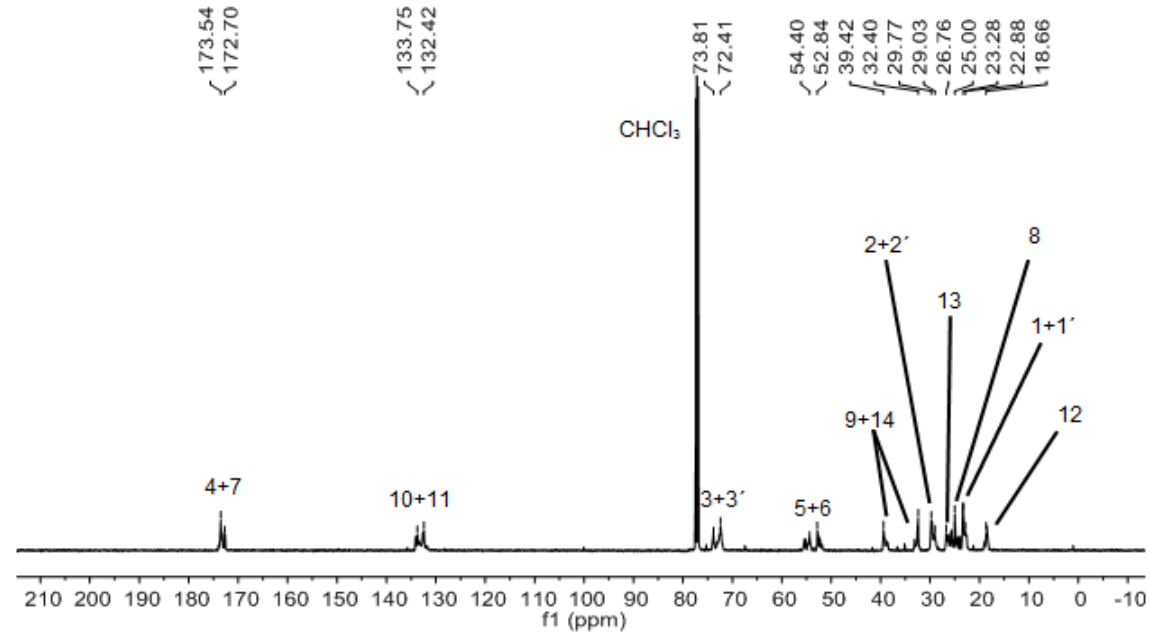

Figure S39. a)[1]H NMR of poly(CHO-*alt*-**1e**) and b) [13]C NMR of poly(CHO-*alt*-**1e**)

a)

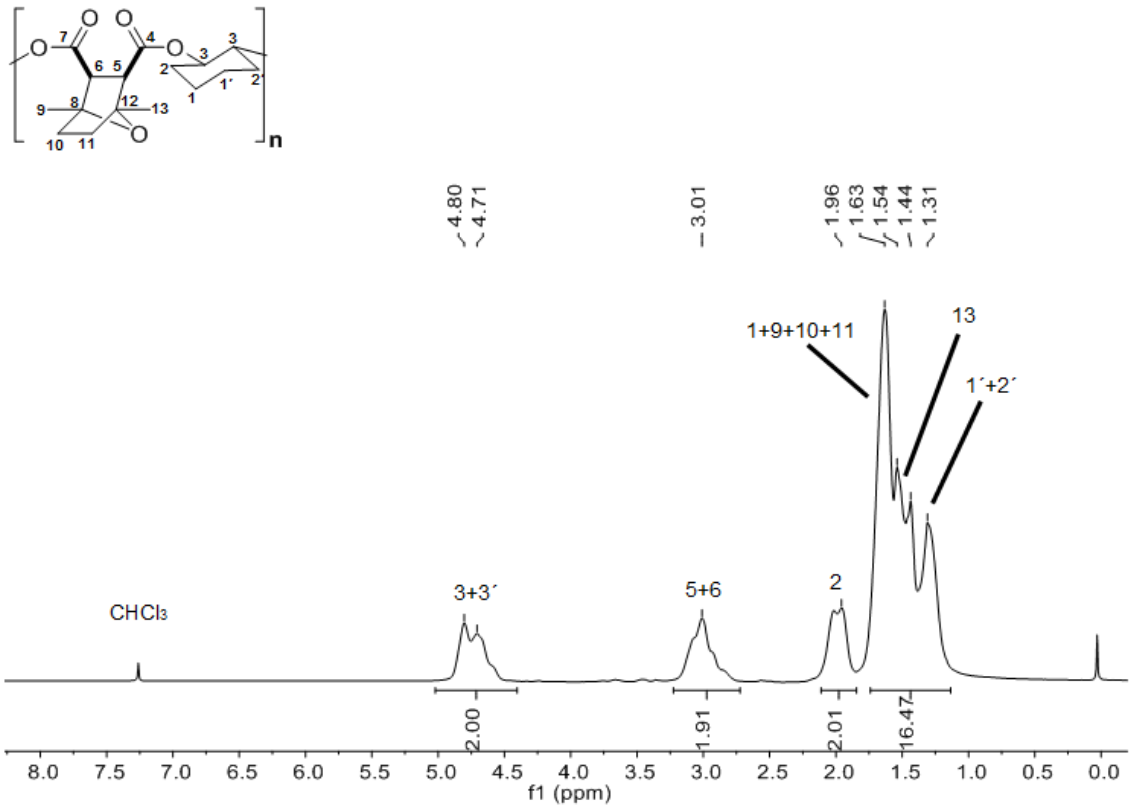

b)

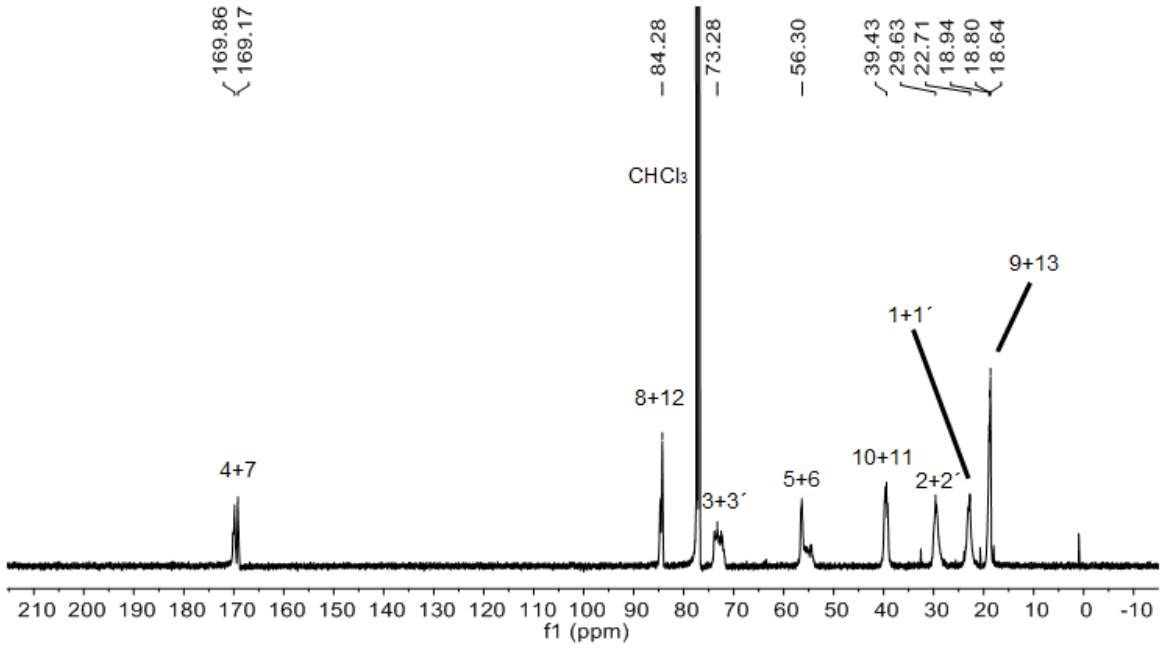

Figure S40. a)[1]H NMR of poly(CHO-*alt*-**1f**) and b) [13]C NMR of poly(CHO-*alt*-**1f**) (Note that while there are multiple possible isomers, the peaks are overlapping and for simplicity's sake only one isomer is drawn.)

a)

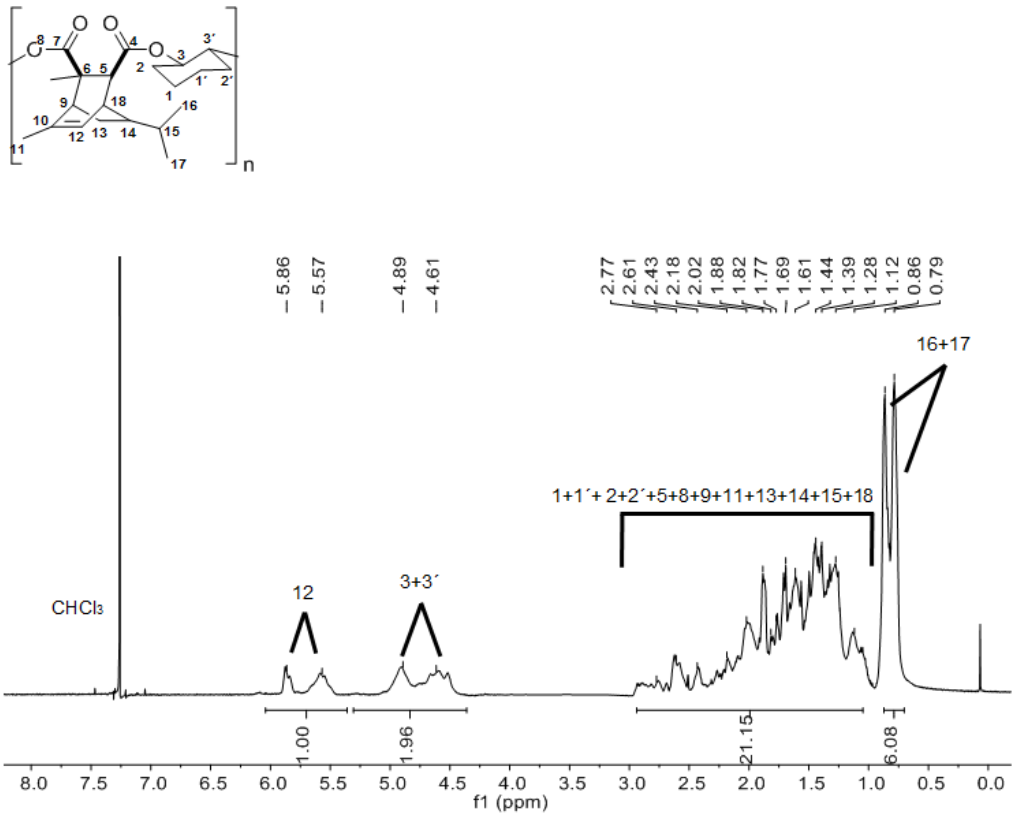

b)

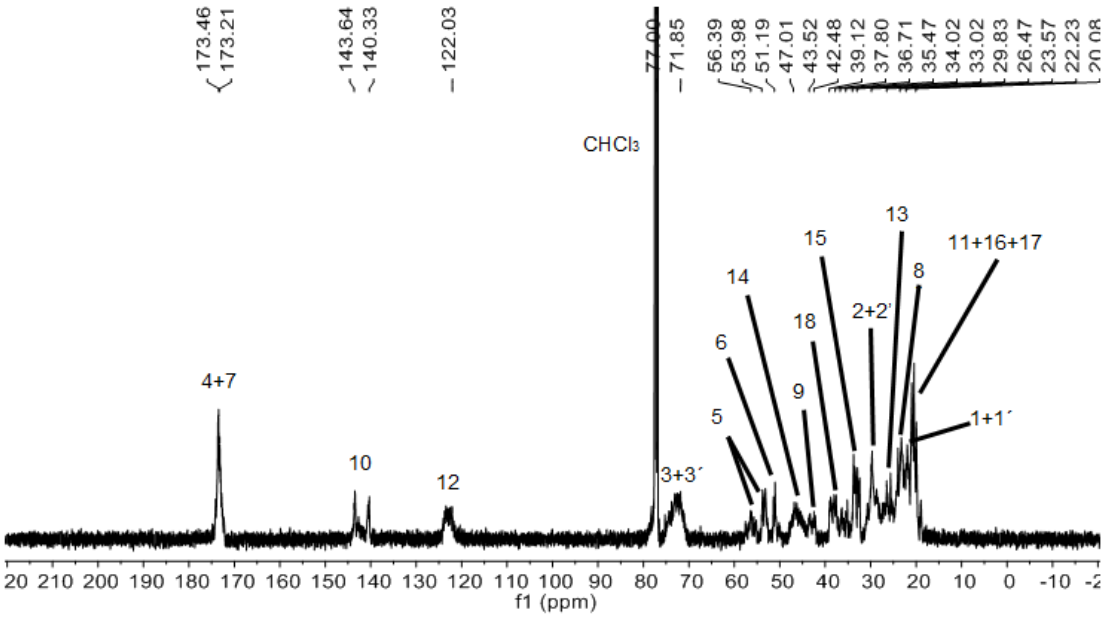

14. References

(1) Huijser, S.; HosseiniNejad, E.; Sablong, R.; de Jong, C.; Koning, C. E.; Duchateau, R. Ring-Opening Co- and Terpolymerization of an Alicyclic Oxirane with Carboxylic Acid Anhydrides and CO_2 in the Presence of Chromium Porphyrinato and Salen Catalysts. *Macromolecules* **2011**, *44*, 1132-1139.

(2) Kurahashi, T.; Fujii, H. One-Electron Oxidation of Electronically Diverse Manganese(III) and Nickel(II) Salen Complexes: Transition from Localized to Delocalized Mixed-Valence Ligand Radicals. *J. Am. Chem. Soc.* **2011**, *133*, 8307-8316.

(3) Coletti, A.; Galloni, P.; Sartorel, A.; Conte, V.; Floris, B. Salophen and salen oxo vanadium complexes as catalysts of sulfides oxidation with H_2O_2: Mechanistic insights. *Catal. Today* **2012**, *192*, 44-55.

(4) Rutherford, D.; Atwood, D. A. Five-Coordinate Aluminum Amides. *Organometallics* **1996**, *15*, 4417-4422.

(5) Licini, G.; Mba, M.; Zonta, C. Amine triphenolate complexes: synthesis, structure and catalytic activity. *Dalton Trans.* **2009**, 5265-5277.

(6) Van Zee, N. J.; Coates, G. W. Alternating Copolymerization of Propylene Oxide with Biorenewable Terpene-Based Cyclic Anhydrides: A Sustainable Route to Aliphatic Polyesters with High Glass Transition Temperatures. *Angew. Chem., Int. Ed.* **2015**, *54*, 2665-2668.

(7) Citron, C. A.; Wickel, S. M.; Schulz, B.; Draeger, S.; Dickschat, J. S. A Diels–Alder/Retro-Diels–Alder Approach for the Enantioselective Synthesis of Microbial Butenolides. *Eur. J. Org. Chem.* **2012**, *2012*, 6636-6646.

(8) Nielsen, L. P. C.; Stevenson, C. P.; Blackmond, D. G.; Jacobsen, E. N. Mechanistic Investigation Leads to a Synthetic Improvement in the Hydrolytic Kinetic Resolution of Terminal Epoxides. *J. Am. Chem. Soc.* **2004**, *126*, 1360-1362.

(9) Inoue, S. Immortal polymerization: The outset, development, and application. *J. Polym. Sci. A Polym. Chem.* **2000**, *38*, 2861-2871.

(10) Van Zee, N. J.; Sanford, M. J.; Coates, G. W. Electronic Effects of Aluminum Complexes in the Copolymerization of Propylene Oxide with Tricyclic Anhydrides: Access to Well-Defined, Functionalizable Aliphatic Polyesters. *J. Am. Chem. Soc.* **2016**, *138*, 2755-2761.

(11) van Meerendonk, W. J.; Duchateau, R.; Koning, C. E.; Gruter, G.-J. M. Unexpected Side Reactions and Chain Transfer for Zinc-Catalyzed Copolymerization of Cyclohexene Oxide and Carbon Dioxide. *Macromolecules* **2005**, *38*, 7306-7313.